eprints@whiterose.ac.uk
https://eprints.whiterose.ac.uk/

Review of Machine Learning for Hydrodynamics, Transport and Reactions in Multiphase Flows and Reactors

Li-Tao Zhu[1], **Xi-Zhong Chen**[2], **Bo Ouyang**[1], **Wei-Cheng Yan**[3], **He Lei**[1], **Zhe Chen**[1], **Zheng-Hong Luo**[1]*

[1]*Department of Chemical Engineering, School of Chemistry and Chemical Engineering, State Key Laboratory of Metal Matrix Composites, Shanghai Jiao Tong University, Shanghai 200240, P. R. China*

[2]*Department of Chemical and Biological Engineering, University of Sheffield, Sheffield, S1 3JD, UK*

[3]*School of Chemistry and Chemical Engineering, Jiangsu University, Zhenjiang, Jiangsu 212013, China*

*Corresponding Author: Professor Z.H. Luo; E-mail: luozh@sjtu.edu.cn.

Tel.: +86-21-54745602; Fax: +86-21-54745602

Abstract

Nowadays, artificial intelligence (AI), machine learning (ML) and data science are leading to a promising transformative paradigm. ML, especially deep learning and physics-informed ML, is a valuable toolkit that complements incomplete domain-specific knowledge in conventional experimental and computational methods. ML can provide flexible techniques to facilitate the conceptual development of new robust predictive models for multiphase flows and reactors by finding hidden pattern/information/mechanism in a dataset. Due to such emergence, we thereby comprehensively survey, explore, analyze and discuss key advancements of recent ML applications to hydrodynamics, heat and mass transfer, and reactions in single-phase and multiphase flow systems from different aspects: (1) Development of multiphase closure models of drag force, turbulence stresses and heat/mass transfer to improve the accuracy and efficiency of typical CFD simulations; (2) Image reconstruction, regime identification, key parameter predictions and optimization of multiphase flow and transport fields; (3) Reaction kinetics modeling (e.g., predictions of reaction networks, kinetic parameters and species production) and reaction conditions optimization. These sections also discuss and analyze the key advantages and weakness of ML for solving the problems in the domain of multiphase flows and reactors. Finally, we summarize the under-solving challenges and opportunities in order to identify future directions that would be useful for the research community. Future development and study of multiphase flows and reactors are envisaged to be accelerated by ML and data science.

***Keywords*:** Multiphase flows and reactors; Hydrodynamics; Transport phenomena; Reactions; Machine learning; Physics-informed neural networks; Data-driven modeling

Contents

1. Introduction and fundamentals of machine learning

In 1959, machine learning (ML) was defined as the study that gives machines the capability of learning without being explicitly programmed[1]. In 1997, Mitchell[2] gave a more descriptive and specific definition of ML: "ML is a computer program able to learn from experience with respect to some tasks and some performance measures, if its performance on tasks, as measured by performance, improves with experience." Venkatasubramanian[3] clarified the applications of artificial intelligence (AI) into several different phases: (i) Expert systems era (~1983 to ~1995), (ii) Neural networks (NN) era (~1990 to ~2008), (iii) Deep learning (DL) and the data science era (~2005 to present). The illustrative relationships among AI, ML, and DL are illustrated in **Figure 1a**. ML can find insights or efficiently predict the desired properties of the target by extracting complex and often hidden patterns or relationships from the available data. ML might be categorized into the following types (**Figure 1b**): supervised, semi-supervised, and unsupervised learning. **Figure 2** illustrates several typical ML methods: artificial neural network (ANN), boosted decision tree, support vector machine (SVM), and physics-informed neural networks (PINN). The major distinctions between these types include the availability of the amount of context and labeling information for the target variable for training ML[4] and whether the physics or constraints are embedded into the ML architecture. Some common types of ML are listed in **Table S1**. Note that the advantages and disadvantages of these ML algorithms in the table are relative, and they may have their own specific application scenarios or tasks. In the following sections, we will explore and analyze their specific advantages and disadvantages combined with the specific application examples. It should also be emphasized that our critical discussions and

comments are in the hope that some references may be useful for future work of readers.
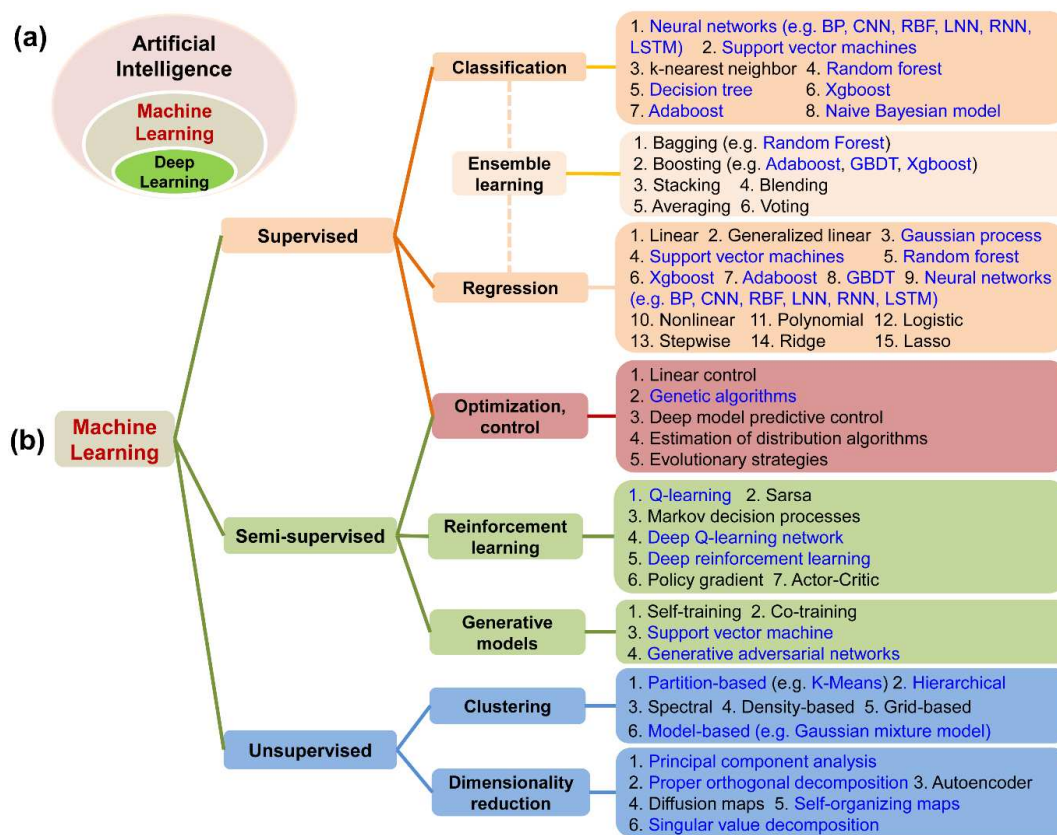
Figure 1 (a) The relationships among artificial intelligence (AI), machine learning (ML), and deep learning (DL); (b) The possible categorization of ML algorithms. Figure 1b was made according to the categorization presented in the reviews of Brunton et al.[5] and Beck et al.[6] The methods marked in blue are applied very often by users.

In recent years, due to the feasibility and flexibility of tools for ML implementation and workflow management, the explosion of new sources of data, and the rapid advancement of algorithms and powerful supercomputer resources, ML is experiencing an immensely fascinating resurgence in numerous scientific and engineering disciplines, such as chemical engineering[3,7], chemistry[8,9], catalysis science[10-12], material science[13-14], fluid mechanics[5,15,16]. Accompanied by this rapidly developing trend, recent advances of ML, especially DL, are also greatly contributing to a new era. In this new era of AI-enabled paradigm, discovery and innovation no longer solely rely on human effort and domain expertise but also significantly supplemented by analytics and mining of knowledge hidden in the data, and the visualization

of information[6,17].
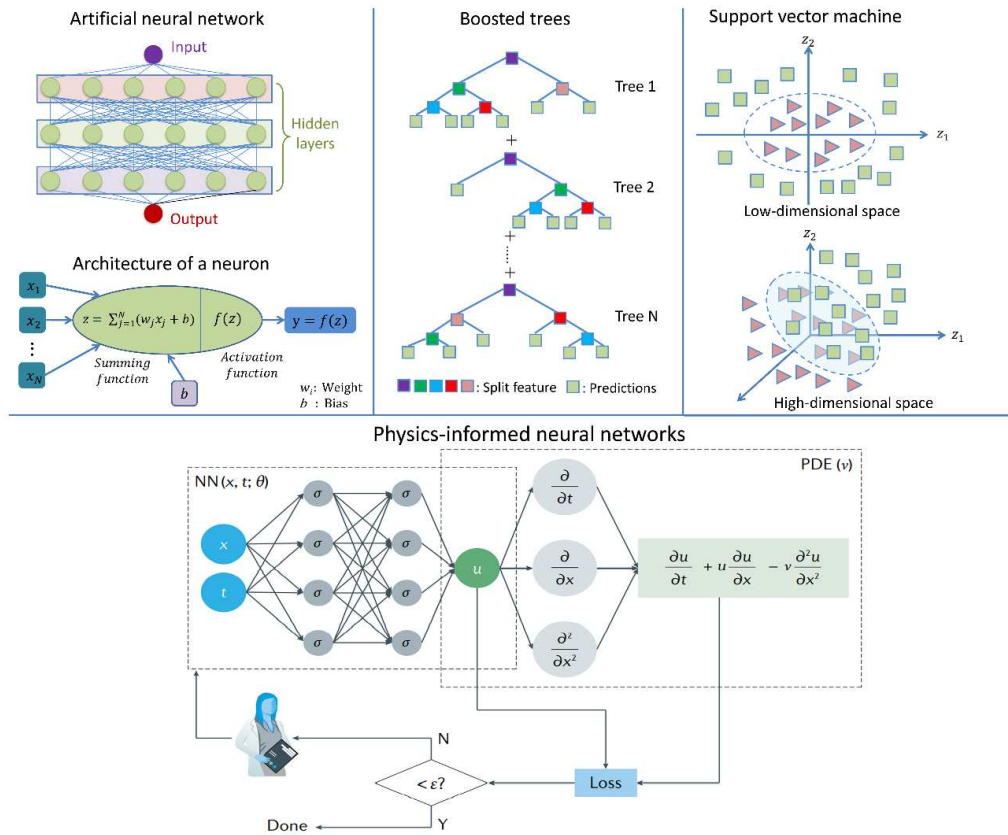
Figure 2 Several typical machine learning methods: Artificial neural network, boosted decision tree, support vector machine, and physics-informed neural networks (PINN). The diagram of PINN was adapted with permission from ref 18. Copyright 2021 Springer Nature.

Recently, ML is also largely impacting research of multiphase flow, transport phenomena, and chemical reactions, especially in multiphase flows and reactors. As illustrated in **Figure S1**, the increase of the number of publications, containing the keywords 'machine learning X' (Here, X denotes fluid dynamics, heat transfer and reaction kinetics) from the Web of Science since 2016, is apparent and research interests related to these topics are expanding rapidly. Multiphase flow and transport phenomena (accompanied by chemical reactions) are widely encountered in various process engineering applications, such as the reactor (e.g., bubble column, external-loop airlift, fixed bed, fluidized bed, stirred tank, trickle bed, etc.), mixer, separator, heat exchanger, boiler, absorber, rotating contactors, and

so on. These phenomena are often very turbulent, dynamic, multidimensional, and multiscale in nature, and exhibit persistent instabilities in flow variables spanning various spatiotemporal scales[19]. Compared with the single-phase fluid flow, the complex interactions between the phases further increase the complexities of multiphase flows and make it intractable to understand and model. Better understanding and accurate prediction of multiphase characteristics can significantly contribute to reaching rational design, scale-up, optimization, and control of multiphase flows and devices. Traditionally, the underlying mechanism of these complex multiphase characteristics can be studied and understood by experimental and numerical techniques. In particular, computational fluid dynamics (CFD) is an effective numerical tool to describe the detailed flow and transport behavior. Historically, the data sets from these techniques are utilized to calibrate or develop simplified engineering correlations (e.g., Ergun equation and Gunn heat transfer correlations) that are useful for engineering design, optimization, and control. Nowadays, multidimensional, instantaneous big data sets (i.e., a massive amount of data) are available. However, this brings a great difficulty to traditional data management, analytics, and modeling, which is laborious and time-consuming. Compared with the conventional data modeling and analytics approaches, ML is promising to provide an efficient analysis of data sets, identification of the flow patterns hidden in the data, discovery of predictive models and thereby facilitate the augmented understanding, design, and control of multiphase processes[20]. **Table S1** summarizes some common ML algorithms, their corresponding basic functions (e.g., Activation functions or kernel functions), and their advantages and limitations. In particular, NN is the most popular and wide spread ML method, probably due to its flexibility of

architectures that can be re-designed to target complicated problems, and its excellent approximation ability to nonlinearities with high accuracy. For example, multiphase flow problems commonly have a large parametric space and the conventional methods have the difficulties in finding complex and accurate functions to approximate the flow properties. However, the structure of NN can be flexibly reorganized to process complicated prediction tasks, and it is thereby effective to provide solution to these multiphase flow problems. So far, there may be mainly three types of ML-based models. In this part, we only provide brief introduction and discussion of these three types of models in order to pave the way for later comprehensive discussion and analysis of their applications in Section 2.

(1) The pure ML-based data-driven model (DDM): It is a surrogate modeling method to replace the complete traditional models. Such a method is black-box in nature and able to well fit the input-output relationship without introducing any domain knowledge such as the prior understanding of physics and chemistry. This type of pure ML-based DDM can be applied for diverse multiphase problems such as the development of closure models for flow dynamics and transport, reconstruction and identification of flow patterns, quantification of uncertainty in physical models, estimation and optimization of key physical or reactive process parameters and reactor performance based on the flow, transport and reaction conditions and device structures, etc. Commonly, pure ML-based DDM can approximate the relationships between feature input and output variables with high accuracy but also probably with a risk of overfitting and lack of interpretability. In particular, its performance is significantly associated with the sufficiency of datasets.

(2) The hybrid model: It includes but not limited to: (a) using ML or traditional

physical models to optimize the hyperparameters/structures of another ML, (b) using ML to optimize the sub-models or constants/coefficients in the traditional physical models, or (c) using ML to replace the sub-models or constants/coefficients in the traditional physical models. The method (a) could potentially improve the ML performance by overcoming the possible limitations or risks (e.g., overfitting) in the pure DDM. The hybrid model is also applicable for predicting the input-output relationship problems mentioned in **(1)** and has a potential to achieve better model performance than the pure DDM. In some specific systems, it has been designed to compensate for the weakness of both the pure ML model and the physical model[21].

(3) The domain knowledge-informed ML model: It is an emerging learning method that can integrate the prior physics, mathematical laws, chemical mechanisms or boundary conditions as constraints into the architecture of ML algorithms[18]. The role of such constraints is to teach the conventional ML models about the prior knowledge, which can not only greatly improve its approximation ability but also boost the interpretability that the pure ML (especially NN) does not have. A typical example of such a new deep learning technique is the recently popular 'physics-informed neural networks' (PINN), as illustrated in **Figure 2**. PINN in its early phase mainly makes the physical governing equations, e.g., the N-S equation, kinetics-ordinary differential equation (kinetics-ODE) and kinetics-partial differential equation (kinetics-PDE), "participate" in the training process by adding the residual of the physical equation to the loss function of NN. Notably, the pioneering idea of using ML to solve ODEs and PDEs was proposed by Lagaris et al.[23] Recently, a residual-based adaptive refinement strategy to boost the training efficiency was implemented

into an open-source library called DeepXDE[22]. So far, there is an increasing number of specifically-designed software libraries for physics-informed ML such as NuralPDE and NeuroDiffEq and others[18]. In this way, the NN optimizes not only the loss function of the network itself but also the residual of each iteration of the physical equation, so that the final training result meets the underlying law. Moreover, the boundary conditions can also serve as constraints to adjust the structural parameters of NN including weights and biases. The major advantage of PINN is to endow ML with more interpretability, high robustness, accuracy and consistency even for extrapolation scenarios.

Furthermore, the applications of ML-enabled discoveries may also be categorized as physical matter, models and processes (see **Figure 3a**)[24]. For example, ML-aided discoveries of physical matter can identify molecules, materials, or flow reactors with optimal performance. Discoveries of processes encompass the synthetic routes to a specific chemical molecule or chemical engineering processes to achieve a desired reaction conversion. Discoveries of models can be the regression models from measured or simulated data, structure-function relationships, or even conceptual mechanistic models. A typical workflow example of ML-enabled model discovery (see **Figure 3b**) may include: (1) Implementation of (high-throughput) experiments/simulations or collection of data from the literature or open database; (2) Construction of database; (3) Selection of descriptors; (4) Determination of algorithm; (5) Model training and validation, including feature selection and reduction; (6) Model testing; (7) Model used for prediction, regression, classification, control, and optimization, to name a few[7].
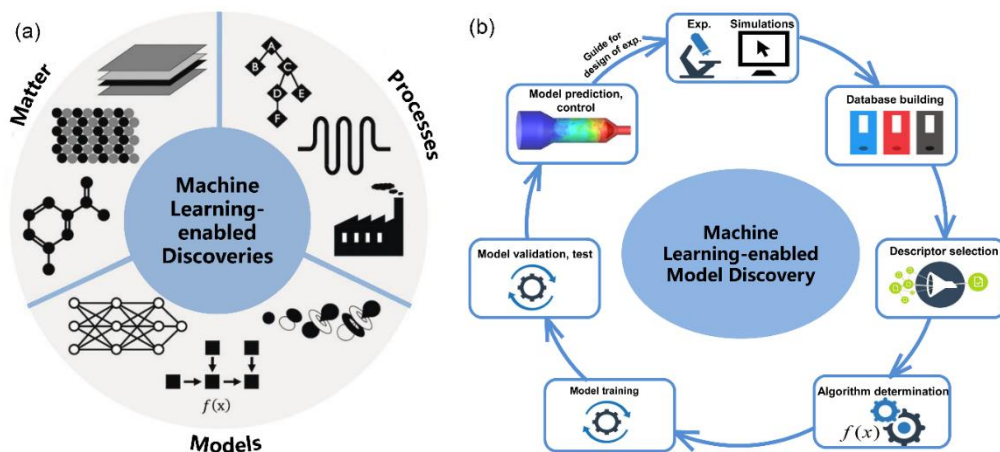
Figure 3 (a) The applications of ML-enabled discoveries may be categorized as physical matter, models and processes; (b) A typical workflow of ML-enabled model discovery. Figure 3a was adapted with permission from ref 24. Copyright 2020 John Wiley and Sons. The simulation contour in Figure 3b was adapted with permission from ref 25. Copyright 2016 American Chemical Society. The workflow in Figure 3b was reproduced with permission from ref 7. Copyright 2021 Elsevier.

Although it is necessary to invest some computational cost in the process of model discovery, the ML method can give fast prediction and classification of the properties of the crucial target with relatively low computational expense once the model is constructed. Usually, three independent datasets, which can be built by randomly splitting the original data set, should be prepared for separate training, validation, and testing of ML models. The training set is used for learning and fitting the parameters (e.g. weights for NN) in ML. The validation set is often employed to tune hyperparameters (e.g. the number of hidden layers and hidden neurons for NN architecture), which is to determine the optimal hyperparameters that aims to maximize the model performance. Meanwhile, the validation set can also be used to check the state and convergence of the ML model during the training process. For instance, it can be utilized to monitor whether the model is overfitted and to determine when to stop training. The test set is only used to evaluate the generalization performance of the model and has never been seen before by the model. To further enhance ML performance, some common cross-validation strategies are often adopted for training operations, such as k-folder

cross-validation and least-one-out cross-validation. For regression-related problems, some basic assessment standards such as the mean squared error (MSE), mean absolute percentage error (MAPE), mean relative error (MRE), coefficient of determination (R^2) and Pearson correlation coefficient can be used to measure the training accuracy. It is desirable that the accuracy is achieved uniformly over the entire data set. **Figure S2** illustrates three typical types of fitting performance in a common regression or classification learning operation: Underfitting, Ideal fitting and Overfitting. **Table S2** summarizes the commonly utilized activation functions, loss functions and optimizers, as well as their advantages and weaknesses. Here, "activation" in the NN means that each layer of the network needs a transformation when it outputs, and it connects the neighboring two layers (**Figure 2**). The nonlinear connection is more preparable because it can greatly increase the information stored in the network and enhance the hierarchical nonlinear mapping learning ability. To sum up, the advantages of having an activation include adding the network system with nonlinearity, differentiability, simple computation, unsaturation, monotonicity, limited outputs and normalization. However, in most cases only some of the above preparable properties can be achieved and each activation function has its specific limitations, as summarized in **Table S2**. Moreover, the loss function is used to measure the gap between the output and real value, which is an indicator of the optimization direction during the training operation. In a training task, many optimizers can be selected (**Table S2**) and their common function is to adjust, calculate and update the hyperparameters affecting model training and learning performance, so as to approximate or reach the optimal value for minimization (sometimes "maximization") of the loss during training. It should be noted that the

advantages and disadvantages for different methods summarized in **Table S2** are also problem-specific. Generally, their development history follows a basic rule, namely, take the essence and discard the dregs. That is, the latest one absorbs the advantages of the old one or/and overcomes the disadvantages of the old one. Thus, one should choose the most suitable ML algorithm, function or optimizer for a specific scenario or task.
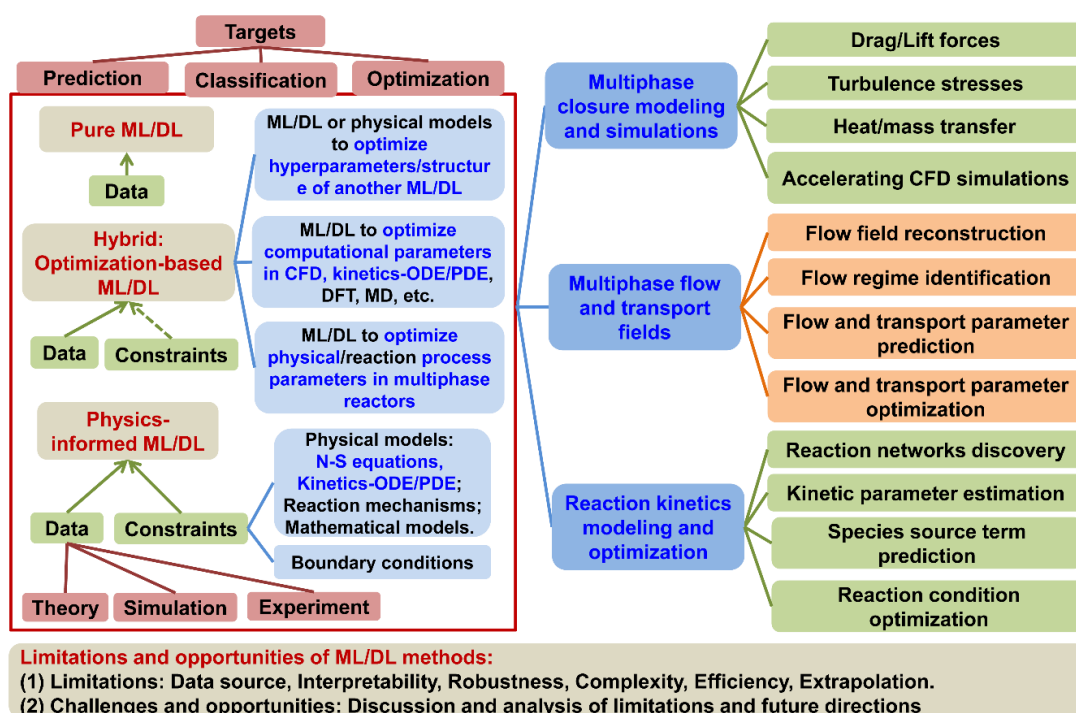
Figure 4 Applications, limitations and opportunities of machine learning for multiphase flows and reactors. The descriptions marked in red and blue indicate the main focus of this review.

In this comprehensive review, we first provide a brief introduction to what ML is and why we do need it. The fundamentals of ML are also briefly summarized. We then survey, explore, analyze and discuss the current status and challenges of ML advances for multiphase flow, transport phenomena and chemical reactions from the following aspects (**Figure 4**): (1) Development of multiphase closure models of drag force, turbulence stresses and heat/mass transfer for the averaged CFD simulation and its acceleration; (2) Image reconstruction, regime identification, key parameter predictions, and optimization of multiphase flow and

transport field parameters; (3) Kinetics modeling (e.g., estimation of kinetic parameters and species source terms) and reaction conditions optimization. The specific survey processes and review summary are illustrated in **Figure S3**. **Section 2** mainly highlights the benefits and challenges of ML promising for addressing longstanding problems in the research domains of chemical engineering and multiphase flow. **Figure 5** shows the relationships among Sections 2.1-2.3 and their role in multiphase reactor engineering. The main idea of this review follows the subject of mass transfer, momentum transfer, energy transfer and reactions, i.e. "Three Transfer Plus Reaction", which lay the foundations of multiphase reactor engineering. In particular, the developed ML-based closure models and the complete CFD models in Section 2.1 can assist to improve the accuracy and efficiency of the estimation and optimization of flow, transport and reaction process parameters in Sections 2.2.3, 2.2.4, 2.3.2 and 2.3.3. Meanwhile, the obtained physics, measured process data and estimated parameters (e.g., flow, transport and kinetics parameters) from Section 2.2.1, 2.2.2 and 2.3.1 can contribute to more reliable and accurate closure models and CFD models in Section 2.1. All of these sections complement and promote each other, and will be useful for better understanding of multiphase flows and rational design, scale-up and optimization of multiphase reactors. Finally, Section 3 summarizes the under-addressing problems, highlights the emerging applications, and provides promising directions probably useful for the research community.
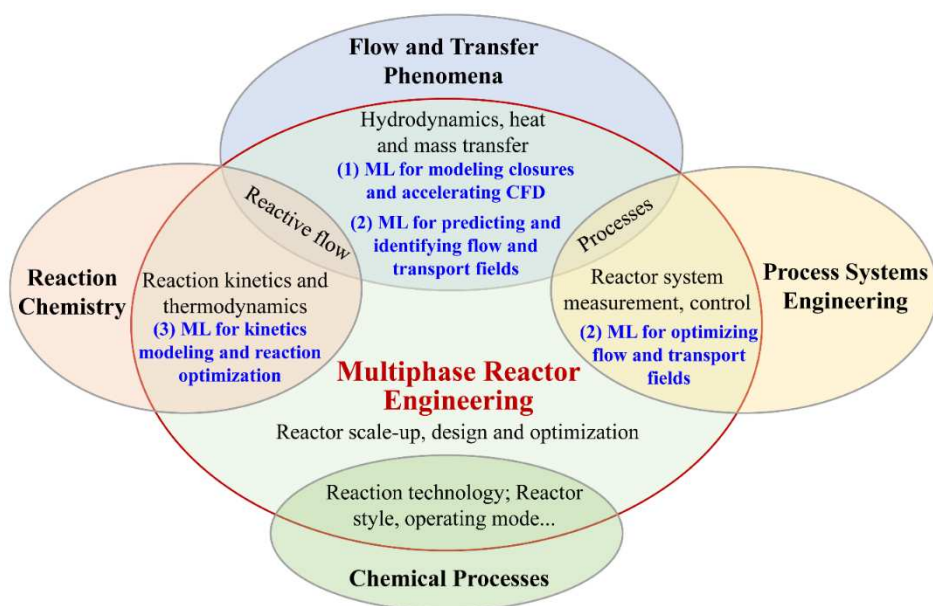
Figure 5 The relationships among Sections 2.1-2.3 and their role in multiphase reactor engineering. The descriptions marked in blue indicate the main topics of this review.

2. Current status and challenges

2.1 Machine learning for multiphase closure modeling and simulations

Historically, extensive theoretical, experimental, and computational approaches have been proposed to capture the complex multiscale characteristics of multiphase flows and transport phenomena. Among these methods, the direct numerical simulation (DNS)[26,27] has emerged as a powerful tool to resolve the full details of fluid flows without additional turbulence closures. Despite the exponential growth of computing power in the last decades, DNS of even a lab-scale multiphase flow device still demands extremely huge computational resources, which makes it still impractical for engineering design and optimizations of large-scale multiphase flow reactors. An alternative numerical method with much reduced computational cost is the large-eddy simulations (LES)[28], which is filtered from Navier-Stokes (N-S) equations to separate the larger scales of motion. The additional term due to filtering procedure above needs to be closed and modeled by a sub-grid scale (SGS)

turbulence closure model. Another popular numerical alternative for simplified engineering approximations is the Reynolds-averaged Navier–Stokes (RANS) method. Similarly, the turbulence closure for the Reynolds stresses is required. A major problem is that the closure constants involved in the turbulence transport equations are usually determined empirically in order to solve these equations. Note that efforts are also made to use more accurate DNS and LES data to model these closure constants[29]. For multiphase flow such as the fluidized fluid-particle flow, the interactions between the phases further increase its modeling and understanding complexity. To efficiently approximate the characteristics of multiphase flow systems, one can perform the averaged methods including the Euler-Euler two-fluid model (TFM) based on continuity theory[30] and the Euler-Lagrange approach[31,32], e.g., CFD-discrete element method (CFD-DEM), CFD-discrete particle method (CFD-DPM). Again, these averaged multiphase methods should be closed by closures.

So far, many closure correlations for descriptions of drag, turbulence stresses, heat and mass transfer coefficients have been formulated based on experimental data or DNS data. However, in many realistic cases, a major difficulty is that it's still impossible to seamlessly integrate such multi-fidelity data into existing multiphase flow models[18]. In the research field of modeling and predicting multiphase flow and transport, the lack of universally reliable closure models underscores the demand for a transformative method. Fortunately, with the increasing computer resources and the available high-fidelity datasets, data-driven and physics-informed ML modeling can complement traditional methods and provide easy-to-use techniques to facilitate the development of new robust closure models for multiphase flow systems by mining hidden information from a dataset. The ultimate goal is to apply the

developed models for the design, scale-up, optimization, and control of multiphase flows and reactors. A conceptual workflow for conventional and ML-aided data-driven multiscale modeling and simulations is plotted in **Figure 6**. However, it is not an entire replacement for traditional physics-based modeling[33]. From a chemical engineering perspective, multiphase flow and transport phenomena problems in multiscale multiphase flow and reactor systems are often clarified into three different scales: microscale, mesoscale and macroscale (**Figure 6**), but don't limit it to just three scales. In multiphase flow and device systems, mesoscale is an intermediate scale characterizing the dynamic inhomogeneity (e.g., aggregation of bubbles and clustering of particles) and thereby bridging the microscale element (e.g., bubble, particle and droplet) and macroscale multiphase devices[19,34]. It should be noted that the single-phase fluid flow lays the foundation of multiphase flows. For example, the mechanistic understanding of flow/transport characteristics and physical closure models obtained from single-phase flow can be very useful for better understanding and modeling of multiphase flows. Therefore, this part will encompass review of closure models for both multiphase and single-phase flows.

Table 1. Recent advances of machine learning applications for developing closure models.

Topics	ML algorithms; architecture, activation, loss functions, optimizer	Data sources and feature inputs	Research performance and contributions	Research gaps and future remarks
➤ **Drag on each particle**[35]	➤ **BPNN**: 1 hidden layer; 25 hidden neurons; Sigmoid; MSE	➤ LES-IBM; 21780 (75:15:15); Re, ϕ, x_i, y_i, z_i	➤ MSE=15% for 68% of particles (ANN with neighbourhood particle effect) vs. MSE=15% for 46% of particles (Mean drag).	➤ Further increase of prediction accuracy by adding more data points.
◇ **Drag correction**[36]	◇ **ANN**: 3 hidden layers; 128, 64 and 16 nodes in each hidden layer; ReLU; Zero-one	◇ Fine-grid TFM; $\widetilde{u_{slip}^*}$, $\bar{\phi}$, $\overline{\nabla P_{g,z}}$, Δ_{filter}	◇ Pearson r=0.99 of ANN vs. r=0.87 of the traditional method; Dramatic accuracy improvement due to introduction of filtered gas phase pressure gradient marker	◇ Need to identify the dependence of filtered drag correction on filter size when introducing gas phase pressure gradient.
➤ **Drag on each**	➤ **PINN**: 5 hidden layers;	➤ LES-IBM; 7260	➤ Improvement of 7.09% average	➤ Improvement is not

particle[37]	128 hidden sizes; Linear; MRE+Loss_PHY	(55:45); Re, ϕ, x_i, y_i, z_i	prediction performance (MRE) compared with Linear, RF and GB regression models.	remarkable. Effects of upstream and downstream particles should be considered.
✧**Drag correction**[38]	✧**BPNN**: 5 hidden layers with 240, 120, 60, 30, 15 hidden units, Adam to optimize learning rate, ReLU, Huber; **XGBoost**: 30 trees, 15 max tree depth.	✧Fine-grid TFM; $\sim 1.525 \times 10^7$ (60:30:10); $\widetilde{u_{slip,y}^*}$, $\bar{\phi}$, $\overline{\nabla P_{g,y}}$, Δ_{filter}	✧ANN: MAPE=9.85%, r=0.98; Xgboost: MAPE=11.33%, r=0.97. Remarkable accuracy improvement of 3-marker model vs. 2-marker model; Successful online integration of CFD with ML.	✧Limited to the simulation of a small domain; Mainly for dense fluid-particle flows while it needs to considering dilute flows.
➤Drag correction[39]	➤**ANN**: 1 hidden layer; 15~20 and 5~9 hidden nodes	➤EMMS; $\sim 1.310 \times 10^7$ (70:15:15); u_{slip}, ϕ_g, $d_p, \rho_p, \rho_g, \mu_g, D_r$	➤MSE=9.62, 8.66, 0.089%; Direct addition of material properties and reactor factors in the drag correction; Initial effort in ML-aided EMMS predictions	➤Difficult to quantify the improved accuracy because it's dependent on the varied properties of gas–solid mixtures; Need to perform the case with evident variations in particle diameters.
✧**RANS stress source term correction** [29]	✧**RF**: 100 trees, 5 maximum tree depth	✧DNS, LES; $q(x)$, e.g., dP/ds, Re_d	✧Relatively initial effort in quantification of RANS stress discrepancies using ML and demonstrating its merits.	✧Potential ill-conditioning of RANS-based stresses still challenge the solution of mean flow by improvements of Reynolds stresses.
➤**RANS stress coefficient correction** [40]	➤**BPNN**: 2 hidden layers and 64 neurons in each hidden layers; Nonlinear	➤Limited experimental data; η_1, η_2, η_3	➤R^2=0.85~0.90; Optimizing the Spalart-Allmaras model coefficient to improve RANS based stress discrepancy.	➤Further improvements by using more elaborate experimental data.
✧**LES stress coefficient correction**[41]	✧**DANN**: 4 hidden layers; Nonlinear	✧DNS; 2×64^3 (70:30); $3 \times \mathbf{D}^{3'}$	✧R^2=0.988~0.995; MRE=0.101~0.155. High accuracy without any fine-tuning by data-driven modelling of SGS coefficients; Relatively low cost and good generalization ability.	✧Need of more physics-based knowledge and constraints to integrate into SGS models; Further improvements of interpretability of DANN
➤**Reynolds stress tensor modelling** [42]	➤**DNN**: 8 hidden layers with 30 nodes per each one, 2.5×10^{-7} learning rate; **MLP**: 10 hidden layers, 10 nodes in each one, 2.5×10^{-6} learning rate; ReLU	➤DNS, LES, RANS; $\mathbf{S}$, $\mathbf{R}$	➤RMSE=0.14 DNN vs. RMSE=0.31 of MLP for duct flow. First attempt to embed the tensorial invariance features in a NN; Evidently improving predictions vs. baseline RANS; Bayesian optimization of hyperparameters.	➤Unable to perfectly approximate DNS results; Need to train and test data over a wider range of flow cases.
✧**Solids stress modelling**[43]	✧**DNN**: 5 hidden layers with 128, 128, 64, 64, 32 and 32 hidden units; ReLU; Huber+MAPE	✧Fine-grid TFM; 7.2×10^6 (80:20); $\bar{\phi}$, $\overline{\boldsymbol{v}_s^*}$, $\nabla \overline{\boldsymbol{v}_s^*}$, Δ_{filter}	✧MAPE=20~25%, r=0.80~0.97 vs. traditional correlation MAPE=60~95%; Early effort to applying ML for mesoscale solids	✧Without considering anisotropy of filtered solids normal stresses; Need of a posteriori analysis.

			stress development.	
➢**Mass transfer coefficient** [44]	➢**BPNN**: 1 hidden layer with 14 nodes; **SVR**: Gaussian kernel function, 763 support vectors, 0.2357 kernel scale, 0.0036 bias; Linear ε-insensitive	➢Experimental data; 814 (BPNN: 70:15:15; SVR: 90:10); U_G, σ, d_o, A_d/A_r	➢BPNN: MAPE=9.64% and R^2=0.9819, SVR: MAPE= 7.26% and R^2=0.9852 for the volumetric gas-liquid mass transfer coefficient k_La; Good generalization performance of SVR.	➢Relatively limited number of experimental data points; a wider range of data should be introduced; Further application of ML for optimizing hyperparameters instead of empirical tuning.
✧**Heat transfer coefficient correction** [45]	✧**BPNN**: 4 hidden layers with 16, 8, 8 and 1 hidden units in each one; Sigmoid; Huber;	✧Filtered TFM data; 2500 (80:20); $\overline{\phi_g}$, $\Delta\tilde{T}$, Δ_{filter}	✧MAPE=11.14%, r=0.98 vs. traditional correlation MAPE=21.11%, r=0.96; Boosting accuracy and discovery of new closure marker.	✧Absent validation with experiments; The closure feature inputs should be rendered in a dimensionless form.

Note: The critical comments above may not be adequate and we present the suggestions with the hope that readers and newcomers may obtain some possible inspirations or thoughts from this table.
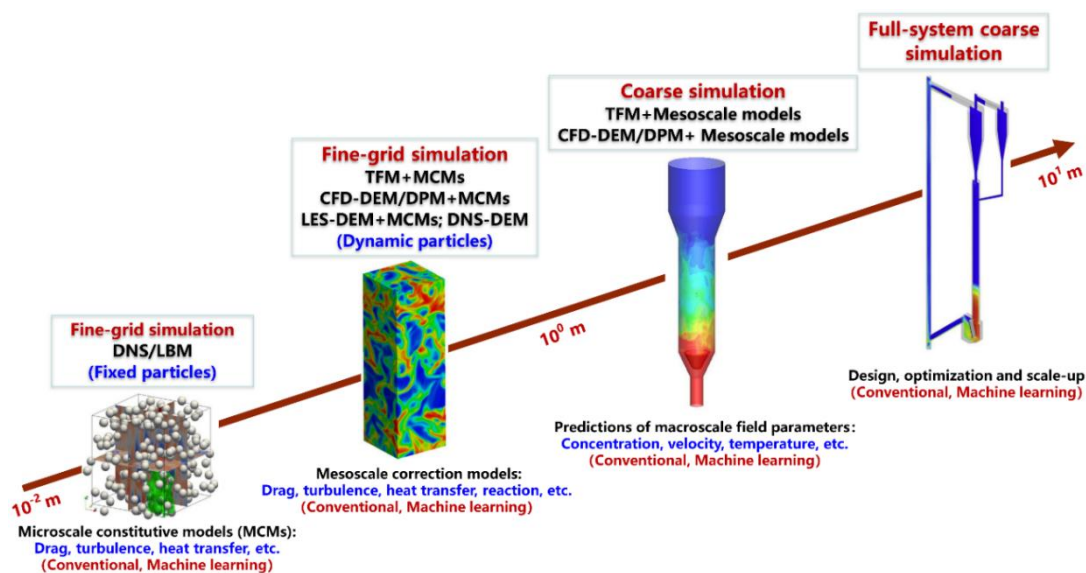
Figure 6 Machine learning-aided multiscale modeling of gas-particle flows. The DNS simulation contour of fixed particles is collected from. The DNS simulation contour was adapted with permission from ref 46. Copyright 2015 Elsevier. The fine-grid simulation contour was adapted with permission from ref 34. Copyright 2021 Elsevier. The coarse simulation contour was adapted with permission from ref 25. Copyright 2016 American Chemical Society. The full-system coarse simulation contour was adapted with permission from ref 47. Copyright 2021 Elsevier.

2.1.1 Drag closure modeling

Interphase drag modeling plays an essential role in the simulation of large-scale multiphase reactors and the identification of multiphase flow states[48]. Recently, increasing attention has been paid to the development of drag models based on ML techniques. **Table 1** briefly summarizes recent advances of several typical applications of ML for modeling of

drag closures, including the specific ML algorithms (including their structures, activation and loss functions), data sources/sizes, feature input variables, prediction performance and contributions, possible research gaps and future remarks. The studies on drag closure modeling may follow the categorizations below:

(1) Data-driven drag modeling of flow passing fixed particles. Most of the studies have used NN to directly predict the drag force on each particle or to indirectly predict the drag force by introducing a drag correction factor. For instance, He and Tafti[35] trained a backpropagation neural network (BPNN) based data-driven drag model using the data produced by the highly-resolved large-eddy simulation (LES) of fixed particle assemblies via their in-house code[47]. This proof-of-concept work revealed that the trained NN can increase the prediction precision of the drag force on each particle with the addition of the relative neighbor particle positions as NN inputs: MSE=15% for 68% of particles (ANN) vs. MSE=15% for 46% of particles (Traditional mean drag). Here, we suggest that further increase prediction accuracy by adding more data points is necessary despite their prediction improvement is evident. In fact, many studies similar to the data-driven drag closure above only consider the fluid bypassing fixed spherical or non-spherical particles[50-52] while the particle velocity fluctuations are not considered. It is thereby suggested that the reliability of the constructed data-driven model using the data source from such a way still needs further verification and improvement.

(2) Data-driven drag modeling of flow passing dynamic particles. Commonly, the actual drag experienced by dynamic particles may significantly differ from the drag calculated from flow passing static particles. Thus, it is desirable to conduct highly resolved

simulations of dynamic fluid-particle flows to generate data used for model training and learning. Luo et al.[53] constructed the ANN-based drag closure model via the introduction of the additional parameters that characterize the particle positions and velocity fluctuations. The prediction results by the ANN-based drag models approximated to the direct numerical simulations-discrete element method (DNS-DEM) data much better than those by pure physics-based models. Note that the particles simulated in the above study belongs to Geldart type D with a diameter larger than ~600 μm[54]. An observable weakness is that the formation of complex clustering structures in real small-particle fluidized bed systems (Geldart type A and B) and its significant impact on fluid-particle transport and reaction behavior are unable to be adequately captured by simulations of large-particle systems (Geldart type D). In fact, the particles widely encountered in industrial reactors such as the fluid catalytic cracking (FCC) riser and the methanol-to-olefins turbulent fluidized bed reactor belong to Geldart types A and B particles. To bridge this gap and accurately understand clustering structures, researchers proposed NN-based and convolutional neural networks (CNN)-based data-driven models to predict the mesoscale drag correction so that the trained model can be used for coarse TFM or coarse CFD-DEM simulations of real gas-solid flows [36,38,55,56]. Particularly, Zhou and coworkers[55] reported that the neighboring flow properties such as the mesoscale fluid pressure gradient could be added as feature inputs to markedly improve prediction performance. However, the relative importance and relevance between the newly introduced variables and the old variables may need to be identified. This is because the filtered drag correction is nearly independent of filter size when introducing the closure marker of the gas phase pressure gradient in traditional physics-based modeling[45]. Moreover, whether the

trained model can be well extrapolated to different gas-solid flow patterns is also an important issue in NN modeling[57]. Based on BPNN and eXtreme Gradient Boosting (XGboost) methods, Zhu et al.[38] proposed data-driven mesoscale drag correction models and optimized the input markers to boost the prediction accuracy. The study demonstrated that the fluid phase pressure gradient can serve as an excellent feature input of the ML for improving predictions of the filtered drag correction. The developed data-driven model was then integrated with a CFD solver and validated with experiments under different flow patterns. However, the data source of this study is generated by simulations of a relatively small domain where there are possible numerical artifacts since the clusters or bubbles can grow to the domain scale and hence lead to unrealistic settlement velocity. Their later study further found that the correction model can still perform well by using the closure maker of the fluid phase pressure gradient in the absence of filter size[45]. Except for the use of simulations to generate datasets, theoretical methods such as the energy minimization multiscale (EMMS) can also provide data for training. Nikolopoulos et al.[39] developed a novel ANN-based framework via the data collected from a custom-built FORTRAN algorithm solving the original EMMS equations over numerous material properties. The learned ANN-EMMS was tested by simulations of a pilot-scale circulating fluidized bed (CFB) carbonator. The prediction difference of mean pressure drop predictions between the CFD-ANN-EMMS and CFD-EMMS was 11.29% while that of CO_2 concentration at the reactor exit was nearly ignorable. There is a possible issue about the difficulty to quantify the improved accuracy as this is dependent on the varied properties of gas–solid mixtures in the reactor. Therefore, it is suggested to further validate the effectiveness of CFD-ANN-EMMS via the cases with

evident variations in particle properties. More recently, the EMMS group[58] further extended to propose a more generalizable ANN-EMMS methodology for simulations of dense gas-particle flows over a broad variety of fluidization conditions and material properties. The developed model was validated by five fluidized beds and could reasonably predict gas-solid fluidization under different flow conditions and material properties.

In summary, many researchers have attempted to apply ML-based data-driven approaches to model and predict the drag force closure. Compared to traditional mean drag correlations, the applications of ML approaches for calculations of drag force reveal several primary advantages: Once the data-driven drag closure is obtained, it's efficient to accurately calculate the drag force with a lower requirement of computer memory storage. This is related to the fact that for example, for a trained NN model only its structure, weights and activations are stored. However, a major weakness is that most of the above contributions have used NN as a black-box approximator to predict the drag force closure with low interpretability. In such a black-box context, the ML model may be difficult to give physically consistent or plausible approximations because of its generalization capability associated with a lack of domain knowledge as constraints in the structure of ML algorithms.

(3) Knowledge-informed drag modeling of flow passing stationary particles. To solve the major disadvantages above, recent works have tried to enforce the prior domain knowledge into the ML architecture and a particularly increasing attention has been paid to the PINN proposed by Raissi et al.[59]. Inspired by such a concept, Muralidhar et al.[37] expanded to propose a PhyNet model which embeds the respective estimations of the pressure and velocity fields around a particle as the physical loss functions into the NN

architecture for learning the drag force. PhyNet can lead to improvements of a 7.09% MRE

compared with Linear, Random Forest (RF), and Gradient Boosting Decision Tree (GBDT)

regression models. However, this improvement seems not very remarkable and the effects of

upstream and downstream particles are suggested to be considered for possible future

improvements. Analogous to PINN above, Moore and Balachandar[60] improved the

performance of a pure data-driven nonlinear regression model by using the model form

provided by their previously-developed point-particle force model[61]. The proposed

physics-informed model can retain both the physical and data-driven models' advantages and

enable the decreased error of the physical model for all cases. Despite the simplicity and

efficiency of the nonlinear regression algorithm, it's hard to deal with the complex

approximation tasks with high dimensionality and nonlinearity. Besides, one may question

whether it is sufficient to train an effective data-driven model using a limited dataset

generated from expensive PR-DNS. That is, whether the trained model is able to learn

generalizable patterns from a relatively small dataset. Despite the integration of prior

knowledge into the ML architecture, there may be still a possible risk of either incapability of

minimizing the overall loss function or overfitting when the number of hyperparameters

greatly grows. This is because the model complexities significantly increase with the

increasing amount of hyperparameters and the model will simply adapt to approximate the

dataset for higher prediction accuracy. More recently, researchers attempted to incorporate

new features into the architecture of PINN inspired by physical observations in constructing

the particle-laden flow model. To improve generalizability, Seyed-Ahmadi and Wachs[62]

introduced two main features into the architecture of the PINN model, including the

superposition of pairwise particle-to-particle interactions and sharing hyperparameters among NN blocks that model the effect of neighbors. In **Figure 7**, instead of simultaneously feeding the relative positions of all influential neighbors to a single fully-connected NN block, effects of individual neighbors are separated into various NN blocks. The number of free parameters can be remarkably decreased and model complexity is controlled without loss of accuracy.
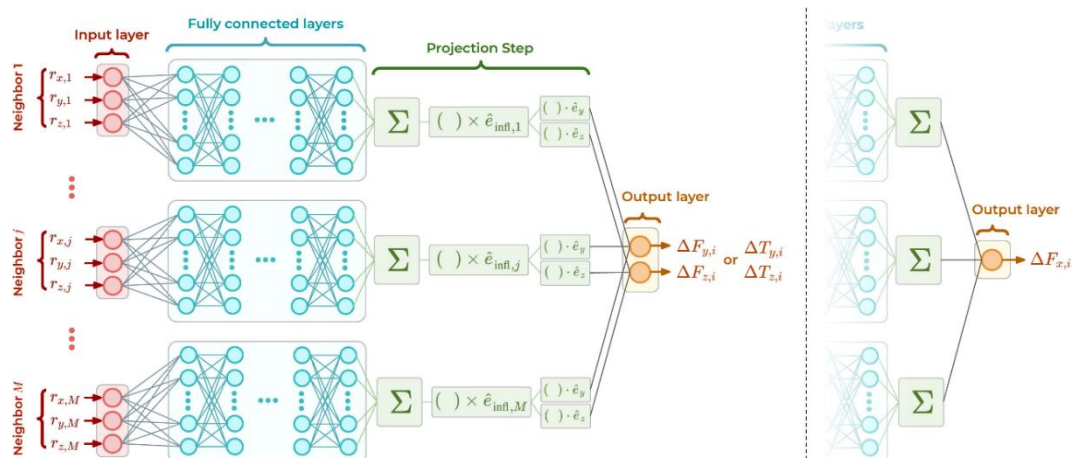
Figure 7 Schematic illustration of a ML model incorporating prior domain knowledge into the architectural design of the NN for learning the force and torque in flow passing fixed spherical particles. Adapted with permission from ref 62. Copyright 2022 Elsevier.

(4) ML-based drag modeling of gas-liquid flows. Overall, most of the above ML-based data-driven and physics-informed studies have been focused on the improvement of modeling gas-solid drag force while researchers have paid much less attention to data-driven modeling of gas-liquid drag force that has equivalent importance as the gas-solid drag force. On the other hand, scientists have made contributions to applying ML for gas-liquid bubbly flows while these significant works are mainly concentrated on quantifying uncertainty in coarse-grid multiphase-CFD simulations of such two-phase flows[63]. Therefore, it is suggested to make an attempt to constitute effective gas-liquid drag closures for efficient coarse simulations of bubbly devices such as bubble columns.

Besides, another important aspect is that most of the above contributions have used NN

to assist the development of predictive drag models. However, a comprehensive cross-comparison investigation of different ML techniques applied for drag model development has been rarely reported. Further investigations are suggested to be specially devoted to the above consideration.

2.1.2 Turbulence closure modeling

Turbulence has been listed as one of the 125 most challenging scientific issues by the Science journal[64]. It has been a long-standing obstacle to precisely represent the turbulence characteristics, which is mainly due to the persistent fluctuations and strong chaos of flow and transport phenomena spanning over a wide range of active spatiotemporal scales. Despite the pioneering theoretical and computational contributions made to successfully understanding and modeling flow turbulence, there are still weaknesses to overcome and a predictive, robust, and accurate turbulence closure is still an underexplored issue. Recently, increasing interest is devoted to applying ML to turbulence closure modeling, especially for the single-phase flow[65,66]. This kind of turbulence closure modeling study may include but not limited to the following categories:

2.1.2.1 Modification of the source terms in RANS models

This kind of study mainly applied ML to quantify and model the discrepancies in the Reynolds stress tensor between the high-fidelity simulation and the RANS simulation. Researchers modified or supplemented the original stress source term in the RANS model to improve its accuracy, namely, by the inclusion of a correction factor or an additional source term in the model[29,67]. As an early example, Xiao et al.[68] employed an iterative ensemble Kalman approach to absorb the prior knowledge and observations in a Bayesian framework,

which enables significant reduction of the discrepancies and achieves much better performance than the existing black-box ML models. Leveraging the data from DNS of single-phase turbulent flow, Parish and Duraisamy[67] applied Gaussian processes (GP) to infer a modification of the production term in the *k-w* equation in RANS modeling. However, there are several possible weaknesses to this kind of study. First, it's still an open question to infer the full Reynolds stress field from the frameworks above. This is mainly because the discrepancy space of Reynolds stresses has high dimensionality and nonlinearity while Bayesian framework and GP are not effective for such a complex problem. Second, the correction model is constructed for a specific RANS model while different RANS models lead to different uncertainties. Therefore, the obtained modification model may be only valid for a specific RANS model, which will limit its universality. Third, **Table 1** shows that most of these contributions have directly used the dimensional variables such as velocity field distributions to construct ML models, which further limits its generalization performance. We suggest that it is essential in further efforts to introduce adequate non-dimensional variables (e.g., Reynolds and Froude numbers) to recover characteristic flow properties and thereby make the model more generalizable.

2.1.2.2 Surrogate modeling of the full turbulence stress

Many researchers applied ML methods for directly mapping the Reynolds stress tensor and subgrid-scale stress to flow variables based on the data obtained from highly-resolved simulations such as DNS. Early work of Sarghini et al.[69] was contributed to training an SGS stress model aided by a multilayer feed-forward ANN using the data of LES, which opens the possibility to utilize ANN methods to identify turbulent flow dynamics. A recent study by

Wang et al.[70] used RF and ANN to train the data-driven SGS closure for LES simulations. Zhu et al.[71] directly reconstructed an ANN-based data-driven model for mapping the filtered flow variables to the turbulent eddy viscosity and obtained a complete replacement of the original turbulence closure model. Note that all of the above three investigations are in the context of black-box ML modeling while no domain knowledge or physical observations was utilized to devise the architecture of ML. An important recent progress is to improve the black-box induced defect by the approach of physics-informed ML. Ling et al.[42] proposed invariant deep neural networks (DNN) based architecture to train and model the anisotropic Reynolds stress tensor using high-fidelity simulation data and the hyperparameters were rigorously optimized by a Bayesian method. To the best of our knowledge, this's the first attempt to embed the tensorial invariance features in a NN. Although the DNN above is unable to perfectly approximate DNS results, it can capture some important turbulence properties that the traditional model fails to characterize. In addition, there is a need to train and test data over a wider range of flow cases. Inspired by the PINN modeling above, researchers attempted to identify input features by introducing non-local features[72] or a systematic physical procedure[73] to generate and evaluate the various mean flow features on stress tensor predictions. Scientists also proposed to separately model linear and nonlinear parts of the Reynolds stress tensor via ML[73]. A recent investigation of Park and Choi[74] was performed to train different ANN-based SGS models with different feature inputs using DNS data. More recently, the hybrid closure was proposed to model the stress in complex multiphase flows. For example, Freund and Ferrante[75] utilized the standard Smagorinsky SGS in the carrier fluid while used NN to estimate the SGS closure terms at the interface. To

sum up, the physics-informed strategies like introducing physical observations or understanding into the model architecture can help to reduce input complexity and improve accuracy. Here, we provide several challenges of this group of modeling methods. First, one of the challenging issues arising in direct surrogate modeling of the full turbulence stress is how to select and optimize feature input variables, in particular, based on physical mechanisms and laws (e.g., the use of various scalar rates, selection of invariants and dimensional analysis methods). However, it's found that lots of existing studies have empirically tuned the hyperparameters. We thereby suggest that a more rigorous hyperparameter optimization using the Bayesian framework and Gaussian processes deserves more future efforts. Second, reducing the dimension and complexity of the DL model is an important direction. Let's take NN modeling as an example. Modeling the full Reynolds stress closure requires complex structures such as deep neural networks which greatly increases the number of hyperparameters for a high-dimension flow problem. This will significantly introduce the computational burden and reduce the overall computational efficiency although such a method does improve the prediction performance of turbulence closure. So, the balance between the model accuracy and computational cost should be taken into account.

2.1.2.3 Modeling of turbulence stress model coefficients

Given that two-equation models for describing turbulence (e.g., k-ε turbulence model) are widely used but inadequate for many complex turbulent flows of engineering interest, Yarlanki et al.[76] attempted to employ an ANN algorithm to estimate and optimize the model constants of the k-ε model. Different from the above study, Matai and Durbin[77] trained a

decision tree algorithm to create zones for establishing a zonal k-ω model with its coefficients optimized. Wang and coworkers[41,78] leveraged NN and deconvolutional NN to construct the model coefficients of the SGS anisotropy stress models. They established the nonlinear mapping between the filtered velocity inputs and unfiltered velocity outputs based on a six-layer fully connected NN. The constructed model had high accuracy (R^2=0.988~0.995; MRE=0.101~0.155) without any fine-tuning and could improve the prediction accuracy of the SGS stress as compared with traditional methods such as the approximate deconvolution approach[79]. However, there is a need to integrate more physics-based knowledge and constraints into DNN in order to improve its interpretability. More recently, Jiang et al.[80] designed an augmented DNN structure that contains two flexible parallel ML-based modules for data-driven turbulence modeling with promising universal interpretability. The key idea of this work is that (a) a frame- and scale-invariant properties, (b) regularization constraints on both trainable parameters and closure coefficients, and (c) fairness constraints were enforced in the model training (**Figure 8**). The proposed framework was able to extract the structural bases and closure coefficients from data, both of which are integrated through a multiplicative layer to constitute the stress anisotropy tensor applicable for coarse RANS simulations. Despite the benefits above, it is essential to further assess the model over other untested multiple classes of complex flows. From a purpose of engineering use, it is an important aspect to assess the newly improved turbulence model by incorporating it into a CFD solver[81]. Another important lesson is that although physics-informed ML can substantially increase the performance of interpretability and extrapolation, special care should still be paid to some strategies preventing overfitting such as regularization, dropout

and early stopping during training and cross-validation of the learned models since NN

modeling are easily prone to overfitting associated with its fundamentally interpolative nature.

Here, it's also suggested that it is necessary to systematically explore a complete and compact

set of input features because there is a possible risk of destroying the generalizable ability

related to incompleteness and redundancy of input features.
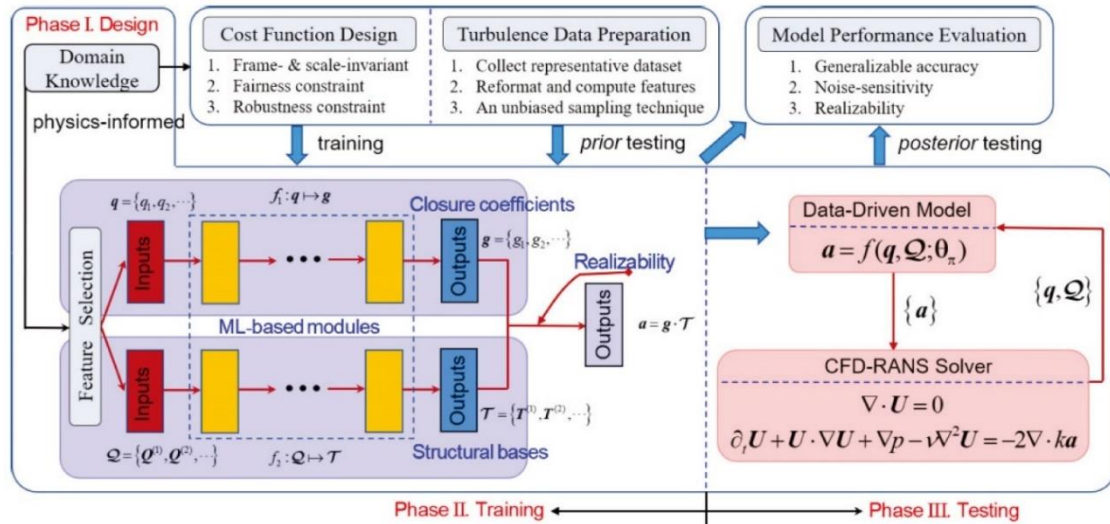
Figure 8 A workflow of the ML-augmented methodology for data-driven turbulence modeling with universal interpretability. The workflow contains several phases: Phase I: Designing the data-driven framework with physics-guided knowledge; Phase II: Training the DNN in a fair and robust way; Phase III: Testing the DNN. Adapted with permission from ref 80. Copyright 2020 AIP Publishing.

So far, most of RANS turbulence closure models used for multiphase flows were

developed based on single phase flows in the absence of dynamic solid particles, droplets and

bubbles. Compared with single-phase flow, multiphase flows such as gas-liquid and

gas-particle flows do have more complex characteristics occurring in multiphase devices.

Based on the resolved data from DNS of bubbly up-flow in liquid, Tryggvason and

coworkers[82,83] employed NN to develop the relations for the closure terms in TFM

simulations of the averaged flow. The overall predictions by their resulting closure relations

agree reasonably well with DNS data which is not part of the training data set. Meanwhile,

Table 1 shows that fine-grid simulations were also used to generate the data sets for learning

multiphase turbulence stresses in gas-liquid flows[84] and gas-particle flows[85]. Particularly, the

kinetic theory of granular flow (KTGF) is often used to close the solid stress for gas-particle

flow systems. In the context of a coarse-mesh TFM, the mesoscale solid stress closure needs

to be considered in addition to the microscale solid stress (i.e., solid stress predicted by

KTGF in the standard TFM), which is about an order magnitude smaller than the mesoscale

solid stress[86]. In this regard, Ouyang et al.[85] recently conducted ANN-based data-driven

mesoscale stress modeling utilizing the data from fine-grid simulations of inhomogeneous

gas-solid flows. It was found that the integration of different loss functions contributes to the

improved prediction performance of solids stress as compared with the use of a single loss

function. A systematic evaluation of closure markers as ML inputs revealed that the

mesoscale solid stress is principally dependent on the additional anisotropic markers, namely,

the mesoscale solid velocity and its gradient. Notably, the prediction accuracy of the above

two studies is dependent on the simulation accuracy itself. Thus, more accurate numerical

methods like DNS-volume of fraction (DNS-VOF) or DNS-DEM are suggested to be

performed to generate datasets.

In addition to the application categories discussed above, recent studies have used sparse

regression to develop algebraic Reynolds stress closures[87,88]. The key benefit of a stress

closure in an algebraic form with Galilean invariance and interpretability is not only its

equivalent prediction performance to that of NN modeling but its pluggable integration into

the existing CFD solvers. Such a very potential strategy was extended to train a multiphase

turbulence closure for fluid-particle flows by leveraging data from highly-resolved

Eulerian-Lagrangian (E-L) simulations[89]. The efforts above highlight the possibility to

decrease the complexity in integrating the data-driven algebraic closure with the CFD solver due to the closure expressed in an algebraic form but still maintaining its predictive accuracy.

To sum up, this part discusses some key advantages, weaknesses and potential directions of data-driven ML modeling and physics-informed ML modeling of flow turbulence. We also note that relatively less studies have been focused on ML modeling of cluster-induced turbulence in gas-solid flows and bubble-induced turbulence in gas-liquid flows. In fact, two-phase flows are very often encountered in chemical engineering devices and the two-phase interactions further increase the complexities of flow turbulence as compared with single-phase flow turbulence. Thus, it is of fundamental importance for future investigations to better understand and predict two-phase flow turbulence behavior assisted by ML.

2.1.3 Heat and mass transport closure modeling

Generally, multiphase flows are unstable, nonlinear and nonequilibrium in nature and their coupling with heat and mass transfer mechanisms further leads to the increasing difficulty in accurate simulations and measurements. Due to such complexities, the prediction of multiphase transport phenomena has been heavily relied on semi-empirical models or empirical correlations and is still a challenging task. So, a possible question is "Can heat and mass transfer phenomena be well understood and predicted by a transformative paradigm such as ML? If so, how and why?" We will try to answer these questions by reviewing recent advances. The advantage of ML-based techniques for multiphase flow transport is that they can introduce the pronounced reduction of the effort to the development of multi-variable transport phenomena models and can easily achieve the expansion of the parameter domain. Due to these advantages, ML for data-driven and physics-informed heat and mass transport

modeling in multifarious scientific and engineering applications is gaining popularity, especially in thermal engineering[90]. Note that our main attention in this section is paid to modeling the interphase heat and mass transfer closures which can be used in CFD solvers or engineering design. Most of these works have been focused on direct modeling of heat/mass transfer coefficients[91-94] or modeling the indirect variables that determine the transfer coefficient such as thermal conductivity, Nusselt number[95], Sherwood number[96] and Prandtl number[97]. Bansal et al.[98] mined the data from the literature over 22,000 experimental conditions and then used ANN and SVM methods to train the data. The trained model was used to predict the interphase mass transfer in terms of the fluid phase Sherwood number for trickle bed reactors. Fairly good accuracy of estimations for the data sets over a wide range of operating conditions was achieved. Zhou et al.[99] compared different ML algorithms including ANN, Adaptive Boosting (AdaBoost), RF, and XGBoost in order to evaluate their prediction performance for flow condensation heat transfer in mini/micro-channels. In particular, the relative importance of extensive feature inputs was also explored in detail. The results revealed that ANN and XGBoost present the best prediction accuracy for the testing dataset with 6.8% and 9.1% MAEs. A key benefit of both studies above is that the authors collected extensive datasets across a wide range of flow cases and can prevent overfitting well. Meanwhile, this may also introduce the errors related to the use of different experimental datasets measured by different researchers. A possible future direction for this issue is suggested to introduce a correction into the ML architecture in order to calibrate the trained model. Similarly, Kojić and Omorjan[44] used BPNN and SVM to estimate mass transport in an external-loop airlift reactor. The prediction accuracy is (1) BPNN: MAPE=9.64% and

R^2=0.9819; (2) SVR: MAPE=7.26% and R^2=0.9852 for the volumetric gas-liquid mass transfer coefficient k_{La}. Zhao et al.[96] applied a principal component analysis (PCA) approach to investigate mass transport of water deoxygenation in a rotor-stator reactor. The established PCA regression model could well estimate mass transfer coefficients with deviations within 15% as compared with experimental values. Kwon et al.[100] employed a RF method to model the convection heat transfer in a cooling channel present with varied array geometries. The data collected from numerical simulations of the channel with variable rib geometries were used for training and testing the ML model. It was observed that ML predictions approximate closely to the test dataset (R^2>0.966). Qian et al.[101] proposed a XGBoost-augmented model for predictions of the heat transfer coefficient in oscillating heat pipes. They established 580 sub-CART trees for obtaining superior prediction results even based on small-scale data. However, there is a general concern for these four works, that is, only a relatively limited number of data points were collected. This may lead to a consequence that once the tested conditions are out of the span used for training, the extrapolation results will not be robust and reliable. Therefore, a wider range of data covering more flow conditions is suggested to be introduced to enhance the model generalization performance and reduce the possibility of overfitting. Moreover, one may perform further applications of optimization methods to systematically optimize hyperparameters instead of manually tunning. Besides, some researchers have also devoted to applying ML to study heat and mass transfer inside porous media[102-105]. However, ML has not yet witnessed extensive adoption to problems of transport phenomena accompanied by chemical reactions in multiphase reactors. To tackle this issue, Zhu et al.[45] implemented ANN-based data-driven modeling of heat transfer and mass transfer

accompanied by chemical reactions in gas-particle fluidized bed reactors, with a prediction accuracy of MAPE=11.14%, r=0.98 vs. the traditional correlation MAPE=21.11%, r=0.96. The key advance of this work is the discovery of a new closure marker (e.g., the mesoscale interphase temperature difference) as the additional feature input and thus boosts the model performance. Despite the improvement, we suggest that the introduced closure feature input should be rendered in a dimensionless form to make it more general.

According to our survey, including the discussion above, it was found that ML-aided predictive modeling of heat transport in thermal energy-related devices and systems has become an active research area. On the other hand, heat and mass transport phenomena are also widely encountered in chemical engineering devices such as fixed bed reactors, which are utilized to produce billions of dollars of chemicals[106]. Despite this critical importance, ML-assisted understanding and modeling of transport phenomena especially accompanied by chemical reactions have not been intensively studied for better design, optimization, and scale-up of chemical process devices. In the future, it is still a major challenge for scientists to discover robust chemical reaction engineering (CRE) models and to identify the hidden patterns in the data for chemical reactors[106]. A possible weakness for most of the researches we discussed above is that they are theory-agnostic black-box models while much less recent studies have turned to the development of physics-informed ML models such as PINN for heat transfer problems[107,108]. Following the PINN modeling of fluid dynamics, researchers typically trained a PINN heat transfer model by incorporating the residual of the heat transfer governing equations into the loss function. And the trained PINN should satisfy the heat transfer PDE. It is considered that PINN modeling of transport phenomena will be of

significance in better generalization performance.

In addition to the sub-model closures discussed above, some other closure coefficients or parameters such as the lift force coefficients[109,110], diffusion coefficients[111], interfacial area[112-115], curvature[116,117] and droplet/bubble size[118,119] should also be informed in advance in Eulerian-Eulerian (E-E), E-L or VOF simulations of gas-liquid, gas-solid and gas-liquid-solid flows. Despite the importance of the lift coefficient calculation in TFM simulations of gas-liquid flows, few reports have used ML to aid in direct data-driven modeling of lift force in such flows. Bao et al.[120,121] proposed a DL-based data-driven method, i.e., feature-similarity measurement[122], to indirectly correct the interfacial momentum closures (e.g., drag, lift, wall-lubrication, and turbulent-dispersion forces) in coarse-grid CFD simulations of gas-liquid flows. The authors applied a three-hidden-layer feedforward ANN method to train and learn the differences between the high-fidelity data (i.e., fine-grid simulation and experimental data) and low-fidelity data of coarse-grid simulations closed by empirical interfacial closures, and then modified such discrepancies to improve coarse simulation predictions. Moreover, researchers used ML as a predictive tool to estimate the interfacial area and droplet/bubble sizes[112,113,118,119] in gas-liquid two-phase flows. Tryggvason and coworkers[117] developed a viable ML-based method to extract a functional relation between the volume fractions and the curvature. The method can return the curvature and specific shape in a VOF simulation solver for numerical parameters. Despite the advantages in prediction accuracy, the authors also suggested that the convergence under mesh refinement cannot be guaranteed without an explicit order. Patel et al.[116] further promoted to deeply analyzing such a promising ML-based method from several different

aspects such as methodology of data generation and model selection using different interface shapes when coupled with a multiphase flow solver. Their results confirmed again that ML-based data-driven modeling that is feasible for accurate computation of the curvature can easily outperform the traditional approaches and even reach the prediction performance of the height function approach in some cases tested.
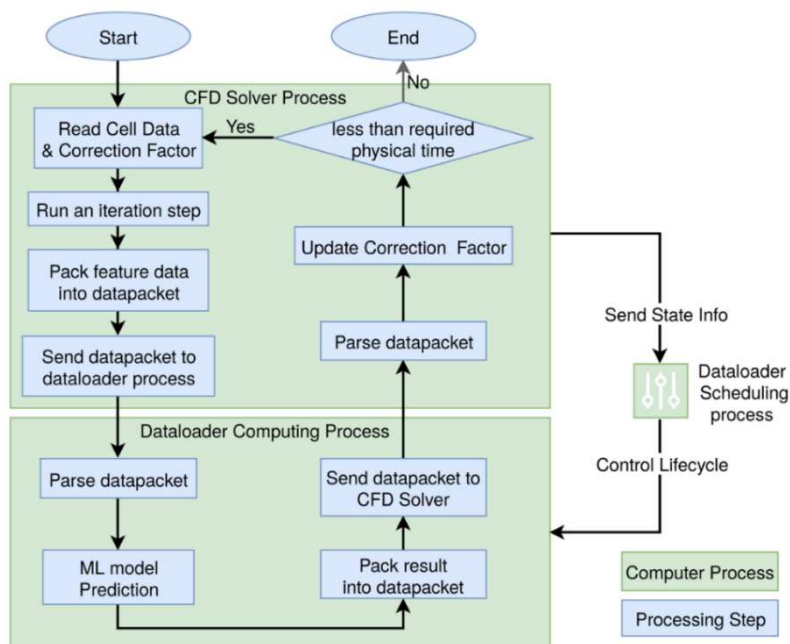
Figure 9 A workflow of data exchange architecture for integration of CFD and machine learning tools. Adapted with permission from ref 38. Copyright 2020 John Wiley and Sons.

2.1.4 Machine learning-accelerated CFD simulations

In the last decades, real-time simulations of multiphase flows with complex multiscale nature are feasible only in the case of certain restrictions although the computing power has achieved huge advancements. High-fidelity DNS of flows and devices is still computationally prohibitive and thereby impractical for most engineering applications. Therefore, attempts have always been made to accelerate simulations aiming to solve this long-standing daunting problem[123,124]. To accelerate simulations, one may consider what algorithms can be used and

how these algorithms can be performed to speed up simulations with adequate accuracy while they do not compromise generalization ability. Fortunately, ML can be applied to accelerate real-time simulations and such kind of major efforts may be categorized into the following types (except for hardware acceleration):

(1) Data-driven surrogate modeling of the entire N-S conservation equations using pure ML. That is, the full N-S simulations will be replaced with a pure ML model as an approximator. One of the typical examples for this group of studies is to use long short term memory (LSTM) network to learn and approximate the time series fluid flow structure data[125]. Such a black-box method is more efficient as compared with extremely time-consuming step-by-step iterations, whose computational speed and numerical stability are heavily constrained by grid resolution and time step in traditional solution approaches of N-S equations such as finite difference and finite element methods[126]. As we have discussed previously, a key disadvantage for a pure ML model is its relatively poor extrapolation and interpretability since the underlying domain knowledge is absent in such kind of model. When using a pure ML method, one has to be very cautious and struggle with the model generalization performance in order to make the model still valid out of the dataset span that was originally utilized for training. In summary, data-driven surrogate modeling of the entire N-S conservation equations using a pure ML can be extremely efficient but its generalization ability is still an open question.

(2) Data-driven and physics-informed closures for coarse simulations. The learned closures in Sections 2.1.1-2.1.3 can be then integrated into CFD solvers to close coarse simulations such as the RANS single-phase model, TFM or CFD-DEM simulations (One

may also call them "averaged models".). Note that in this part the principal effort is to show how these closures can be embedded into a numerical solver and how the simulations can be accelerated. For example, the proposed data-driven mesoscale drag and solids stress models were successfully integrated with the coarse simulation via a data loader (**Figure 9**)[38,85]. It was found that the computational speed of the coarse-grid CFD-ANN simulation is decreased by about 10% as compared with the conventional coarse-grid CFD model[38]. The reduced speed was due to invoking the data loader in each time step. Although the introduction of the data loader does not affect computational cost significantly, the development of such a data loader introduces additional complexity as the data-driven models are probably developed by different ML platforms and have a relative lack of universality. Another typical kind of study is to apply the DL method to accelerate DEM simulations through direct calculation of particle-particle and particle-boundary collision interactions in a numerical solver. This is mainly motivated by the fact that DEM's applicability is remarkably limited by the great computational expense due to the detection and computation of collisions. In particular, Lu et al.[127] trained and tested a CNN model using the datasets from the DEM simulations of granular flow using MFiX solver and the TensorFlow accelerated via a GPU. Notably, they proposed a multi-scale loss function to reduce the model fluctuations associated with training steps. The reported method can accelerate DEM computation speed by orders of magnitude. Altogether, compared with highly resolved simulations, coarse simulations are much faster and satisfy a short turnover duration required in engineering decisions[128]. Despite its benefit to remarkably reduce the computational cost, in fact coarse simulations still need huge computational resources for large-scale flow devices. For example, in industrial gas-solid

FCC riser flow reactors, the mesh resolution requirements are $\sim10^{-3}$ m, which is computationally prohibitive for reactor-scale simulations ($10^0 \sim 10^1$ m). Furthermore, if one uses DEM or coarse DEM to track the dynamics of each particle, it will further greatly increase the computation cost since $10^{12} \sim 10^{14}$ particles are generally present in such riser reactors. This major limit calls for the emergence of a new paradigm in further efforts.

(3) Knowledge-informed ML solution of conservation equations. In efforts to improve the disadvantages in **(1)** and **(2)** above, scientists have performed knowledge-informed ML to accelerate simulations from different aspects such as acceleration of Eulerian fluid simulations or acceleration of Lagrangian particle dynamics simulations. Particularly, Ladický et al.[129] developed a novel ML-based regression forest method allowing for a large time step to estimate the discrete particle movement for smooth particle hydrodynamics simulations. More specifically, a feature vector that directly modeled individual forces and constraints from N-S conservations was designed to enhance the generalization capability of providing reliable predictions of particle positions and velocities. The advantage is that the model can quickly approximate the next-frame position and velocity of the current particle according to the state input of the neighboring particles. A weakness is that this method might not be directly extended to Euler fluid simulations. To address this problem, Tompson et al.[130] trained a CNN solution of the Poisson equation offline, and then used it to replace the preconditioned conjugate gradient solver of pressure projection in Euler fluid simulations. Their novel unsupervised strategy could solve a large sparse linear system with numerous free parameters in the incompressible Euler equations with a standard operator splitting approach. The presented real-time simulations with a good

generalization ability outperformed the data-driven approaches recently proposed in the literature. Another recently notable acceleration progress is that the Google research team[131] replaced the traditional solver component mostly affected by the resolution loss with its learned components (i.e., learned interpolation and learned correction) from high-fidelity simulation data, that is, the data-driven discretization solution is used to interpolate the differential operator into the coarse grid without sacrificing accuracy or generalization in coarse-mesh simulations, as shown in **Figure 10**. DL-based time-varying predictions achieved the same accuracy as baseline DNS while it utilized an order of magnitude coarser mesh than that conventionally required in DNS. Note that this method remained stable during a long-time evolution process. Here, further considerations regarding this work are provided: First, in their final generalization test of 2D simulations, the maximum Re is limited to 4000, and there seems almost no visible inertial region, which may motivate readers to consider how much small-scale structures can be captured. Future efforts are suggested to test the model performance at a much higher Re regarding that it's only a 2D simulation. Second, statistics only give an energy spectrum and vorticity correlation function, and other statistics may also be given in order to make it more convincing to readers. Besides, for all of the works above, one key challenge is that the coarse-grid simulation using data-driven or physics-informed ML closures appear to be more efficient than the current group of methods since the trained closures can be more easily integrated into the coarse-grid CFD solver. This possible limitation deserves to be further investigated in future knowledge-informed ML solution of conservation equations.

In addition to the ML-aided acceleration methods above, recently scientists have also

developed accelerators by optimization of ML architectures and interested readers may be referred to the literature review[132].
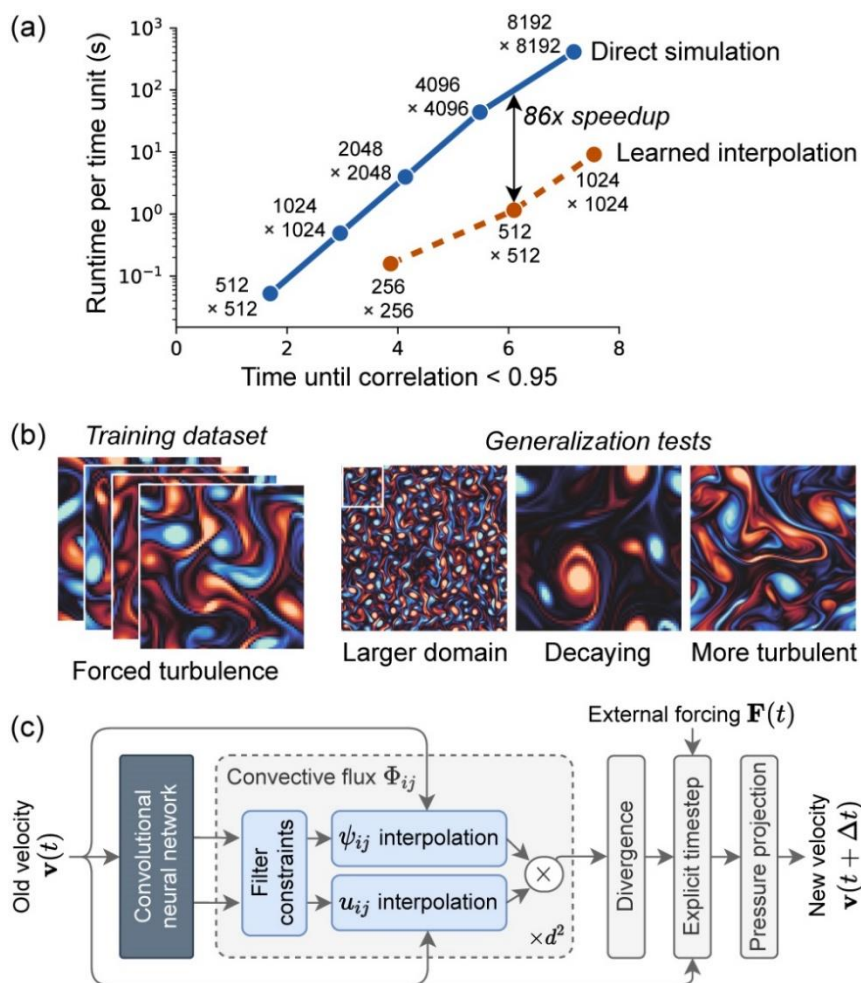
Figure 10 (a) Accuracy vs. computation expense with baseline DNS and DL accelerated solvers. (b) Illustration of training and validation results. (c) Structure of the learned CNN model over a time step. The figure is obtained from the literature of Kochkov et al.[131]

2.2 Machine learning for multiphase flow and transport fields

Modern non-intrusive experimental detection techniques such as electrical capacitance tomography (ECT)[133], electromagnetic tomography (EMT)[134], electrical resistance tomography (ERT)[135], computed tomography (CT)[136], particle image velocimetry (PIV)[137,138], particle tracking velocimetry (PTV)[139], high-speed camera (HSC)[140], laser-induced fluorescence (LIF)[141] and magnetic resonance imaging (MRI)[142], have been widely applied for the study of flow and transport phenomena. Some additional references for each technique

are provided in **Table S3**. These advanced measurement techniques are capable of providing abundant measured data or images used for understanding the underlying flow and transport mechanisms. The collected data or images can be processed by many traditional algorithms. For example, selecting key features from each image is an important step in traditional methods[143]. However, with the increase of the number of categories, feature extraction becomes more and more troublesome. Determining the features that can best describe the corresponding target classification critically depends on the judgment and long-term trial-to-error expertise of engineers. In addition, each feature definition also needs to deal with a large number of parameters and their fine-tuning is severely dependent on the knowledge of engineers. Compared with the traditional techniques, ML especially deep learning can process images with higher accuracy and efficiency in the problems of classification, object detection, segmentation, and (super-) reconstruction and denoising (**Figure 11**). The commonly-used ML methods include the discriminative model and generative model, which were used by some typical fluid flow applications, as shown in **Figure 11**. In this section, we focus on how to use ML including DL to assist identification and prediction of single-phase and multiphase flow fields such as the reconstruction of the flow fields, recognition of flow patterns/regimes, prediction of key flow field parameters, as well as performance optimization of multiphase flows and transport. For most cases in this part, the datasets are obtained based on experiments. **Table 2** summarizes recent advances of the applications above, along with the specific ML algorithms (including their structures, activation function, and loss function), data sources/sizes, input variables (if involved), prediction performance and contributions, possible research gaps and future remarks.

44
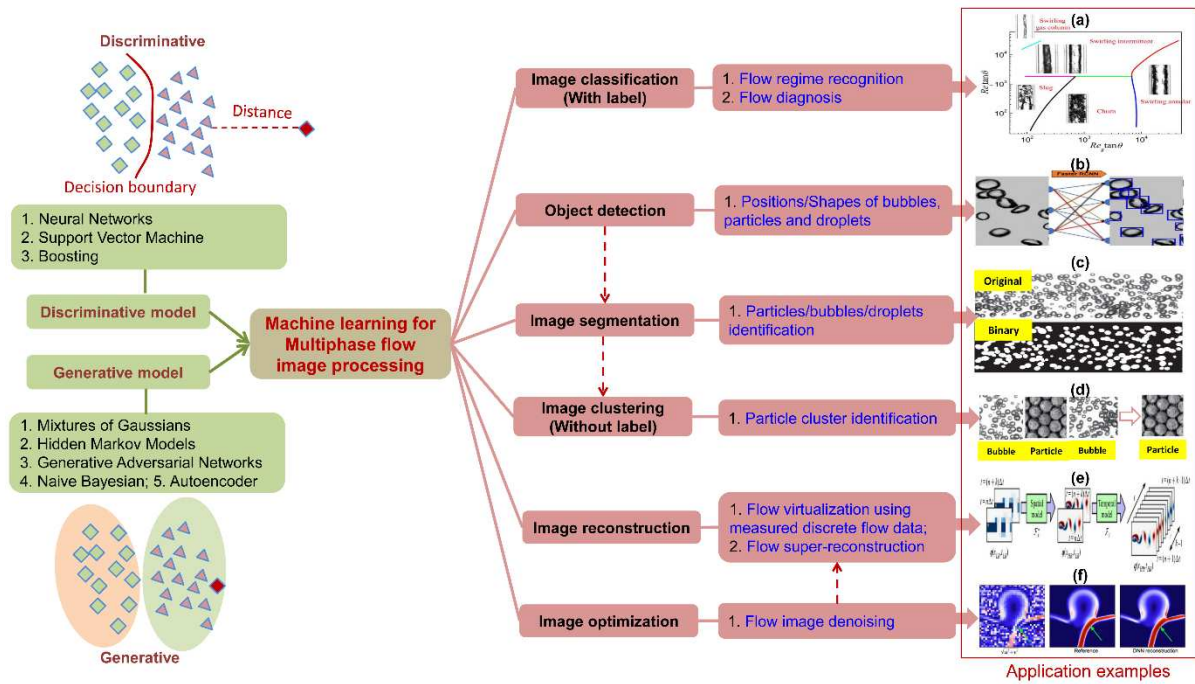
Figure 11 Applications of machine learning or deep learning for multiphase flow data and image processing. The origin of flow images on the right side of the figure were described below: (a) Adapted with permission from ref 144. Copyright 2019 Elsevier. (b) Adapted with permission from ref 145. Copyright 2020 Elsevier. (c) Adapted with permission from ref 146. Copyright 2021 Elsevier. (d) Adapted with permission from ref 147. Copyright 2019 John Wiley and Sons. (e) Adapted with permission from ref 148. Copyright 2021 Cambridge University Press. (f) Adapted with permission from ref 142. Copyright 2020 Elsevier.

Table 2. Recent advances of ML applications for targeting multiphase flow and transport fields.

Topics	ML algorithms; architecture, activation, loss functions, optimizer	Data sources and feature inputs	Research performance and contributions	Research gaps and future remarks
➤ **Bubble detection and shape reconstruction**[145]	➤ **CNN**: Final fully connected layers with 50 neurons, Max pooling layer with 2 pool size, 0.01 learning rate; MSE, MAE	➤ Experiment: High speed camera; One image with ~200 bubbles; Image input with a size of 64*64*1 pixel	➤ MRE=0.151; Locating bubbles via a faster region-based CNN detector; Estimating bubble shape parameters by a shape regression CNN;	➤ Not reasonable to assume bubbles with ellipsoidal shapes and not valid in bubbly flows with high Reynolds numbers and Eotvos; Probably necessary to operate and train ML in an opensource platform.
✧ **Reconstruction of flow fields**[149]	✧ **PINN**: 10 hidden layers with 50 in each one; Adam 0.001 learning rate; Swish;	✧ Experiment, DNS; 10000 per iteration; C(t, x, y)	✧ High accuracy: Real error=6.59~6.84%; Virtualizations of flow fields by encoding the N-S equations into the NN; Very applicable for the	✧ Extend to apply the PINN model for non-Newtonian and compressible flows, pr other flow cases; Try to learn the constitutive law from the flow images.

			flows with complex geometries and initial/boundary conditions.	
➢ **Recognition of gas-liquid-solid flow regimes**[150]	➢ **CNN**: 5 convolution and maxpooling layers; 0.005 learning rate; ReLU	➢ Experiment; 2,500 images for each condition; 349 training images in each model and 1 for testing; Binary image inputs	➢ High accuracy: MRE=4.6%; Successfully identifying transitions of trickle-to-pulse and bubble-to-pulse flows;	➢ Need of extending to flows with higher superficial fluid inlet velocity; Further consideration of speedup procedures for flow image sampling.
✧ **Recognition of liquid-liquid flow patterns**[151]	✧ **CNN**: 5 convolution and maxpooling layers; Adam; Softmax; Categorical crossentropy	✧ Experiment: high-speed camera; 32383 images (7:2:1); 3D array with 150pixels ×450pixels ×3 channels	✧ R^2=0.986~0.998 vs. traditional correlation R^2=0.491; Able to recognize flow patterns under extensive conditions in microchannels; High-throughput automatic experimentation platform via the proposed model.	✧ Need to include time-sequence factors; High computation and memory cost due to a large amount of images involved; Necessary to include flow physics into the network.
➢ **Identification of importance of gas-particle flow field parameters**[152]	➢ **SOM**: 100 neurons (i.e., 10 neurons by 10 neuron 2D map)	➢ Experiment; 1188 data sets; SOM: Cluster appearance probability, duration and frequency	➢ SOM: Easier interpretation of the relationships in clustering riser flows by reducing the data dimensionality; RF: Flexible to determine the variable importance.	➢ Need to render input variables in a dimensionless form to have more theoretical universality and less model complexity; SOM: Lack of guidance to what underlies the two data assemblies identified.
✧ **Identification of cluster characteristics in gas-particle flows**[153]	✧ **K-means**: K=3	✧ Experiment: high speed camera; >500 images for each condition; Image inputs	✧ Demonstrating the reliability of K-means used for extracting clustering features; Revealing a novel strategy for studying complex clustering phenomena.	✧ Need to include the difference of the computational time between the conventional image processing and K-means methods.
➢ **Prediction of local mass flux in riser flows**[154]	➢ **RF**; **BPNN**: 1 hidden layer with 300 neurons	➢ Experiment; 1320 data sets; BPNN: d_{ave}, ρ_s, r/R, h/H, Us, Gs;	➢ Good accuracy: BPNN: R^2=0.9, NRMSE<0.04 for predictions of local mass flux; RF: Determination of the relative importance of variables.	➢ Need to nondimensionalize the input features; Further validation of the model is necessary.
✧ **Prediction of minimum fluidization velocity**[155]	✧ **BPNN**: 1 hidden layer with 16 neurons; ReLU	✧ Experiment: ~40 000 papers (70:30); d_p, ρ_s, ρ_g, μ_g, φ_g, ψ_p	✧ High accuracy: RMSE=9.144%, MAE=2.357%, R^2=0.918 vs. the empirical correlations; Revealing the possibility to construct a big database using a novel technique of text mining, which provides a new effective and efficient way	✧ Need to quantify potential uncertainties in the process of text mining; May need to consider the system errors due to different experimental detection techniques applied; May still contain wrong information extracted from papers

			for calculating fundamental fluidization parameters.	due to format issues.
➢ Optimization of cyclone separator performance [156,157]	➢ **Hybrid: GA-RBFNN:** 1 hidden layer with 98 neurons; MSE	➢ Experiment: 98 samples, LES-DPM: 25 data sets; Experiment: E_u, ρ_g, V_{in}; LES: x_1, x_2, E_u, S_{tk50}	➢ High accuracy: MSE= 1.31e-4 ~5.84e-4, R^2=0.9967~0.9996; An effective strategy to establish the predictive model of pressure drop for optimizing cyclone separator performance.	➢ Possible overfitting for RBFNN due to the limited number of data; The datasets should cover a wider range of operating conditions; Further conducting study of robust parametric design to probe the uncertainty in the optimization operation and geometrical factors.
✧ Optimization and control of reactor performance [158]	✧ **Hybrid: GA-BPNN:** 3 hidden layers with 15, 41, 20 neurons; SELU, ReLU, ReLU for three hidden layers; MSE; Adam.	✧ CFD: 56 data sets (8:1:2); T_i, G_g, Y_i	✧ High accuracy: MRE=98.8%, R^2= 0.9898; Successful development of a integrated CFD-BPNN-GA for both predictions and optimization control of reactor performance.	✧ Dataset generation efficiency is low and may be accelerated by ML; Automatic optimization of hyperparameters using ML instead of manually tunning; Possible overfitting due to the limited amount of data.

Note: The critical comments above may not be adequate and we present the suggestions with the hope that readers and newcomers could obtain some possible inspirations or thoughts from this table.

2.2.1 Flow and transport field reconstruction

The key to image reconstruction is determined by the precision and speed of the image reconstruction algorithms[159] but it is a complex, nonlinear, ill-conditioned and under-determined problem. To date, multifarious traditional algorithms (e.g., sensitivity/Jacobian matrix and gradient estimation approaches) for flow image reconstruction have been proposed and have made great contributions to measurements of practical multiphase flow systems. One limitation for these traditional algorithms is that the image processing steps and outline segmentation algorithms are critically dependent on the user-defined parameters, requiring to be tuned by trial-and-error for varied operating conditions and multiphase device structures[146,160]. Other possible challenges include the hard-to-capture flow physics in a high-frequency range, low sampling frequency, and relatively low spatial resolution and accuracy in the reconstructed images. Due to the

exceeding desirability to image reconstruction with high speed and precision, researchers have applied ML methods for processing fluid or particle flow images from the data measured by different experimental measurement methods, as summarized in **Table S3**. The existing reconstruction methods based on ML or DL may be divided into several categories:

(1) Data-driven reconstruction approach using experimental data. For instance, some early contributions[133,161] used nonlinear ANN techniques to reconstruct ECT images of flow fields. Fan and coworkers[133,162,163] systematically studied the ANN-based nonlinear techniques for image reconstruction of two-phase and three-phase flows using ECT. They combined the multilayer feedforward ANN with the analogue Hopfield network to train a set of ECT data based on a regularized back-propagation algorithm. Comparison with the other commonly-used iterative techniques, the developed method significantly improved the accuracy and consistency, and showed superior stability of reconstructed images. Yadav et al.[164] applied different ML algorithms including ANN, Support vector regression (SVR), and relevance vector regression (RVR) for fast reconstruction of gas-liquid flow images based on the data detected by radioactive particle tracking (RPT). It was found that SVR performs best in the position reconstruction accuracy for all cases while RVR reconstruction speed outperforms SVR considerably due to the sparser nature of RVR. Except for these ML methods, researchers applied an encoder-decoder CNN to estimate the next-frame solid holdup pattern based on learning the first several frames as an input in a gas-particle fluidized bed[165]. However, a possible challenge for this encoder-decoder DL is that the encoder must compress all input information into a fixed-length vector, and then pass it to the decoder. Compressing long and detailed input sequences with a fixed-length vector may lead to

information loss. This possible limitation is suggested to be mitigated by allowing the decoder to access the entire encoded input sequences via further assessments and investigations. Moreover, RNN methods[166,167] such as LSTM and gated recurrent units (GRU) have also been applied for processing sequence-to-sequence flow images due to the inconvenience of ANN for this kind of problems. However, the methods like LSTM and GRU to process flow images have two evident limitations: First, it assumes that the image data used for training LSTM is sequence-related. As a consequence, it is not easy for LSTM to use time-series image data that is not completely formed according to step-by-step time variations. Second, when the sequence length exceeds a certain limit (e.g., >1000), one will suffer from the low training efficiency and the gradient will still disappear. Overall, this kind of method directly establishes the mapping relationship between the under-sampled data input and the output, and can directly obtain reconstructed images with a quality potentially more accurate and efficient than the traditional algorithms. However, they share one universal disadvantage of relatively poor interpretability that the pure ML or DL methods have. The other possible drawbacks for DL (especially CNN algorithm) processing of complex flow images may include: (i) the increase of network layers is generally accompanied by the dramatically increasing consumption of computing resources, as well as (ii) the challenging problems of overfitting, gradient disappearance or explosion.

(2) Knowledge-informed reconstruction approach using experimental data. Such kind of research efforts mainly attempted to re-design the NN architecture by coupling the image processing domain expertise[168], the physical meanings associated with reconstruction algorithms of multiphase flow images[169,170], another type of physics-aware understanding[171]

or even a concept of 'human attention'[172]. This can contribute to the remarkable improvement in the quality of image reconstruction such as reduction of the deformations and reconstruction artifacts. Notably, a new deep residual neural networks, i.e., ResNet[171] was proposed to substantially improve the performance of CNN and is much easier to train very deep neural networks without degradation by residual learning. Recently, researchers tried to apply this new method for modeling the evolution of dynamical multiphase flow systems[173]. Another typical example[174] is to develop CNN-based DL methods for reconstructing flow images of ECT measurement data where the inaccurate capacitance property is considered. In order to enhance the solution stability and reconstruction quality, the authors used a combination estimation approach and an improved stabilizing item, and proposed a new cost function to reduce the reconstruction artifacts and deformations. Besides, there are other advanced experimental techniques such as MRI, which has not yet gained enough efforts in applications of ML or DL to facilitate MRI image reconstruction[175,176].

(3) **ML-based super-reconstruction approach using simulation data.** Recently, another particular interest for fluid flows is to utilize ML, especially DL, to reconstruct the high-resolution flow images from low-resolution flow images and this process is called super-reconstruction[177]. Fukami et al.[148] proposed a novel data reconstruction approach using a supervised DL technique. The authors utilized a CNN-based down-sampled skip-connection/multiscale model and the multiscale characteristics of turbulent flows were integrated into its network structure. They presented that the CNN-based approach can recover the flow fields using a small number of training data for spatiotemporal models. However, paired data for training are required for supervised techniques for super-resolution

recovery of fluid flows. Different from the above method, Kim et al.[178] developed an unsupervised ML methodology that employed a cycle-consistent generative adversarial network (GAN) capable of being trained by unpaired flow data for super-resolution reconstruction, as shown in **Figure 12**. It was revealed that the unsupervised GAN for learning flow data could be feasible for applying to the super-resolution reconstruction over a wide range of turbulent flows. Meanwhile, some scientists have employed DL methods to reconstruct the temperature fields in both microfluid[179] and nanofluid[180] heat transfer problems. In particular, Kong et al.[179] extended the CNN strategy to target the super-resolution reconstruction of temperature fields using the data from low-resolution coarse temperature fields. The authors proved that the two CNN approaches investigated is capable of significantly boosting the reconstruction accuracy while the novel multiple path super-resolution CNN gives a superior reconstruction performance as compared with the classical CNN. More recently, Mikhaylov et al.[181] reconstructed the temporal evolution of large-scale flow structures in a stirred tank using the data from DNS. The proper orthogonal decomposition (POD) aided reduced-order modeling was applied for extraction of the dominant modes and their temporal coefficients. The system identification was used to establish an estimator for capturing the relationship between the velocity signal inputs and POD coefficient output. It was revealed that the constructed estimator is applicable to operating conditions that were not used in the process of its construction. This work represents a recent popular trend that uses hybrid DL methods to reduce the network architecture complexity and also boost the model universality for a wide range of flow cases.
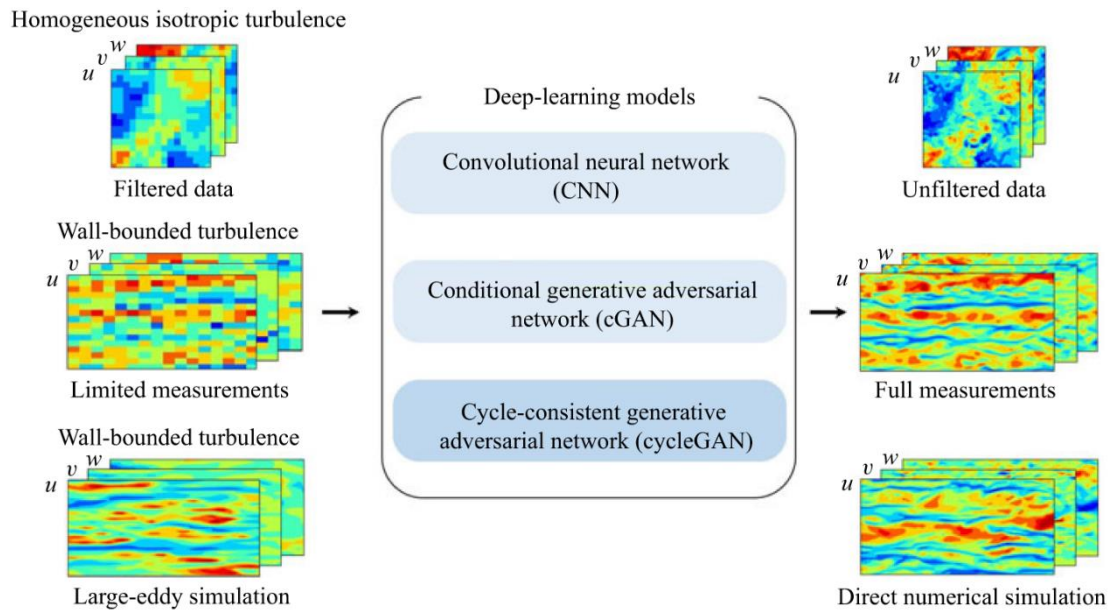
Figure 12 Unsupervised DL for super-resolution reconstruction of several typical flow turbulence images. Adapted with permission from ref 178. Copyright 2021 Cambridge University Press.

2.2.2 Flow regime identification and bubble/particle detection

Detailed knowledge about identification of multiphase flow patterns/regimes and particle/bubble detection is of key importance to rational design and control of multiphase devices (e.g., fluidized bed reactors, bubble columns and microreactors), and the improvement of product quality and process efficiency. Although considerable progress using the existing traditional methods has been made in identifying multiphase flow patterns, they appear to have inadaptability, and are practically difficult to provide reliable identification in the case that multi-variables need to be accounted for. The identification workflow is strongly dependent on operating conditions, and few general process procedures have been proposed. To solve the problems above, ML is becoming a popular tool in assisting with flow regime identification and cluster/bubble/droplet detection.

(1) Gas-liquid flow regime identification. Pioneering studies[135,182-185] mainly applied SVM and ANN to recognize the transition region between the gas-liquid two-phase flow

regimes in bubble columns or tubes. Ishii and coworkers[182,183] applied supervised self-organizing NN methods to categorize gas-liquid flow regimes using the data generated by measuring impedance or simulations. Identification results conclusively demonstrated that NN can appropriately classify up-flow patterns and the databases from both numerical simulations and experiments have reliability. Liu and Bai[144] developed a novel methodology by integrating the use of a self-organizing NN and an image processing method to identify the swirling gas-liquid flow regime. The swirling flow pattern was then mapped and a comparison between the swirling and non-swirling regime maps was revealed. Quintino et al.[186] used RF and ANN models to identify the transition of gas-liquid flow regimes based on the database from both experiments and physical models. The trained hybrid model even with a relatively small dataset could improve prediction accuracy and the graphical comparison of transition boundaries presented a better understanding of the model performance than the conventional metrics. However, a possible problem among most of the above studies is that the output is usually related to many variables which can be selected as feature inputs but this will increase the input space complexity. So, PCA can be used to extract the feature vector that still well represents the feature space for identifying various flow regimes[187-189]. Recently, researchers also used RNN approaches such as LSTM to predict the time-series chaotic dynamics and forecast two-phase flow regimes[190]. More recent investigations were extended to develop a novel DL method aided by an image segmentation technique for identification of thermally gas-liquid two-phase flow regimes including annular/semi-annular, elongated plug, slug-plug and bubbly flows[191]. To sum up, a major drawback is that most researchers have trained a pure ML model based on relatively limited experimental datasets, which leads to a

risk of overfitting and thus reduces the model generalization capability. On the one hand, it could be an effective solution to establish a vast databasing for flow images and some recent works have present an excellent example of how to improve this kind of weakness in identification of condensing two-phase flow patterns using CNN[192]. On the other hand, this common limitation for pure ML models may be fixed by embedding the prior identification knowledge, physics or constraints of flow regime identification into the ML structure, as we have emphasized in previous sections. Therefore, more future efforts should be devoted to physics-informed or physics-constrained ML identification of multiphase flow regimes.

(2) Gas-solid and gas-liquid-solid flow regime identification. Compared with lots of efforts to ML-aided recognition of gas-liquid flow regimes, few references on ML-assisted identification of gas-solid and gas-liquid-solid flow regimes could be of guidance to provide available information. The existing studies mainly applied SVM and NN methods to recognize the gas-solid flow regimes based on some typical characteristic parameters, e.g., the cepstral coefficients[193,194], pressure drops[195], solid hold-up[196], superficial velocities[197], and recurrence rate[198]. One problem encountered is that feature selection has not been approached and tested in these studies. Commonly, ML's capability of accurate identification of flow regimes is closely associated with the feature selection that can leads to reducing the feature space dimensionality and improving the prediction accuracy. It is henceforth suggested to perform a comprehensive feature selection task for gas-solid flow regime recognition problems. For gas-liquid-solid trickle bed and fluidized bed reactors, the initial efforts involving ML-based flow regime identification is available[199]. Recently, Wang et al.[147] proposed a general workflow of the CNN-assisted image analysis approach for recognizing

the trickle-to-pulse and bubble-to-pulse flow transitions in a conventional gas-liquid-solid trickle bed reactor, including four steps, as illustrated in **Figure 13**. Their study showed a 4.6% MRE between the manually segmented liquid fraction and the identified liquid fraction, indicating the high recognition performance of the proposed method. One important point is that their method was established based on relatively low superficial fluid inlet velocity, which may limit its applicability to a wide range of flow conditions. Besides, it is suggested to apply ML procedures to accelerate flow image sampling with much higher processing efficiency than the traditional methods.

In addition, recent studies have paid attention to the other flow patterns such as liquid-liquid flows in microreactors. Shen et al.[151] built a CNN-assisted platform with the expert-level capability of automatic recognition of liquid-liquid flow patterns. Their study showed the generalized liquid–liquid flow pattern map in microchannels and the comparison of the predicted slug flow patterns between CNN and conventional models, R^2=0.986~0.998 vs. traditional correlation R^2=0.491. This work perfectly demonstrates the applicability of ML on microreactor technology and is beneficial for circumventing the difficulties in labor-intensive investigations of hydrodynamics. However, their platform did not include the time-sequence factors, that is, it's unable to timely handle a developing flow pattern changing due to time varying. Thus, future attention may be paid to including flow physics into the network or directly using the DL mode with the ability to process sequential data.
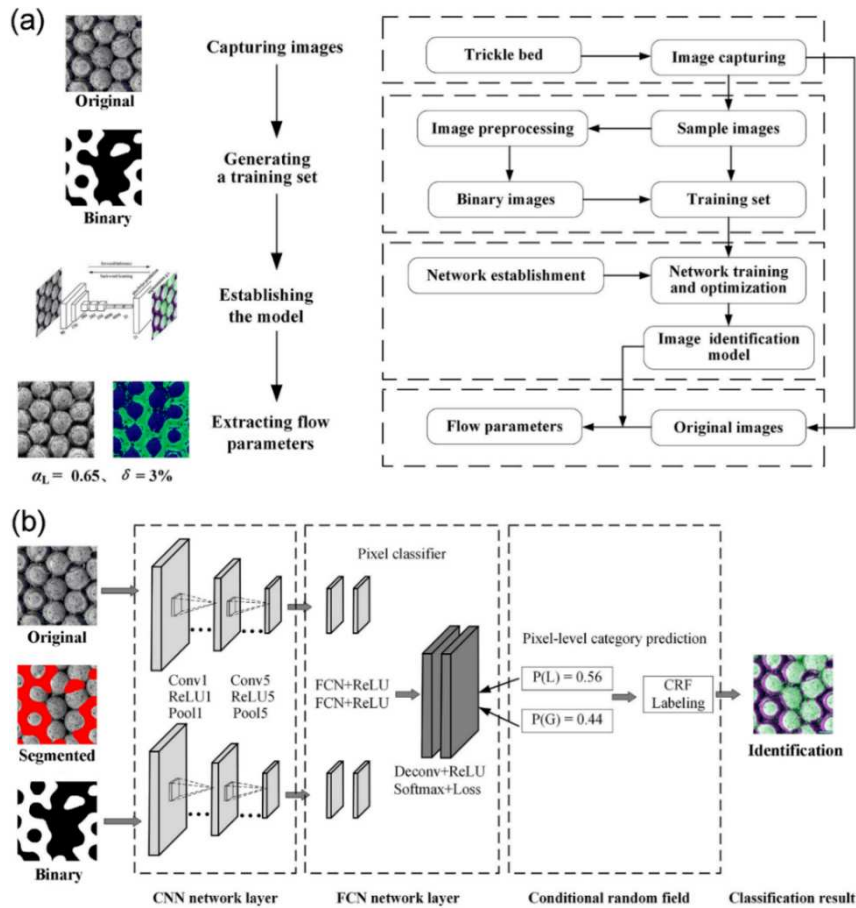
Figure 13 Machine learning for gas-liquid-solid trickle bed reactors: (a) Flowchart of the processing procedure of the deep learning-assisted image analysis method; (b) The architecture of fully convolutional networks (FCN). Adapted with permission from ref 147. Copyright 2019 John Wiley and Sons.

(3) Particle/bubble detection. In the literature, the ML algorithms, especially CNN, have also been increasingly applied for detection of characteristics of bubbles, clusters and droplets from experimental flow images. The interesting characteristics include their location, shape, diameters and velocities[200,201]. For example, Poletaev et al.[200] proposed a ready-to-utilize CNN powered software for bubble detection in gas-liquid two-phase flows. The performance comparison indicated that the average processing time of experimental images using CNN on a single CPU core is about 6 to 8 times faster than the conventional correlation algorithm. Notably, the CNN was deployed on a CPU and a GPU while the conventional method was executed on a single CPU. Moreover, half the bubbles within the whole probable range of bubble sizes were identified by the conventional correlation method,

which were much less than the NN. However, both methods predicted a very close mean bubble diameter with a ~11% difference. Haas et al.[145] developed a region-based BubCNN workflow used for faster detection of bubble location and shape from the gas-liquid flow images detected by HSC. Note that the BubCNN contained two modules: a rapid region-based CNN for recognition of bubbles and a shape regression CNN for reconstruction of the bubble shapes through ellipses. However, it may not be valid to assume bubbles with ellipsoidal shapes in bubbly flows with high Reynolds numbers and Eotvos, where bubble shapes are more complex and irregular. Therefore, it's suggested that the BubCNN could be further extended to more flow conditions to enhance its case-specific applicability. Moreover, it's probably necessary to operate and train BubCNN in an open-source platform in order to make it more flexible and easier to be integrated with other platforms or numerical solvers. Meanwhile, some researchers not only detect the bubbles but also further developed the 'mask' extraction tool to reconstruct the bubble pattern[140,202]. For the disk-type bubbles classified with an eccentricity of less than 0.46, it was suggested to segment them along with the path parallel to the bubble macro-axes. on contrary, segmenting bubbles along with the path perpendicular to their macro-axes was recommended for the ellipsoidal or spherical bubbles with an eccentricity of larger than 0.46. To be easier and more flexible for users, some tools modules like a fuzzy inference system have been thereby developed for bubble mask extraction with a friendly graphic user interface[203]. In addition to bubble detection above, another increasingly popular trend is to detect particle and droplet characteristics by ML[204,245]. Li et al. investigated the non-spherical biomass particles and spherical polyethylene particles in a lab-scale fluidized bed using PIV and PTV techniques[205]. The ML

pixel-wise classification methodology was trained and used to acquire particle masks for PIV and PTV processing. Recently, using a K-means algorithm with optimal hyperparameters, FCC particle clusters were identified from flow field images of the gas-solid CFB riser and downer[153]. The authors successfully revealed the reliability of K-means used for recognition of the challenging particle clustering phenomena. However, their model only considered the particle cluster characteristics over a fast flow condition while it did not further test the model performance for the bubbling and turbulent flow conditions. That is, the cluster identification model may not be generalizable out of the span where the model was trained. At least, the optimal hyperparameter valid at the fast flows probably need to be optimized again for the other conditions that the model has not covered. The consideration above demands further efforts to systematically assess the generalization performance of the ML model in the future.

Before closing our discussion in this part, several suggestions are summarized here for future efforts to probably promote the development of flow pattern identification. First, it is important to embed the prior knowledge, physics or constraints of flow properties into the ML structure, especially for the case with very limited experimental datasets. This will make the developed identification model more generalizable and significantly improve the recognition and detection reliability. Second, it is suggested to apply ML procedures to accelerate on-line flow image sampling and thus to boost flow identification and detection efficiency. We also suggest to operate and train the recognition and detection models based on open-source ML platforms in order to make these models more flexible and easier to be coupled with the other platforms or numerical solvers. In addition, it is considered that the ML model should be trained under a wide range of operating conditions as far as possible and

highly-resolved simulations could be performed to circumvent the difficulty in the labor-intensive and high-cost experiments.

2.2.3 Flow and transport field parameter prediction

Persistent lack of physical comprehension continuously stymies preferable prediction performance of the key parameters in multiphase flow and reactor systems although scientists have made systematic contributions to experimentally-formulated correlations throughout the past decades[206-208]. The correlations of the key parameters in multiphase units are commonly expressed by gas/liquid/solid phase properties, operating conditions (e.g., phase concentration, velocity, and temperature), devices configurations (e.g., height and diameter), or a combination of them in dimensionless forms like Archimedes, Froude, Nusselt, Reynolds, Sherwood, and Weber numbers. However, the prediction discrepancies between the existing empirical correlations of key parameters such as the particle entrainment and minimum fluidization velocity in gas-particle riser flows can reach several orders of magnitude[209,210]. Fortunately, the advanced research and development of flexible ML tools have a potential to complement the incomplete knowledge to boost the prediction ability of key multiphase field parameters, such as mass flow rate/flux[211-214], minimum fluidization velocity[155,215], mixing rate/index[216,217], overall/local hold-up[218-224], pressure/pressure drop[225-230], velocity[119,231-233], temperature[234-236], and other parameters[237-239] in multiphase/particulate flows and reactors. Note that interested readers may be referred to a relatively comprehensive list of the existing literature summarized in **Table S4**.

Joshi and coworkers[114,240-242] performed systematic studies of developing SVR-assisted correlations to predict the overall/local gas hold-up and effective interfacial area in gas-liquid

bubble column reactors. Their investigations showed that it is potential to apply SVR for online prediction and monitoring of the local parameters in bubble columns reactors. Shaban and Tavoularis[211] leveraged multi-layer back-propagation ANN technique to estimate the flow rates of liquid and gas phases in two-phase bubbly flows. The authors revealed that a PCA of feature components contributes to a reduction of input dimensions. It was also found that the prediction performance of their approach outperforms that of the previously reported approaches over various flow regimes and conditions investigated in their work. Khare and coworkers[119,243] employed a Gaussian process-assisted method to build a data-driven surrogate model trained by the data from highly-resolved simulations (i.e., DNS-VOF and E-L based LES) of liquid jet injection in turbulent gas crossflow. They presented a detailed prediction study of flow field parameters including the evaporated liquid vapor fraction, temperature, pressure, velocity, and spray penetration and Sauter mean diameters in the liquid phase with reasonable accuracy (ranging from 0.05 to 13.5%). Chew and coworkers[152,154,206,213,244,245] directed efforts towards a deep understanding and an enhanced prediction of fast gas-particle riser flow characteristics assisted by several common ML methods including ANN, RF, and self-organizing map (SOM). In their essential study on the determination of the relative dominance of the riser flow parameters, it was suggested that the radial position is of key importance to the local solids flux and elutriation, and the overall solids flux has the most dominant effect on the local solids hold-up. It was also revealed that the formation of clusters in the monodisperse gas-particle flow system is much more pronounced than that of polydisperse ones, indicating that particle polydispersity hinders the cluster formation and is thereby beneficial for homogeneous particle distributions. Further

possible improvement may need to render the feature input variables in a dimensionless form to make their method have more universality and less complexity. Yang and coworkers[239,246] combined an SVM-based data-driven method and DEM modeling to predict key granular flow parameters such as the angle of repose and collision energy in a rotating drum. Zhong et al.[247] proposed an improved strategy beneficial for finding the optimal ANN to significantly enhance predictions of the particle phase fraction distributions in gas-particle CFB risers. This work provides a possibility to reduce experimental workload (up to 1/3 experimental sets) and hence is of practical meaning to experiments, especially for large-scale reactors.
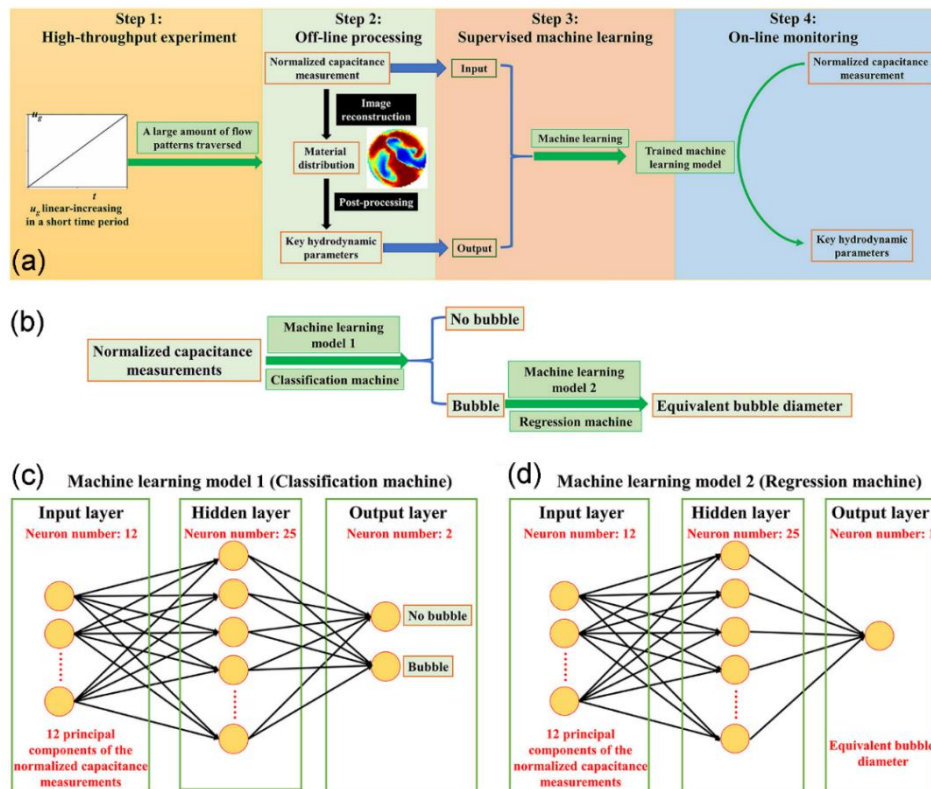
Figure 14 Machine learning for bubbling gas-solid fluidized bed reactors: (a) Flowchart of the ML applied for predictions of key hydrodynamic parameters using the ECT measurement data; (b) An example: Steps for predicting of the bubble diameter using two ML methods; Feedforward network structure of the classification machine (c) and (d) regression machine. Adapted with permission from ref 196. Copyright 2019 John Wiley and Sons.

As shown in **Figure 14**, Guo et al.[196] presented a flowchart of the supervised ML and applied it for mapping the high-throughput ECT measurement data to key hydrodynamic

parameters in a bubbling gas-particle fluidized bed reactor. The trained model was able to directly predict the key parameters from the on-line normalized capacitance measurement. More recently, Li et al.[248] proposed a new high-precision real-time model for predictions of the void fraction in gas-liquid two-phase flow based on ensemble learning. The model integrated the XGBoost with an empirical modal decomposition approach and a kernel ridge regression. The lasso regression method was used to further assess the prediction performance of XGBoost. The integrated model not only had good prediction accuracy, but also was able to eliminate abnormal data without losing the feature information of the original dataset, superior for online control of gas-liquid flow parameters. Zhou et al.[155] proposed a novel text mining method to construct a database by extraction of experimental data of minimum fluidization velocity (U_{mf}) from open reports. In particular, a pipeline of natural language processing was applied for identification and extraction of the parameters associated with prediction performance of U_{mf} with 83% precision from $\sim 4 \times 10^4$ papers. Their promising ML-aided data-driven approach was demonstrated to outperform the existing empirical correlations over a wide variety of fluidization systems. It is noteworthy that, first, there may be a risk that the extraction decisions made by text mining are not always correct and interpretable. Once the text mining algorithm gives unreasonable results, it can be difficult to recognize and repair the problem in the later stage. Second, the fluidized bed device factors such as the effects of bed size and bed internals are not considered as the feature inputs and the feature inputs are not nondimensional. These will probably limit the universality of ML-aided estimation of minimum fluidization velocity. Third, there is a requirement to quantify the potential uncertainties in the process of text mining. Another

possible uncertainty is the system error due to the historically measured data from different experimental detection techniques.

Here, we further provide some summary discussion regarding the studies surveyed in this section. **(1)** From a perspective of data source for all of Sections 2.2.1-2.2.3. It can be readily found that most often only very limited experimental data points were used for training although some authors have tried to collect data from various open reports. It was also suggested that integration of the traditional physical model with ML algorithms into an aggregation function model can work by the core of ensemble methods[249]. This is because reasonable predations can be achieved by traditional models even in the case of only a few data points available. In fact, it is a concept of physics-informed ML modeling. **(2)** From a perspective of ML algorithms used. The ANN, SVM and tree models are mostly used to predict the key flow parameters in these studies (including **Table 1**), probably due to their simplicity and high accuracy in the investigated span, especially compared with other complex DL methods. Moreover, Python programming language and Matlab software are most often used by researchers and some secondary-development ML tools are based on them. **(3)** From a perspective of feature inputs for all of Sections 2.2.1-2.2.3. One may have a major concern that lots of researchers have directly used the common flow variables as feature inputs to predict the output, instead of the nondimensionalized form of the input variables. The advantage is that it may be very easy to select the most commonly used flow variables or geometric factors as the inputs. The main disadvantage is that too many inputs will increase the model complexity and thereby slow the learning operation. To reduce input complexity such as dimensionality reduction[250], one can implement the relative importance analysis using

the decision tree model or the PCA method. However, sometimes the search space can be very large in order to obtain an optimal input solution. In this situation, one can select techniques to overcome this drawback such as greedy search, particle swarm optimization or genetic algorithm (GA) to optimize the feature inputs[251].

2.2.4 Flow and transport field parameter optimization

In the literature, ML has played a vital role in chemical process systems engineering (PSE) design, optimization and control, which was well reviewed and extensively studied by many researchers[252-254]. In this section, we will mainly focus on how to apply ML techniques to combine with the field data of flow and transport for multiphase device performance optimization. This aspect has received relatively little attention, compared with the topic in PSE. Commonly, there are two general frameworks for optimizing the physical performance of flow devices, namely, single-objective optimization and multi-objective optimization.

(1) Single-objective optimization. It aims to either maximize or minimize an objective function. Early contributions[255] were focused on the development of flow models and optimization techniques, and then applied the developed model as an efficient and effective enabler for elucidating the governing flow phenomena such as turbulence control mechanisms. Based on this, high-performance devices could be thereby devised for significant drag reduction. Recently, Zhang and Li[256] reported an ANN-assisted method for control of the local non-fluidic solid phase flow pattern by learning the relationship between the inlet flow rate and recirculation zone. The trained ANN was then used to optimize the input energy consumption to fit a continuous multiphase flow process over the long term. Nikita et al.[257] proposed a novel reinforcement learning-based method for optimization of the

process flowrate in order to reach the maximum yield for continuous processing of

biopharmaceuticals. Overall, most of the above studies mainly applied the pure ML models to

optimize a single parameter of flow and transport processes while most often the

maximization of multiphase flow and device performance needs to optimize multiple

parameters simultaneously.
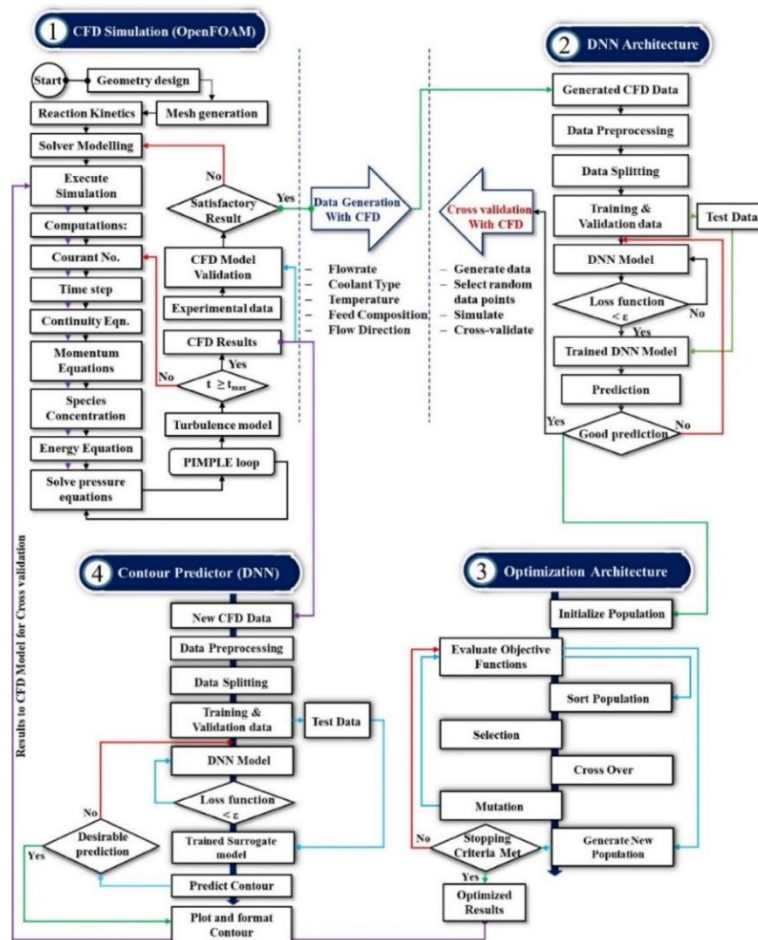
Figure 15 A unified CFD-DNN-GA framework for multi-tubular reactor design and optimization. Adapted with permission from ref 158. Copyright 2021 Elsevier.

(2) **Multi-objective optimization.** Multi-objective optimization problems are usually

involved in the design and control of industrial multiphase devices, which aims to

simultaneously optimize multiple objective functions using multi-disciplinary aspects such as

the incorporation of CFD model, the coupling of traditional physical models and sometimes

manufacturing cost constraints. In a multi-objective optimization problem, usually, there are

multiple maximization or minimization objective functions at the same time, which are not independent of each other. There will be some possible conflicts between them, which make them fail to meet all the objective functions simultaneously. One may perform Pareto optimality algorithms to solve this kind of problems. Here, the original meaning of Pareto optimality refers to an ideal state of resource allocation. In multiphase device optimization, we can assume there are three desirable objectives: minimization of pressure drops and particle attrition while maximization of separation efficiency. One may not reach all of the above three objectives but at least make one objective better while does not make the other two objectives worse. For instance, Chen et al.[258] performed well-validated CFD simulations of the continuous flow and temperature profiles of a microchannel within a microwave applicator. They applied a gradient boost regression tree model to study the correlation between the parameters. The application of the proposed model for optimization of the dimensions and operating conditions showed a trade-off between the outlet temperature and energy efficiency (i.e., a Pareto optimal). Hamad et al.[259] reported a novel ML-facilitated multi-objective optimization approach for polymerase chain reaction flow systems. The data from CFD simulations of a prototype three-zone thermal flow was used to train a fully-connected NN for later creation of Pareto curves that could show the trade-off between the temperature uniformity and pressure/heating costs. The trained model was applicable for efficient evaluation of the effect of geometrical configurations and flow conditions on the pressure drop, temperature field uniformity, and heating power requirements, useful to achieve an optimal thermal flow system.

Recently, researchers[260] proposed to train an ANN-based predictive controller and then integrated it with a fixed-bed catalytic reactor model using the data from CFD simulations., which could safely operate the reactor with output tracking. Such a kind of reactor model was also used to maximize the operating profit and calculation of the best set-points for controlling a continuous stirred tank reactor[261]. More recently, there is a growing tendency to use deep learning methods combined with optimization algorithms for multiphase reactor performance optimization. Gbadago et al.[158] proposed a novel integrated framework for flow and transport modeling, data analysis, and optimization of reactor systems utilizing CFD, DNN, and GA (**Figure 15**). The optimization results outperformed those of other traditional methods while the optimization speed was remarkably boosted. Despite its evident potential, herein we provide several possible considerations of this work. First, the dataset generation efficiency seems very low and only a limited data is available, which is critically dependent on the computation speed of the CFD simulation. Therefore, further development of acceleration strategy of CFD by ML or hardware is suggested. Second, the proposed framework is relatively complex since it consists of four modules including two DNN models, which may hinder its flexibility and applicability for users. Besides, automatic optimization of hyperparameters using ML (e.g., Bayesian optimization, particle swarm optimization, or GA), instead of manually tunning hyperparameters, deserves more attention in future work.

In the literature, it is an active area where researchers have significantly contributed to the combination of CFD and ML for multi-objective optimization of cyclone separator performance, as summarized in **Table S5**. For instance, Elsayed and coworkers[156,157,262-264] performed very systematical studies of applications of advanced CFD methods (e.g.,

LES-DPM) and ML techniques (e.g., RBFNN, ANN, and GA, etc.) for design and optimization of gas-solid cyclone separators. The CFD simulation results were used for the construction of the data set. The ML was utilized for training a surrogate model. The multi-objective optimization results revealed the optimal geometric factor and operation condition to maximize the cyclone separator performance. Ye et al.[265] performed VOF-E-E simulations of gas-liquid-solid cyclone separators to generate data sets for ultra-fine particles classification using SVM and RBFNN. The coupled non-dominated sorting genetic algorithm-II (NSGA-II) was applied for the multi-objective optimization to obtain the Pareto front. Deng et al.[266] extended the above methodology to study gas-liquid cyclone separators. Based on the database from E-L simulations of gas-liquid annular flows, they established an SVM-based surrogate model, which was then integrated into the NSGA-II. The integrated model was used to implement the optimization, and the special characteristics of Pareto optimal solutions were probed.

Here, we provide further discussion and analysis regarding the survey above. First, there is a need to conduct the study of robust parametric design to probe the uncertainty in the optimization operation and geometrical factors. Second, **Table S5** shows that most of the studies have been focused on gas-solid flow systems in cyclone separators while the solid-liquid or gas-liquid flows have received very limited attention. Regarding their equal importance in multiphase process engineering applications, future studies of more flow patterns are suggested to be enhanced. Finally, it can be found that there is an increasing trend in rendering the input features in a dimensionless form but the input variables have been most

often nondimensionalized by the device diameter. The other combined characteristic length may be used to replace the device diameter in order to make the model more general.

2.3 Machine learning for reaction kinetics modeling and optimization

Reaction kinetics plays a fundamental role in multiphase reactor engineering because the obtained mechanistic understanding and kinetic models are of useful guidance for estimating and optimizing reaction outcome and reactor performance based on flow, transport and reaction conditions, and thereby achieving rational design and scale-up of reaction processes and reactors. On the other hand, industrial chemical processes such as FCC, polymerization, methane reforming, and coal/biomass pyrolysis/gasification/combustion involve complex reaction networks consisting of hundreds of components and numerous reactions. The considerations above motivated the authors to present this section for highlighting the significance of reaction kinetics modeling and optimization in reactor engineering. It should also be noted that prior Section 2.2.4 is focused much more on optimizing flow and transport conditions to maximizing device performance while current Section 2.3.3 is focused on not only the above conditions but also the reaction-related conditions/properties/factors. Better understanding of selecting suitable flow and transport conditions lays the foundation of kinetics modeling and optimization of reaction conditions and reactor performance. These sections complement and promote each other, and will be of useful guidance for rational design of reaction processes and reactors.

The traditional reaction kinetics modeling considering the transport effect can be described by nonlinear PDE with an example as follows:

$$\frac{\partial(\varepsilon_f \rho_f Y_i)}{\partial t} + \nabla \cdot (\varepsilon_f \rho_f \boldsymbol{v}_f Y_i) = -\nabla \cdot (\varepsilon_f \boldsymbol{J}_{f,i}) + S_i \tag{1}$$

where Y, J and S denote species mass fraction, diffusion flux and kinetic reaction source term, respectively. If one assumes that chemical reactions evolve with time in a spatially homogeneous system, namely, without considering the effect of transport phenomena, then reaction kinetics can then be solved by the ODE, for example:

$$\frac{d(\varepsilon_f \rho_f Y_i)}{dt} = S_i \tag{2}$$

The forward and reverse rate constants of S can be solved by the Arrhenius equation:

$$k_r = k_{0,i}\exp\left(-\frac{E_i}{RT}\right) \tag{3}$$

where k_r, k_0, E, R and T are the rate constant, pre-exponent factor, activation energy, universal constant, and temperature, respectively.

Commonly, the kinetic reaction source term can be mathematically described at different levels: (1) The phenomenological lumped model, which groups the species into lumps and aims to contain the primary characteristics of the observed rates without the chemical details such as the specific structure-property relationships; (2) The elementary step model involving molecules or reaction intermediates with detailed kinetic mechanisms. The lumped reaction models can be obtained by experiments while the detailed kinetic mechanisms can be obtained by the first-principles theory (e.g., the molecular dynamics (MD) simulations and density functional theory (DFT)) or kinetic Monte Carlo (kMC). Note that many of the kinetic models have been developed without considering the effect of transport phenomena. This problem may be addressed by coupling the obtained description of the reaction source term with CFD simulations of reactive flows. The fact is that the computational speed of the lumped models coupled with CFD can be relatively fast but this will lead to loss of accuracy. Meanwhile, the kinetics with the detailed kinetic model (DKM) in CFD simulations of

reactive flows enable high accuracy while computation cost will arise due to the requirement of solving hundreds of PDEs of reaction kinetics for each time step in every grid cell in CFD simulations.
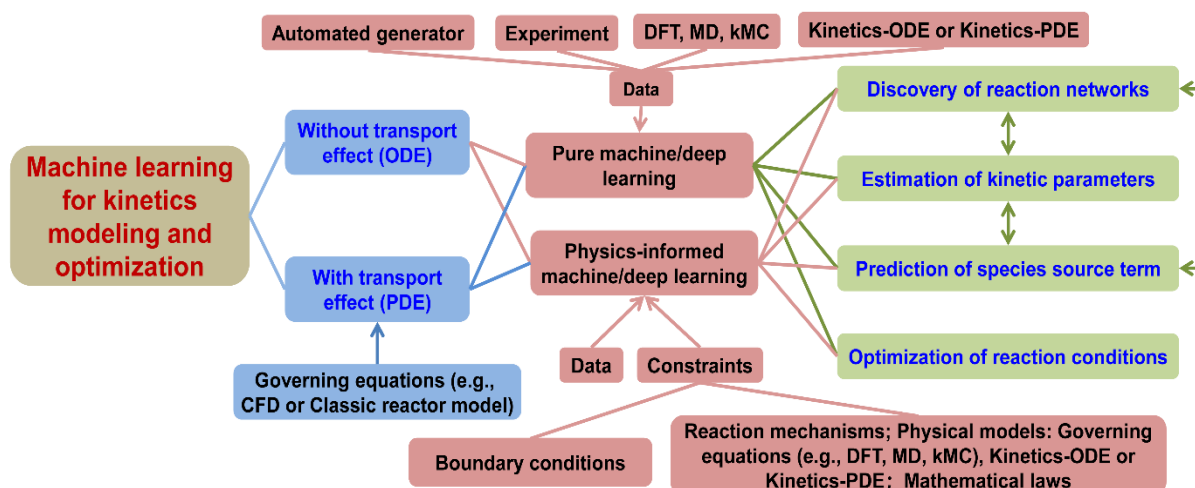
Figure 16 Applications of pure ML/DL or physics-informed ML/DL for kinetics modeling with and without transport effect.

To this end, there is an increasing tendency to use pure ML/DL or to combine ML/DL with the traditional physical models (e.g., CFD, pure kinetics-PDE/ODE, kMC, MD, DFT and lumped kinetics models, or other kinds of prior knowledge) for reaction kinetic modeling with and without transport effect from different aspects, as seen in **Figure 16**. For the latter, it can be called as physics-informed ML/DL, kinetics-informed ML/DL or mechanism-informed ML/DL. Some typical applications include the discovery of reaction networks, predictions of reaction source term of each species (e.g., the mass concentrations related to yields/selectivity/conversion), determination of reaction kinetics such as reaction rate parameters, and optimization of reaction conditions. **Table 3** summarizes some typical examples of recent advances along with the specific ML algorithms (including their structures, activation and loss functions), data sources/sizes, feature input variables, prediction performance and contributions, research weaknesses and future directions.

Table 3 Recent advances of machine learning applications for the determination of kinetic parameters and reaction conditions.

Topics	With transport?	ML architecture, activation, loss functions, optimizer	Data sources and feature inputs	Research performance and contributions	Research gaps and future remarks
➢ **Estimation of reaction rate constant**[267]	➢ No	➢ **DNN**: 3 hidden layers of 64, 24, 24 neurons per layer; Softsign (Hidden layer), Tanh (Output layer); MSE; Learning rate=5×10^4.	➢ Reactant partition function; $\sim1.5\times10^6$ datasets; m, V_1, V_2, w_1, w_2, T, d, s	➢ MRE=1.1%; Difference between DNN and TST is 31%. A large dataset for training is necessary.	➢ Future work may include physical knowledge to reduce prediction error, e.g. the TST rate constant as an input.
✧ **Estimation of activation energy**[268]	✧ No	✧ **Transfer learning**; **PCA**; **DNN**: Hidden size=300, depth=3; 10-fold cross-validation; Learning rate=$10^{-5}\sim10^{-6}$.	✧ DFT; 5.7×10^4 (85:5:10); t-Distributed stochastic neighbour embedding	✧ RMSE=2.28 kcal mol^{-1}; Development of a template-free DNN strategy for estimation of the activation energy.	✧ Uncertainty in NN predictions of molecular properties should be quantified. The applicability of the developed model can be tested by more reaction systems.
➢ **Reduction of reaction networks**[269]	➢ No	➢ **Gaussian process**	➢ DFT; Group additivity fingerprints	➢ Reducing reaction networks of syngas on the surface of Rh(111) catalyst; A substantive step for applying ML in the field of computational catalysis	➢ Expensive computational cost. GP is limited to relatively low-dimensional problems due to loss of its effectiveness in high-dimensional feature input space.
✧ **Simultaneous estimation of species sources term and kinetic parameters**[270]	✧ No	✧ **PINN**: 3 Hidden layers with the same number of neurons (ranging from 5 to 20). tanh, swish and tanh for each hidden layer.	✧ ODE solver; Forward problem: Boundary conditions (t_0, x_0), **p**, n_{max}, tol; Inverse problem: (t, $\tilde{x}$), n_{max}, tol.	✧ MAE=$1.79\times10^{-5}\sim8.93\times10^{-3}$; MSE=$4.27\times10^{-10}\sim2.49\times10^{-4}$; $R^2\approx1$; Robust clarification of elementary reaction pathways and estimation of kinetics parameters. Inclusion of physical knowledge and boundary conditions enables high robustness and generalization performance.	✧ Need to consider transport effect in order to used it as a more practical tool; May be coupled with CFD solver or classics reactor model.
➢ **Simultaneous estimation of species sources term and kinetic**	➢ Yes	➢ **PINN**: 5–7 hidden layers, 256 neurons per layer; Tanh; Loss= $MSE_{Govern}+MSE_{Boundary}$	➢ MATLAB; $10^3\sim10^4$; Forward problem: Initial conditions, Boundary conditions; Inverse problem:	➢ Enhanced accuracy: a 0.3% error even for a limited number of datasets; With transport effect considered for the catalytic CO_2 methanation.	➢ The reactor model is limited to a 1D plug-flow isothermal fixed bed reactor model; Future efforts may couple the PINN with a 3D CFD solver.

parameters[271]			✧Observation data; Boundary conditions		
✧**Estimation of species sources term**[272]	✧Yes	✧**RF**, **DT**: 25 trees; 4 tree depth.	✧ODE solver of micro-kinetics; 8^6 training and 5×10^4 testing sets; T, P_i, θ_i	✧High accuracy: MRE<1.5%; High efficiency: 558 times faster than ODE solver; Able to recognize the importance of variables; Successful coupling of RF with CFD.	✧Need to validate with experiments; Absence of comparison between the PRCFD-RF and pure PRCFD; Need to quantify the increasing computational time due to integration of RF with CFD.
➢**Estimation of species sources term**[273]	➢Yes	➢**DNN**: 3 hidden layers with respective 32, 64, 128 neurons; ReLU and Sigmoid; RMSE	➢RANS k-ε model; 71820 (90:10); k, ε, Y_A, Y_B	➢RMSE=8.50×10^{-3}; High accuracy vs. finite-rate model; Acceleration of 14 times vs. the time-consuming Lagrangian PDF approach; Considering the turbulence-chemistry interaction effect on reaction source.	➢The reaction rate model should be trained based on more high-fidelity DNS or LES data; Need of further test of its effectiveness in multiphase flow simulations.
✧**Estimation of species sources term**[274]	✧Yes	✧**BPNN**	✧CFD; x, y, Tg	✧Species concentrations: R^2=0.73~0.91, MSE= $3.633e^{-5}$~$3.85e^{-2}$; High accuracy for biomass fast pyrolysis predictions.	✧Need of additional performance metrics such as MAPE; Future work may need to map the relationship along with flow time.
➢**Optimization of reaction conditions**[275]	➢No	➢**Hierarchical NN**: Step 1: Fully connected layers (ReLU, ReLU, ReLU, Softmax); Step 2: 2 fully connected layers (ReLU, Softmax); Step 3: 2 fully connected layers (ReLU, Linear).	➢Reaxys; $\sim10^7$ datasets; (1) Product and reaction fingerprints; (2) Catalysts, solvents, and reagents	➢Top-10 predictions: For catalyst, solvent and reagent: 69.6% accuracy, individual species: 80–90%; Within ±20 °C for temperature: 60–70%. Potential generalizable performance; Much faster to select suitable reaction conditions.	➢A possible weakness is that the number of estimations per each stage is limited to top-10 combinations in a short time period since the predictions are in a sequential manner; Potential improvement of the prediction ability through a better curated dataset.
✧**Optimization of reaction conditions**[276]	✧No	✧**GP**; **PCA**; **Bayesian optimisation**; **GA**	✧Literature; A library of 459 solvents; Descriptors	✧Cross-validation R^2=0.84; Inclusion of physical knowledge in ML; Enabling rational solvent selection and temperature optimization for catalytic reactions.	✧Future efforts of DoEs may be conducted for reduction of the number of experiments.
➢**Optimization of reaction**	➢No	➢**PCA**; **NN**: 7 hidden layers; ReLu, Adam; Loss=MSE; 5-fold	➢718 data points from 46 papers; 4 compositional	➢R^2>0.85; Generalizable and satisfactory accuracy for catalyst screen and	➢Need to establish a bigger, standard database for renewable reaction

conditions[2] 77	cross-validation.	features of feedstock, operational conditions, catalyst descriptors	5 5	supercritical gasification optimization;	water condition	processes by some recent advanced techniques such as text mining.

Note: In this section, reaction conditions/factors denote reagents, catalysts, solvents, reactants, products, and operating conditions (e.g., flow rate, temperature and pressure), etc. Besides, the critical comments above may not be adequate and we present the suggestions with the hope that readers and newcomers could obtain some possible inspirations or thoughts from this table.

2.3.1 Prediction of reaction networks and kinetic parameters

It is a longstanding bottleneck in discovery and design of novel products due to its requirement for enormous efforts and costs in finding a combinatorically large space of potential candidates[278]. Therefore, the capability of predictions of reaction networks without performing extensive simulations and experiments is of crucial significance. The study of reaction networks may be categorized into three types[279]: forward open-end study, backward open-start study, and start-to-end study. These reaction networks are very complex since the network size is usually very large and reacting species can highly interconnect. As a consequence, a large number of interconnected ODEs or PDEs should be resolved. In the early development stage, this solving process heavily relies on manual operation while numerous recent network generators such as ReNGeP PRIM, MECHEM and NetGen have been developed to automatically generate and design reaction networks[280]. Despite its automated benefit, these generators still have some challenges such as the reduction of model complexity, simultaneous estimation of kinetic parameters, lack of generality and relatively difficult-to-use, etc. In recent years, ML is increasingly employed to support the automated discovery of reaction networks and determination of kinetic parameters[281,282]. There are several general ways to achieve these purposes and they may be categorized as follows:

2.3.1.1 Single determination of kinetic parameters

The first type is to use pure ML/DL to estimate the rate constants or activation energies by fitting the database from experiments, traditional quantitative structure–reactivity relationship (QSRR) and computational methods (e.g., MD, DFT and kMC). Recently, there is a rapid growth of study using ML/DL to assist calculations of kinetic parameters[283]. This kind of studies may be further categorized as follows:

(1) The dataset from new experiments or readily available experimental database: Among these researches, ANN is one of the most popular methods used for predicting activation energies[284] and reaction rate constants[285-287]. Rizkin et al.[288] reported a novel NN-assisted methodology for exploring polymerization reactions based on an automated microreactor in conjunction with in-situ infrared thermography. The developed methodology using efficient and high-speed experimentation could map the reaction space of a zirconocene polymerization catalyst to kinetic parameters. This work demonstrated that high-fidelity datasets on a complex chemical reaction system can be obtained by integrating advanced microfluidic techniques with ML algorithms. Unlike the above investigations, Quaglio et al.[289] proposed an ANN-aided approach for the selection of an appropriate kinetic model based on the available experimental evidence. The generality of the model was assessed by varying the experimental design and system noise. This method does not need to fit kinetic parameters and is suitable for the case involving diverse candidate mechanisms. Moreover, many efforts were also spent on combining pure ML (e.g., RF, NN and XGBoost) with molecular fingerprints to estimate the reaction rate constant of the radical-induced oxidation reactions of aqueous organic pollutants[286].

Note that most of the reaction systems above are assumed to be homogeneous without

considering the effect of transport. A clear bottleneck is that the black-box ML/DL such as NN requires large datasets to train the algorithms. As a consequence, obtaining the large datasets from traditional experiments can be very challenging due to the material usage cost for traditional reactors with large volumes, especially for expensive materials. One solution is to perform high-throughput flow chemistry experiments in microreactors. Researchers have developed a fast, automated ML-aided platform to determine reaction models and kinetic parameters[284]. This kind of method can remarkably improve current industrial determination techniques and significantly reduce computation time, overall cost and labor. However, the developed platform may be only appropriate for some specific flow rection systems lacking universality. Another alternative is to collect data from some existing databases but the data distribution may be very uneven and the reaction rate constants are often not given. We would suggest these databases should be gradually improved and become more and more feasible for all users in the future. At the moment, one may improve the training performance by choosing a suitable data sampling/handling strategy specified to their data characteristics/qualities/distributions, such as random sampling, greedy sampling on (both) inputs/output, and variational sampling[290]. The last option is that the theory-based methods can provide large datasets for training ML, which has become an effective methodology for calculations of rate parameters of kinetic models. However, there still exist problems for these approaches, for example, the ab initio computation of exact rate parameters will result in a huge computational burden, which hinders fast quantitative predictions of the coupled reaction kinetics involving large datasets. In order to overcome this hurdle, combinations of ML/DL with computational methods can be performed.
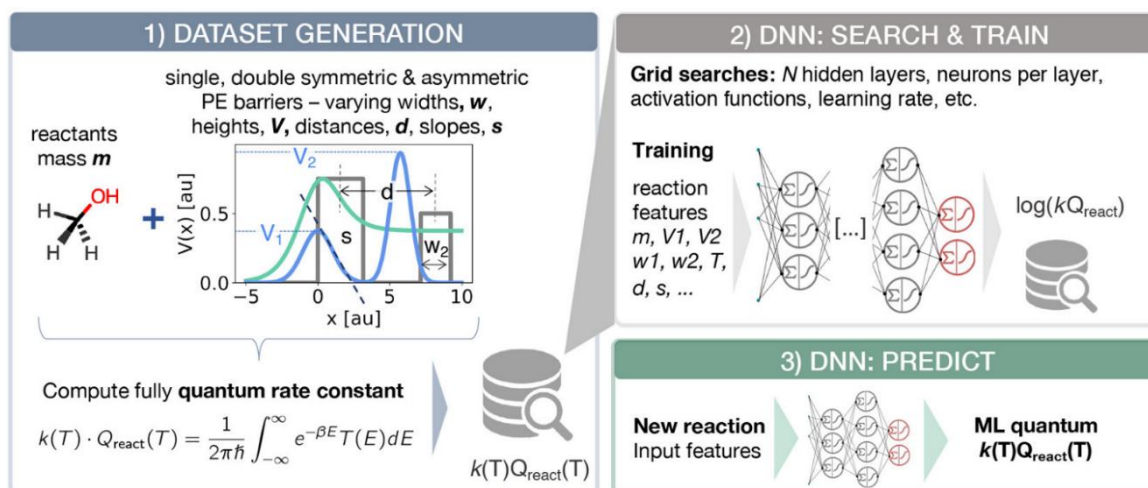
Figure 17 Flowchart of deep learning quantum reaction rate constants. 1) Data generation. 2) DNN model inputs, outputs and structures. 3) DNN to estimate rate constants. Adapted with permission from ref 267. Copyright 2020 American Chemical Society.

(2) The dataset from the traditional transition state theory (TST) or first-principles theory. These methods can be trained to estimate activation energies[268] and reaction rate constants[267,283,291]. The common steps for this group of studies include (i) data generation from computational methods, (ii) selection of suitable ML/DL methods, (iii) design of ML/DL structures, (iv) training the model and optimization of these structures, and (v) application of the trained model, as shown in **Figure 17**. Grambow et al.[268] constructed a template-free directed-message-passing NN model (i.e., a type of graph CNN) to estimate the activation energy for a given reaction. The model was trained based on a DFT dataset spanning a diverse set of reactions, achieving correct predictions and good agreement with an intuitive comprehension of chemical reactivity. Komp and Valleau[267] trained a DNN model to estimate the quantum reaction rate constant-related terms based on the datasets obtained from in-house calculations. In particular, $\sim 1.5 \times 10^6$ rate constants are contained for various types of 1-D potentials, which covered a wide variety of reactant masses and temperatures. The trained DL model can estimate the logarithmic rate product with a 1.1% relative error and the difference between the TST and DFT can be up to 31%. This difference suggests that future

efforts may include the rate constants computed from traditional TST as input features. Instead of directly training the DL model based on the datasets from TST or DFT, there are also studies[291] directly training the Gaussian process model to regress and assess the difference between different computational methods such as TST and DFT. One possible limitation for this kind of investigations is that only a relatively small range of temperatures is commonly used for most of the studies. This will limit the applicability of the trained model although the authors have claimed that their models have good generalization performance. This issue may be fixed by combining more computational methods and experimental data to sufficiently take advantage of their strengths and conduct further cross-validation tests.

2.3.1.2 Simultaneous determination of pathways and kinetic parameters

The second type is to directly apply physics-informed ML/DL to train the data from experiments, kinetics-ODE solvers or quantum computation to discover unknown pathways and simultaneously estimate kinetic parameters. The kinetics-ODE, the other types of governing equations and boundary conditions can be added as the constraints to make the obtained model follow the physical fundamentals and have much more interpretability and robustness. A typical PINN example is to design and train a reaction neural network using the basic physical laws (e.g., the mass action law and Arrhenius law) as constraints. Ji et al.[292] revealed that such a physically interpretable model can find the unknown reaction pathways and estimate the rate constants at the same time according to the weights of NN. To obtain the solution of kinetics-ODEs, one can apply the feed-forward NN as basis functions and the microkinetic differential algebraic equations as constraints, which enables simultaneous

determination of reaction pathways and kinetic parameters (**Figure 18a**)[270].
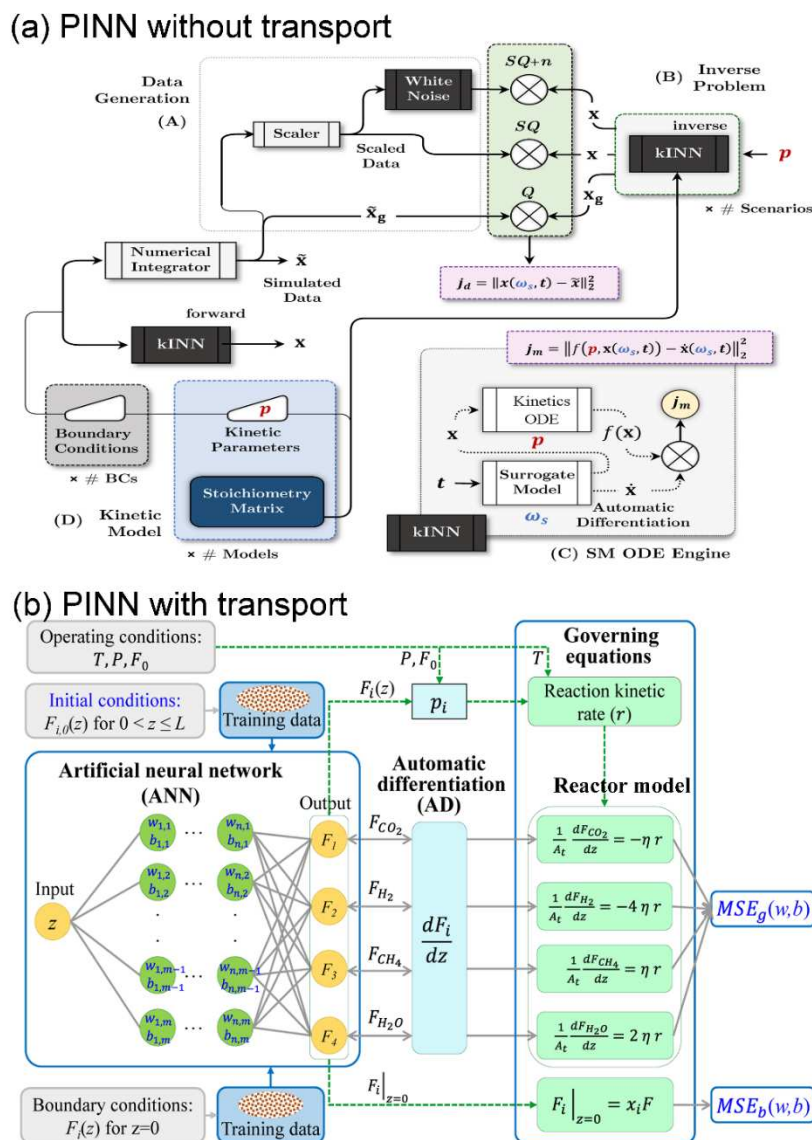
Figure 18 (a) PINN without transport effect, able to solve both inverse and forward kinetic problems (Gusmão et al.[270]); (b) PINN with transport effect in a fixed bed reactor for catalytic CO_2 methanation, able to solve inverse kinetic problems (Ngo and Lim[271]). Figure 18a was adapted with permission from ref 270. Copyright 2022 Elsevier. Figure 18b was adapted with permission from ref 271. Copyright 2021 MDPI.

One primary advantage of the above studies is that the reaction NN can give robust clarification of elementary reaction pathways of the investigated reaction systems with high dimensionality when suggesting the candidate network. However, in the former study, it may be difficult for their model to deal with the reaction systems where a large variety of timescales and concentration levels are involved. Another possible problem of this kind of

study is that different authors usually enforce different constraints into the NN structure while the un-encoded candidate constraints are not demonstrated further. It is true that enforcing all constraints into the NN structure will make the model very complex, but there may exist an optimal solution of which constraints should be embedded into the NN architecture. This may be of interest for future work. Another kind of representative study is to encode kinetics-ODEs into the loss functions of NN for reactions[293,294]. It should be of practical use to integrate this physics-inform kinetics-ODE framework into a CFD solver or a reactor model to give forward predictions of species source terms.

2.3.1.3 Reduction of reaction networks

The third type is to perform ML/DL such as PCA, tree models and CNN for complexity reduction of reaction networks from different aspects. The motivation of network reduction is that rapid and accurate predictions of reaction compositions are greatly beneficial to reaction processes design, optimization, and control[295]. However, the establishment of a comprehensive kinetic scheme is computationally prohibitive due to the highly complex chemical space. Most of the studies tried to simplify the reaction mechanisms from the known comprehensive reaction mechanisms. In fact, the key idea of these studies has some similarities, such as learning local representations from complex reaction networks, the discovery of the key components and interactions, the identification of the suitable coarse quantities of the reaction network, and the sparse identification of the most influential reactions using component concentrations and the reaction rates. Several representative application examples are discussed and analyzed below. Hough et al.[296] applied ANN and decision trees for reduction of the computation cost by four orders of magnitude as compared

with the DKM of biomass pyrolysis. The trained ANN was generalizable to give predictions of the DKM with an accuracy of over 99.9% on the unseen test dataset. The outlined ML method did not depend on the underlying kinetic correlation between inputs and outputs, which is applicable to any varied kinetic relationships, no matter whether the reaction relation is known. Ulissi et al.[269] reported a novel Gaussian process-based surrogate methodology for optimizing and reducing heterogeneous catalysis reaction networks of syngas on the surface of Rh(111) catalyst. The surrogate method was trained by adsorption energies on the basis of group additivity fingerprints in conjunction with transition-state scaling relationships and a simple classifier for the determination of the rate-limiting step. The presented model was iteratively applicable for predictions of the key reaction step to specific products via the explicit DFT calculations. This work is a substantive step for applying ML in the field of computational catalysis. However, the computational cost of DFT is relatively expensive and more importantly the GP is usually limited to relatively low-dimensional problems due to the loss of its effectiveness in a high-dimensional feature input space. Given the relatively poor generalization of ANN because of complete ignorance of the reaction network topology, Qiu and coworkers[297] reported a high efficiency CNN-aided framework able to learn local representations from complex reaction networks. Methods for characterizing large-scale networks were adopted for extraction of features of naphtha pyrolysis reactions. Using the selected features as inputs in CNN architectures, the optimized CNN models enabled a 300 times acceleration of the computation speed as compared with the traditional kinetic model and the prediction accuracy of yields of major products reached 97%. Their later work[298] developed a unique multiple sub-network reconstruction characterization module used for

effective discovery of the key components and interactions in the co-cracking process and for elucidation of the evolution mechanisms in the co-cracking reaction network. Van Geem and coworkers[295] proposed four DNN-based frameworks for the steam cracking production process. Based on a limited amount of practical naphtha indices and fast accessibility of process characteristics, their novel methodology enabled the determination of a detailed composition of the steam cracker effluent, showing a high accuracy of predictions of the networks and an ignorable computational burden. Thus, their method was very applicable for continuously monitoring/controlling hard-to-access process parameters and for providing a real-time optimization strategy. Unlike these contributions, Katsoulakis and Vilanova[299] proposed a new scalable methodology by combining an information theory tool with a variational approach for efficiently reduced modeling of high-dimensional reaction networks. The reported ML method allowed for identification of the suitable coarse quantities of the reaction network by sensitivity analysis, and for the development of a best-fit reduced model with the control of the information loss. The effectiveness of the data-driven reduced model was well demonstrated for several high-dimensional biochemical reaction networks. Harirchi et al.[300] proposed a novel data-driven sparse-learning method for identifying the key reactions in complex combustion reaction networks. The presented optimization method was applied for sparse identification of the most influential reactions using component concentrations and reaction rates. The required computational resource was minimal and no additional data or simulations were required.

It can be concluded that the results by ML accord well with the existing understanding of chemical kinetics and the developed model is able to reduce the complexity of kinetic

modeling, thereby accelerating the discovery of reaction kinetics. However, most of these established models appear to be only valid for a specific reaction system since the datasets used for training are usually limited to a specific composition space. Another notable similarity is that whether using the GPU to speed up the reaction network modeling has not been indicated for most of the above papers. To this issue, some researchers have recently turned their attention to this important aspect[301] and increasing efforts need to be devoted to boosting the discovery efficiency of reaction networks.

2.3.1.4 With transport effect

The fourth type is to perform pure ML/DL or physics-informed ML/DL of reaction kinetics with transport effect. Note that the discussion of the first three types mostly ignored the effect of transport phenomena on reaction kinetics modeling. To account for the transport effect in kinetics modeling, one can collect plant data from large-scale reactors[302] but the economic cost is usually very high. Alternatively, one can also combine ML/DL with the CFD or the classic simplified reactor model. The first typical example is to use the pure data-driven ML to map the relationship between the rate constants and the temperatures. Spencer et al.[303] first performed transient coarse-grid CFD simulations to generalize a series of 'snapshots' at an assigned time interval $\Delta t = 0.1$ s when the temperature ranged from 473 K to 633 K for a CVD process. The recorded vector data of flow variable distributions were then reduced to a low-dimensional description by a POD method. After that, ANN was used to train and map the reduced data. The mapped relationship was subsequently regarded as the initial condition of the coupled steady-state fine-grid simulations with the detailed kinetic models and this could accelerate the convergence. However, in the fine-grid simulations the

kinetic rate constants should be adjusted so that the predicted deposition rate can approximate to the experimental data within a reasonable tolerance. The benefit of this work is that the reduced order model based on coarse CFD predictions can serve as a preconditioner for the fine-grid CFD which accelerates its convergence. The possible disadvantage is that there are several different processes involved, and this could increase the implementation complexity and uncertainty in different processing steps. Another typical example is illustrated in **Figure 18b**, where the classic reactor model is used to consider the transport effect in an isothermal fixed bed reactor for catalytic CO_2 methanation. Ngo and Lim[271] trained an effective physics-informed feed-forward ANN. In particular, a classic plug-flow fixed bed reactor model was introduced to consider the effect of transport phenomena and the unknown effectiveness factor existing in reaction kinetics can be estimated with a 0.3% error even for a limited number of datasets. In their model, the forward problem aimed to optimize the weights and biases and then predicted the unknown effectiveness factor; meanwhile, the inverse problem estimated the effectiveness factor by directly optimizing the loss function where the effectiveness factor was involved. We note that very limited studies have reported PINN-based inverse modeling of reaction kinetics parameters with transport effect. It should also be noted that this work is limited to a 1D isothermal plug-flow reactor model. We thereby suggest that future efforts can be extended to investigations on more complex 3D reactor geometries and considerations of thermal effects.
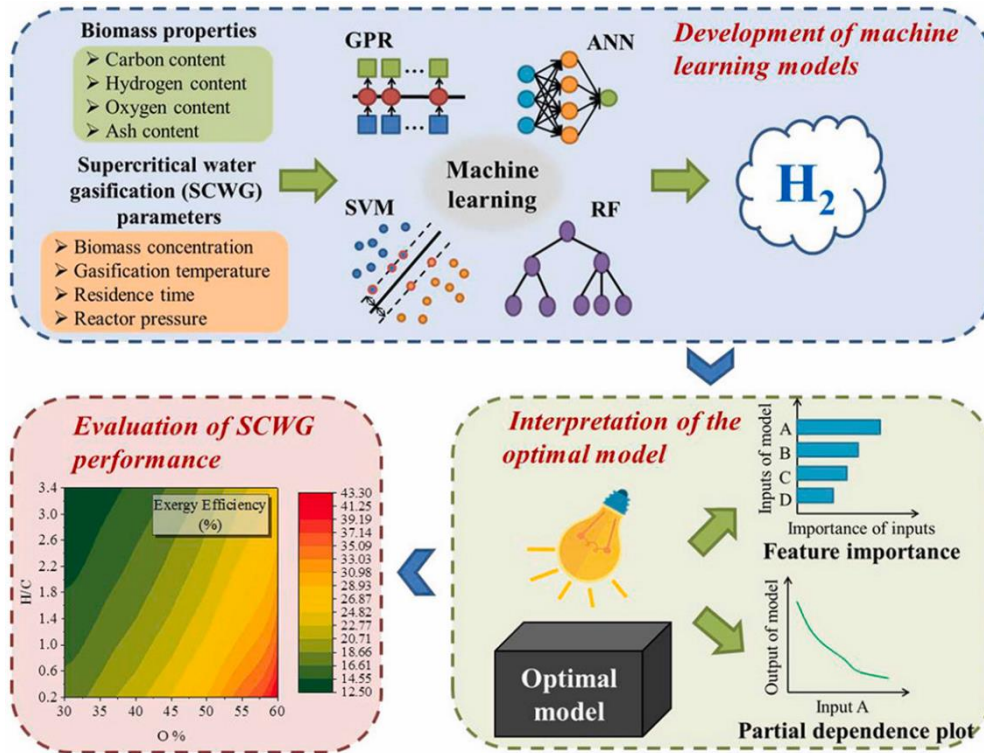
Figure 19 A workflow for assessing the performance of different machine learning methods to estimate H_2 production through supercritical water gasification of biomass. Adapted with permission from ref 308. Copyright 2021 Elsevier.

2.3.2 Prediction of species production

Similar to inverse problems of estimating kinetic parameters above, study of the forward prediction of species source terms can also be categorized into different classes: pure/physics-informed ML/DL with or without transport effects.

2.3.2.1 Without transport effects

This class of investigations can be further divided into two types: (i) Pure ML/DL without transport effects; (ii) Physics-informed ML/DL without transport effects. Most of the previous researchers have used pure ML/DL for data-driven predictions of the species production using the datasets generated from the coupled CFD solvers with the detailed kinetic models or the experiments. The pure ANN, SVM, RF, decision trees and gradient boosting (GBoost) are the most popular algorithms for the regression purpose above. Chen et

al.[304] reported ANN and SVM models for estimation of the product profiles and biomass pyrolysis bio-oil heating value. It was indicated that both models are able to well predict the yield of pyrolytic product and the bio-oil heating value while SVM manifests a better estimation performance for biomass pyrolysis. Mutlu and Yucel[305] proposed RF-based and least-squares SVM-based data-driven models applicable for estimation of syngas composition for downdraft biomass gasification based on the downdraft gasification data from an experimental fixed bed system. In addition to using the experimental data as the data source, recent studies have also used molecular-level kinetic models to generate data for training ML approximators to completely represent the time-consuming molecular-level kinetic models for predicting the product yields. Agarwal and Klein[306] developed several data-driven regression models based on the decision tree, GBoost, and ANN to predict component yields. Zhu et al.[307] applied RF model for predicting the yield and carbon contents of biochar using the data of lignocellulosic biomass pyrolysis. The model could give accurate predictions of the biochar yield and C-char based on characteristics and conditions of biomass pyrolysis. Besides, the model identified that temperature was the key factor affecting both carbon contents and yield in pyrolysis processes. Zhao et al.[308] developed a novel methodology to evaluate the performance of different ML methods, including RF, GP, ANN and SVM, and to estimate H_2 production through the supercritical water gasification of biomass (SCWG), as displayed in **Figure 19**. For the investigated SCWG, the RF model outperformed the prediction ability of the remaining models. The optimal RF was then utilized to assist the relative importance and partial dependence analysis of biomass properties and process parameters for maximizing the efficiency of H_2 reaction and exergy consumption. To sum up,

the studies above may be improved from the following optimization perspectives. First, we suggest again that the data size required to train a high-accuracy and generalizable ML model deserves more future efforts. In particular, Agarwal and Klein[306] showed at least 10^3 data sets are required in an ANN modeling to reach sufficient accuracy while this requirement can be up to over 10^4 datasets for decision tree models in the systems they studied. In fact, it is hard to achieve such a high requirement for the data from experiments, which suggests that there may be a risk of overfitting to train a pure ML using very limited datasets. It should be noted that the specific amount of data required could only be of guidance for the corresponding type of specific systems. Second, most of the studies above have not presented a relatively systematic optimization of hyperparameters and it is unknown how much uncertainties are involved in their models and thus in their predictions. In efforts to improve this weakness, some optimization-based ML algorithms are suggested to be performed in the future. Third, input feature reduction using some common ML methods can be conducted to deal with the complex systems with hundreds of compositions[309] since the combinations of input parameters can be up to 2^{13} for estimations of on the yield of biochar. This highlights the need to identify the key input features using high-performance ML algorithms. In particular, Ullah et al.[310] developed a novel GA-assisted method for feature selection and evaluated several different ML-based data-driven regression models based on the selected features. It was found that data-driven models could offer reliable predictions of bio-oil yield, and particularly the RF-based data-driven model outperformed the remaining models in the case that the complex relationship between the inputs and output target was considered. In the future, this kind of work may be further trained and tested over more systems to probably

'formulate' a universal feature reduction rule. Finally, we want to emphasize that in recent years the physics-informed ML/DL methods have been rapidly applied to improve the major weakness of pure ML/DL, and an increasing number of new ML/DL structures has been designed and reported. However, applications of ML have not been widely absorbed in physics-informed ML/DL modeling of reaction kinetics. In fact, forward physics-informed ML/DL can be applied for the prediction of the composition source terms once the inverse physics-informed ML/DL model is well constructed (**Figure 18a**) or the kinetic parameters have been known. Therefore, more efforts are suggested to investigate forward physics-informed applications in reaction kinetics, especially the comparison between different orders of reaction kinetics models from a perspective of algorithm optimization.
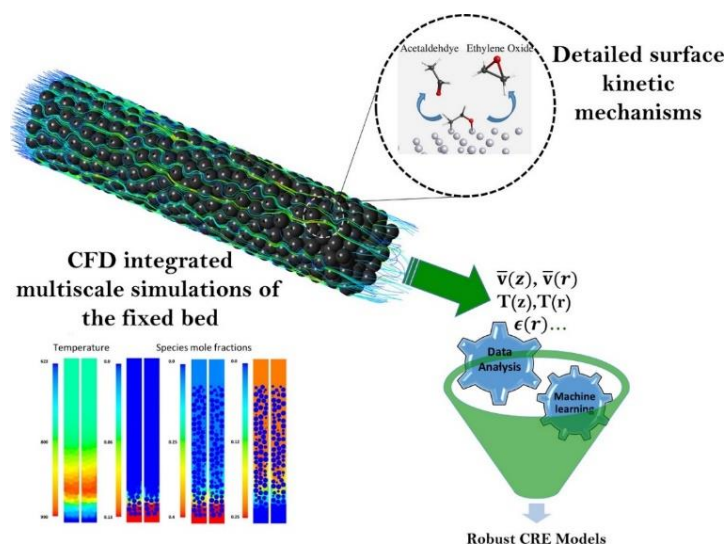
Figure 20 Flowchart for data analytic- and machine learning-aided chemical reaction engineering model development for fixed bed reactors. Adapted with permission from ref 106. Copyright 2019 American Chemical Society.

2.3.2.2 With transport effects

There are basically several ways to consider transport effects in predictions of reaction source terms including mapping the relationship between the reaction rate and the input variables (e.g., operating conditions) or direct mapping the relationship between the mass

fraction of components and the coordinates of each numerical cell. Bracconi and Maestri[311] designed a novel procedure using Random Forest and Extremely Randomized Trees to approximate computationally-intensive first-principles kinetic models (e.g., the mean-field microkinetic models) in catalytic reactions. The results using the trained ML model excellently agreed with those by the full first-principles models within an error of 0.2%. The tree model was then coupled with reactor models to predict the reaction rate used as the reaction source term of CFD simulations. Moreover, there are also ML studies directly training and learning the data from the coupled CFD and kinetic models. Zhong et al.[274] also conducted back-propagation ANN to improve predictions of the species distributions in a gas-solid biomass fast pyrolysis reactor. They explored the effect of the sampling approach and number of outputs, and optimized the hyperparameters (e.g., the number of neurons in the architecture of ANN). The species mass fraction data of TFM simulations were successfully mapped to the coordinates of each numerical node and temperature of pyrolysis in the reactor. Partopour et al.[272] proposed a novel RF method for ensemble learning the pre-computed microkinetics data and then integrated the learned mapping predictor with the CFD in order to estimate the reaction rate needed in particle-resolved CFD simulations of fixed bed reactors. In particular, their trained reduced kinetics model showed high accuracy with MRE<1.5% and high efficiency (558 times faster than ODE solver). It is necessary to implement further validation with experimental data of their trained model and comparison between the PRCFD-RF and pure PRCFD. Besides, quantification of the increase of computational time due to the integration of RF with PRCFD may also be needed. Partopour and Dixon[106] further proposed a workflow for data analytic- and ML-aided reaction

engineering model development for fixed bed reactors (**Figure 20**). In this workflow, the high-precision CFD tool coupled with the detailed microkinetic models was utilized to generate multiscale data sets of flow, transport, and reactions useful for later development of reliable data analytic- and ML-aided reaction engineering models. Using the high-quality large dataset from an industrial-scale FCC device, Yang et al.[312] proposed a novel data-driven hybrid model which successfully embeds the mechanistic lumped kinetic model into an ANN framework. More specifically, the authors considered the predictions given by the mechanistic model as an auxiliary input and concatenated this input layer with the second hidden layer. The hybrid model enabled better representation of the petrol yield data than those estimated by a pure mechanistic model and a pure data-driven ANN model. Recently, we performed data-driven modeling of the filtered subgrid reaction rate source term to correct the reaction rate observed in a coarse-mesh TFM simulation based on the data from fine-grid simulations[45]. Due to a relatively simple relationship between the filtered reaction rate output and two feature inputs (filter size and solid hold-up), conventional fitting and data-driven methods showed comparable prediction performance of a solid-catalyzed first-order reaction. More recently, Ouyang et al.[273] proposed an ANN-based data-driven methodology to approximate the reaction rate in order to speed up the time-consuming simulation of turbulent reactive flows. Their constructed model is able to compute the reaction rate with a satisfactory accuracy (RMSE=8.50×10^{-3}) and a boosted efficiency (an order of magnitude speedup while keeping accuracy) over "unseen" testing operating conditions and new geometry cases. Notably, the proposed model considers the effect of turbulence-chemistry interaction on reaction source terms and is 14 times faster than the time-consuming

Lagrangian PDF approach.

To sum up, most of the studies have directly used the trained pure ML/DL as a black-box approximator but do not endow the prior knowledge into the approximator to keep its robustness and to enhance extrapolation ability. As a consequence, these black-box approximators are probably only applicable for simulations with reaction mechanisms accounting for the identical set of components as the one utilized in the training span. One solution to address the possible overfitting could be increasing the dataset size (if the database is obtained from simulation snapshots) or applying 2%~3% of uncorrelated random noise to perturb the training data[313]. The solutions above may not completely eliminate the overfitting for pure ML-base data-driven modeling, but lower the degree of the overfitting. In addition to applications of pure DL above, there are relatively few efforts focusing on applications of physics-informed DL in the modeling of the mean reaction rate. In particular, in a DNN learning of combustion reaction processes based on DNS data, some researchers have attempted to revise physics-informed loss functions by introducing the mass conservation laws of the mixture and elemental species in a specific formulation which can produce extensive conditions as constraints[314]. Besides governing equations, boundary conditions and reaction kinetics can also be used as physics-informed constraints[273]. When using the kinetics-ODEs as constraints, some mathematical laws may also be considered for the case where the matrix is close to singular value and this consideration can be considered in some specific cases.

2.3.3 Optimization of reaction conditions

Chemical reactions typically have numerous controllable reaction conditions/factors. Accurate suggestions of such conditions/factors play an essential role in yielding the desirable products. In this section, reaction conditions/factors denote reagents, catalysts, solvents, reactants, products, and operating conditions (e.g., flow rate, temperature and pressure), etc. Traditionally, experimental approaches can probe suitable combinations of these factors. However, conventional recommendation of suitable conditions depends heavily on researchers' knowledge and experience. Moreover, the experimental determination process is usually time-consuming, and leveraging big data further brings a great challenge. ML is flexible and efficient to recommend the most suitable solution based on reaction data[315-317]. So far, there may have been three general types of applications of ML for optimization of reaction conditions to maximize the reaction yield/selectivity/conversion: **(i)** Coupling ML/DL with physical models; **(ii)** Coupling ML/DL with experiments; **(iii)** Coupling ML/DL with robotic platforms as an optimizer. In particular, multi-objective optimization is most often applied for the identification of the trade-offs between the criteria of conflicting performance. In order to solve reaction optimization problems, nowadays it has to leverage multidisciplinary knowledge including chemical engineering, chemistry, mathematics, physics and especially computer science. We will discuss the recent progress from perspective of reaction condition optimization while perspective of chemistry such as optimization of chemical synthesis[318] is paid to relatively less attention.

2.3.3.1 Coupling ML/DL with physical models.

(1) The first kind of applications is to perform ML/DL to train the data from the physical models such as CFD model and classic reactor model. After the model is well trained, it can

be used as an approximator to perform a rapid sensitivity analysis of reaction conditions and find the optimal conditions to maximize the yield of the main products and minimize the conversion of other side products. Moreover, the trained ML model can also be used as an objective function in an optimization function, such as GA to optimize reaction conditions[158].

(2) The second kind of application is to use ML/DL to optimize the parameters involved in the physical models and then to use the constructed model to optimize reaction conditions. Chaffart and Ricardez-Sandoval[319] conducted the continuum models and stochastic PDE to simulate the multiscale deposition behavior and ANN was adopted to estimate the model parameters in the stochastic PDE, which was verified by kMC. The established hybrid model was then applied to optimize and control the growth of thin film under various scenarios. An important consideration is that there exists parametric uncertainty because the surface roughness of thin film deposition is probably out of range of the targeted values. Besides, it is still time-consuming to use a stochastic PDE to capture the microscopic film growth deposition. To address this issue, the later work[320] directly used ANN as a surrogate model to capture the microscopic deposition dynamics while a linear parameter varying model was used to simulate the macroscopic deposition behavior. This multiscale data-driven model can significantly accelerate the computational process up to $O(10^4)$ as compared with the pure CFD simulation.

(3) The third kind of application is to employ ML/DL or physical models to optimize the hyperparameters involved in the ML/DL and then to use the optimized model to optimize reaction conditions. For instance, researchers first combined Monte-Carlo sampling with CFD simulations of combustion to generate the database used for later training of

super-learner ML-GA. In particular, the hyperparameters in the ML base learner were optimized by a Bayesian method. Once the ML was well established, the ML-GA can be used for the optimization of combustion processes. This general framework can be integrated into the CFD solver to optimize other reaction systems.

2.3.3.2 Coupling ML/DL with experiments

Here, the optimization process does not involve other physical models and the datasets are collected from experiments. So far, ML/DL has been applied as an optimizer for different reaction systems and notably growing attention has been paid to flow chemistry systems[321-323], renewable energy systems such as hydrothermal carbonization[324] and hydrothermal liquefaction of algae[325,326], etc. These studies may be further divided into two categories: with and without physical knowledge. Physical knowledge includes material properties (e.g., solvent, molecular and catalyst properties, namely, the so-called descriptors) or other kinds of knowledge (e.g., DFT). The ML methods with and without descriptors are discussed below:

(1) Without descriptors: Zare and coworkers applied a RNN for optimization of chemical reactions by iteratively recording the results of a chemical reaction and then selecting varied reaction conditions to enhance the reaction result[327]. The proposed DL model outperformed the current optimization method and required 71% fewer steps on both simulations and real reactions. One notable issue is that this refinement learning using LSTM may suffer from the relatively low training efficiency in training and operation. The sequence length cannot exceed a certain limit in order to avoid the gradient disappearance. Jensen and coworkers proposed a novel hierarchical NN-based method enabling predictions of the reaction components (e.g., reagents, catalysts, reactants, products, and solvents) and the

temperature optimal for a specific chemical reaction[275]. Using ~10 million examples from Reaxys, they trained a model able to recommend conditions, and the test results reached a close match to the recorded data very fast (<100 ms for one reaction). An important weakness is that the number of estimations per stage is limited to top-10 combinations in a short time period since the predictions are in a sequential manner. In particular, Lapkin and coworkers have conducted very systematically essential studies towards AI- and ML-guided automated design and optimization of reaction processes. Schweidtmann et al.[328] conducted a multi-objective Bayesian method to approximate a Pareto front for self-optimization of reaction conditions, including simultaneous optimization of productivity and environmental impact or impurity. Note that the physical knowledge has not been directly considered in the learning operation. The same self-optimization platform was further extended to optimize the complex pharmaceutical reaction processes involving liquid-liquid separation[329]. More recently, Liang et al.[321] presented a typical example of how to apply the Bayesian method to optimize reaction conditions for complex continuous gas-liquid-solid flow systems. Comparison with the conventional approach revealed that their developed optimization method can significantly boost both yields and prediction efficiency. In addition to the reaction systems above, recently researchers have also shown interests in other kinds of reaction systems. Kim et al.[330] reported a novel decision tree-based method to predict the most suitable non-oxidative reaction outcomes of methane to C2 compounds by optimization of the reaction parameters with metaheuristics. Their developed model could simultaneously boost the C2 yield and suppress the formation of coke through an improvement of the multi-objective optimization. An evident issue for this work is that there is a need to integrate

the catalyst descriptors in the training operations for a catalytic reaction process. We will further discuss such an urgency in the following discussion.

(2) With descriptors: Recently, there has been a rapidly increasing tendency combining ML/DL with molecular descriptors for optimization of reaction conditions based on closed-loop experimental platforms[331] with the inclusion of physical knowledge. Amar et al.[276] integrated the physical knowledge including the traditional molecular descriptors, reaction-specific descriptors and screening charge density-based descriptors into Gaussian process surrogate modeling (with a cross-validation $R^2=0.84$), aiming at rational solvent selection for simultaneously maximizing the conversion and diastereomeric excess for asymmetric catalytic reactions. After identification of potential solvents, a black-box Bayesian optimization method was performed to determine the solvent mixture composition and optimize reaction temperature. This work was further improved in terms of the following aspects: An Autoencoder was utilized to the dimensionality of descriptors; The trained NN for the design of experiments (DoEs) was conducted in an active learning mode for reduction of the number of experiments due to the reaction optimization requirement[332]. In summary, ML/DL as the core of process development workflow provides a promising solution to design experiments and optimize reaction conditions, which can be transplanted to future robotic platforms. However, a further identification of which ML/DL strategy is applicable to a specific experimental system still requires further efforts. Such an existing issue has driven an initial effort to compare several typical strategies such as GRYFFIN, SOBO and TSEMO on virtual benchmarks for reaction optimization[333]. Overall, Bayesian optimization methods showed excellent performance across the different types of reaction optimization problems.

As we have stated previously, a much more systematic identification is still needed to make the optimization schemes more compatible with different reaction systems in the future. Moreover, it can also be readily found that the amount of database involved in the past studies ranges from hundreds to tens of millions and the authors usually claim that their machine learning models have excellent, satisfactory or good generalization ability. However, there is at least one point clearly indicating that the ML model generalization performance is still a challenging problem since different numbers of the fold for cross-validation in different papers have been adopted to tune the hyperparameters involved in the ML architecture. We find that some efforts have attempted to train a generalizable NN model by using the datasets from different hydrothermal liquefaction systems involving the alkali-catalyst dataset, transition-metal-catalyst dataset and non-catalyst dataset, which may help overcome the potential overfitting and enhance the model extrapolation capability[277]. Particularly, the authors first performed feature extraction of inputs by a PCA method and established a comprehensive dataset covering different systems, which were then used for training an improved NN with the inclusion of catalyst descriptors ($R^2 > 0.85$). Such a workflow for feature engineering is illustrated in **Figure 21a**. The trained NN was finally used for catalyst screening and reaction conditions optimization (i.e., maximizing the production of H_2 and minimizing the yield of CO_2), as shown in **Figure 21b**. Although the authors have tried to collect as many data points as possible from publications, in fact a total of 718 data points were applied in their study. This highlights the great need to establish a big, standard database for renewable energy reaction processes by some recent advanced techniques such as text mining. Alternatively, a combination of automated high-throughput experimentation with AI

for many reaction problems such as flow reactors, organic synthesis and drug formulation

will be an important future direction for targeting these specific reaction systems.
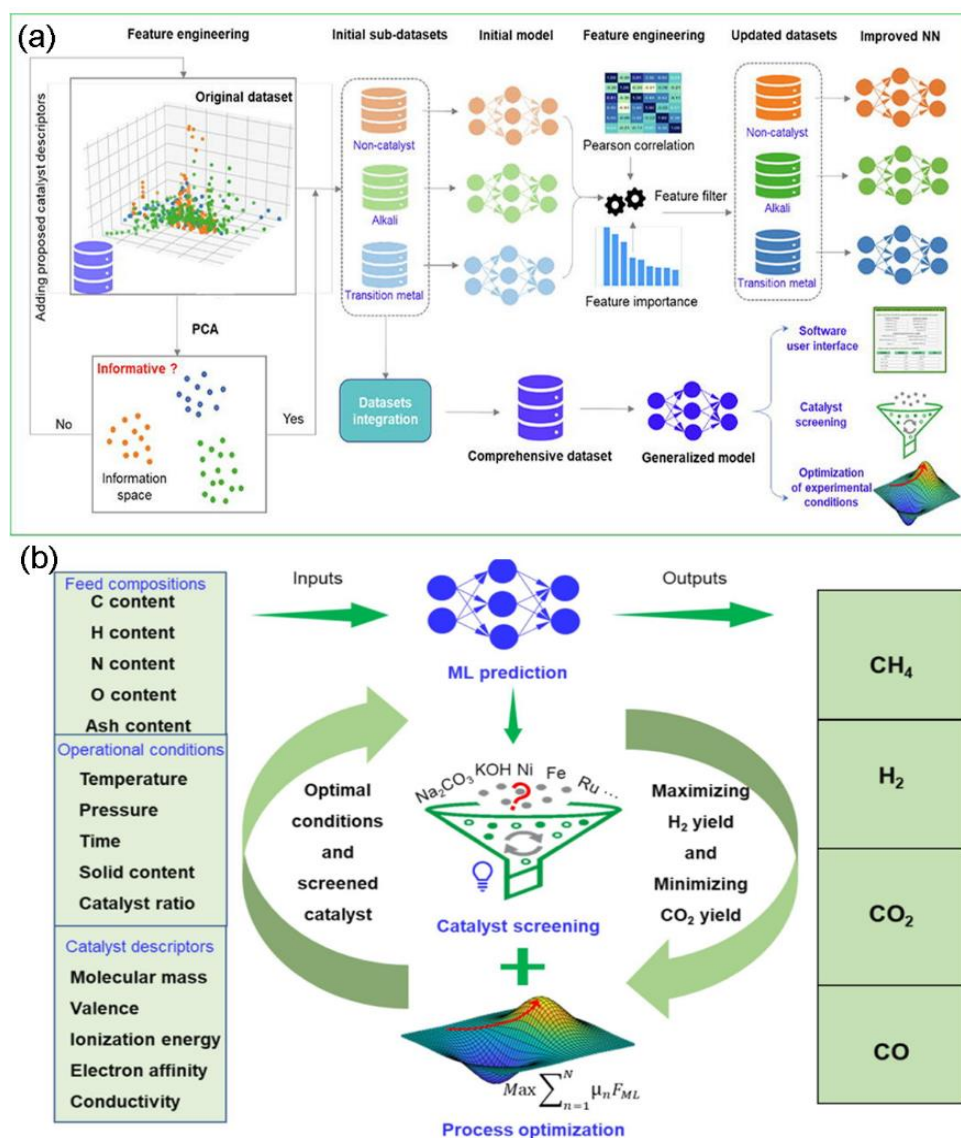
Figure 21 (a) A workflow of feature engineering assisted ML; (b) Schematic diagram of ML-aided optimization of operating conditions and catalyst screening for H_2-rich syngas production from supercritical water gasification. Adapted with permission from ref 277. Copyright 2021 Elsevier.

2.3.3.3 Coupling ML/DL with robotic platforms

With the latest development of robotic automation and computer-aided synthesis

planning, coupling computer AI with robotic platforms has led to exciting results in synthesis

route design and reaction condition optimization. Jensen and coworkers reported a robotic

continuous flow chemistry platform combining an AI-informed synthesis-planning module for the design of synthesis routes and robotic execution of high-throughput experiments[334]. The feedforward NN algorithm was trained to learn millions of reactions based on the existing database, which can propose the synthesis route for a given molecule, including optimal reaction conditions, and evaluate the best path according to the number of steps and predicted yield. Meanwhiles, there still exist several challenges in such a platform including the need for reduction of reaction time, reduction of solids formation to avoid clogging, difficult prediction of suitable purification methods especially for non-column chromatography, and the growing complexity in optimization of multi-step reaction due to the propagation of parameters. Moreover, scientists have also successfully achieved the combination of the robotic platform with Bayesian reaction optimization algorithms for applying to typical batch chemistry systems[335,336]. Doyle group developed a state-of-the-art easy-to-use parallelizable Bayesian-based software platform allowable for daily laboratory optimization of diverse types of reactions in typical batch processes[336]. In particular, researchers conducted a systematic comparison between the human decision-making and Bayesian method in reaction optimization based on a big benchmark dataset for palladium catalyzed direct arylation, as well as applications of Bayesian optimization to other reactions. Benchmarking is done through an online game that links the decisions made by professional chemists and engineers to daily laboratory experiments. It was found that Bayesian optimization is superior to human decision-making in average optimization efficiency (number of experiments) and consistency (variance between the results and initial available data). This study showed that using Bayesian optimization in daily laboratory practice can

promote more efficient reaction synthesis by making more informed, data-driven decisions about running experiments. Notably, there is an important limitation for such kind of study. Because it is assumed that all component variables have identical initial importance, and Bayesian optimization has certain blindness. Another important weakness is that the robotic search cannot capture the existing chemical knowledge, nor can include theoretical or physical models. From this perspective, future efforts should embed more prior knowledge (such as computed structures and properties) into the platform to make the current platform can behave more like a robotic chemist with a computational brain able to generate and test scientific hypotheses. In addition to organic reactions, recently there have been studies coupling the ML-assisted closed-loop optimization workflow of formulations with robotic experiments for automated DoEs[337] and an elaborate description of this robotic AI-informed formulation platform was well reviewed[338].

3. Summary

3.1 Conclusions

It has been a long-standing problem to find a proper methodology for targeting complex multiscale flow and reactor systems[339]. Nowadays, we are excited to witness a promising transformative paradigm induced by AI, especially ML, in data extraction, data analytics, data-driven modeling, and data management, which is useful for the discovery of unknown information/knowledge and innovation in different kinds of applications. Meanwhile, we realize that ML is not likely the solution to every problem in multiphase fields and it is not a complete replacement of the traditional methods. We emphasize again that ML is a valuable toolkit that complements incomplete domain-specific knowledge in conventional

experimental and traditional models. ML can also provide easy-to-use techniques to facilitate the conceptual development of new robust predictive data-driven, physics-informed, and hybrid models for multiphase processes by finding hidden information in a dataset. Besides, ML can assist to develop emerging analytical theories and mechanism-based causal explanations[3,340], a research area needed to be strengthened. Due to such emergence, we hence provide a comprehensive review, discussion and analysis of recent key advancements of ML applications to hydrodynamics, transport phenomena, and chemical reactions in single-phase/multiphase flows and reactors from different perspectives: (1) Development of closure models of drag force, turbulence stresses and heat/mass transfer for the averaged CFD simulations, and its acceleration; (2) Image reconstruction, regime identification, key parameter predictions and optimization of multiphase flow and transport fields; (3) Kinetics modeling (e.g., discovery of reaction networks, estimation of kinetic parameters and species source terms) and reaction conditions optimization. These parts primarily discuss, identify and analyze the advantages and weakness of ML for solving the challenging issues for multiphase flow and reactor systems.

3.2 Summary of challenges and opportunities

Here, we further summarize the under-addressing challenges and opportunities in order to provide future directions probably useful for our research community's study. Some important aspects are illustrated in **Figure 22**. In fact, some perspectives have been identified and discussed in the previous parts and here we mainly aim to provide an overview and analysis of challenges and opportunities of applications of ML in multiphase devices and systems. We summarize these separated aspects together in order to illustrate a better skeleton

for readers. We also hope this part might be viewed as a potential starting and guiding point for interested readers.
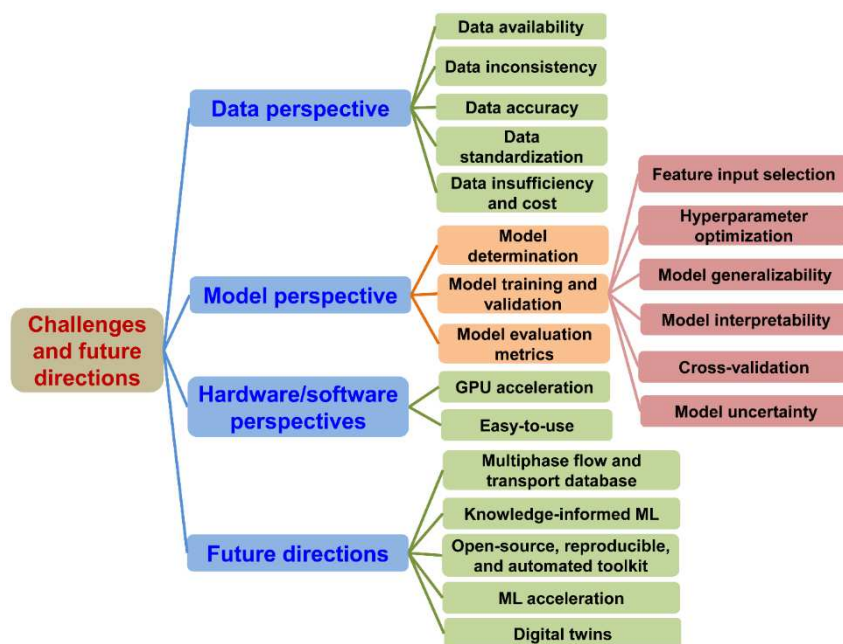
Figure 22 Some important aspects of challenges and future directions in applications of ML for chemical engineering and multiphase flows.

3.2.1 Data perspective.

(1) Data availability. the performance of pure ML-based data-driven models is severely dependent on the availability of homogeneously-distributed large datasets. The reaction database such as Reaxys and Scifinder and rapidly developed automated high-throughput flow-chemistry experimentation platforms have been available to provide large datasets. However, there has been no public, large database available for multiphase flows and transport. Future long-term efforts should be devoted to establishing large databases which store robust, reliable and homogeneous datasets with detailed descriptions accessible to the users. In the short term, an alternative strategy is that, if there is only a small data set available, it is also feasible to embed the prior knowledge into the ML structure to enhance its generalization performance and to avoid overfitting. Besides, to overcome the disadvantages

due to data insufficiency in some cases, researchers can utilize some advanced DL techniques such as transfer learning, in which, taking DNN as an example, one can pretrain a model served as starting network using the relevant large data set from a general database. Subsequently, the weights of the last few layers are trained and optimized again using the small dataset available in hand while the remaining network is kept frozen. Although such a transfer learning process is very clear, it is still challenging to determine which layers are retrained while the remaining is kept frozen. The study in this direction deserves more and more efforts in the future.

(2) Data inconsistency. For instance, although the gas-solid heat transfer rate in terms of Nusselt number can be well predicted by the data sets of Reynolds number, solid volume fraction and Prandtl number, these data sets may be collected from different sources of open reports based on different device configurations (e.g., horizontal or vertical; with or without internals), radius and height, and even based on different experimental techniques or different numerical simulations. In this situation, when attempting to train a model using the simulation data from the existing databases, one has to keep in mind whether the data were generated under the same or at least highly comparable operating conditions and device configurations[341].

(3) Data accuracy. Multiphase flow and transport experiments can be performed to generate data sets used for training and testing. However, due to the data from different experiments probably with different degrees of accuracy associated with the complexity of multiphase processes, the uncertainty in the experimental technique itself needs to be identified before the safe use of the measured data. If possible, a cross-study comparison of

different experimental methods should be conducted. Compared with data generated through experiments, the multiphase simulation is an efficient numerical tool with relatively low cost to produce the data for training and testing ML. However, the reliability and accuracy of a trained ML model employing data from simulations principally depends on the simulation itself's capability of approximating real experiments. That is, the use of simulation data leads to the difficulty for ML to go beyond the simulation accuracy. Thus, it is still an underexplored problem about the way to include the uncertainty of simulation data in the trained ML model.

In addition to data perspective above, it is also important that data sets should cover a broad range of the parameter space of the target problem in order to efficiently leveraging ML with confidence. In this case, a vital transformative paradigm for enlarging the amount of the data friendly to users is to standardize, normalize, or nondimensionalize the data format. This could contribute to the elimination of the errors caused by different dimensions, self-variation or large difference in values.

3.2.2 Model perspective

(1) Model determination. How to choose the best ML model for a given task of flow, transport and reaction problems? One noticeable evaluation metric is that the ML should be easily used, and require relatively less computational cost than the other candidate approaches while still maintaining its forecast reliability and accuracy. To some extent, the appropriateness for a given issue of interest does not solely depend on the sophistication of ML models and the increased complexity is not always better[8]. Another important aspect is that one has to be aware of the applicable characteristics of each ML technique corresponding

to a given problem. In addition, Selvaratnam and Koodali[342] suggested that automated ML tools (e.g., NN intelligence: https://github.com/microsoft/nni) could be applied for finding the best ML pipeline including the choice of model, approaches for data selection and transformation, and selection of hyperparameters. This strategy can be extended to multiphase flow and transport problems in the future work. In the case that only a small dataset is available, the choice of the unsupervised ML method, the supervised knowledge-informed ML, or other types of ML models could be effective to improve the prediction performance. One of typical examples in the context of unsupervised ML is to boost ML prediction capability through unsupervised contrastive pretraining that leverages small datasets of reactions[343]. It should also be noted that integrating ML with first principles models[344] will play an increasingly important role in diverse multiphase research areas.

(2) **Feature selection**. In a feature-target prediction problem, the selection of suitable feature inputs directly affects whether the ML model could be successfully trained. Despite the success of ML's applications, one remaining infancy is that training and development of a model are most often empirically driven. That is, the choice of feature quantities as ML inputs is mainly dependent on the user's domain expertise while more theoretical methods for feature selection still deserve further special attention. It is important to add the prior domain information and constraints as the feature inputs. This will not only ensure that the trained ML model obeys some physical or chemical knowledge but also contributes to a more generalizable and easier-to-train model. Another important consideration is that feature extraction of inputs by ML tools such as PCA can be performed to reduce the training complexity when handling high-dimensionality problems.

(3) Hyperparameter optimization. What depth or complexity of DL models? Or how to assign the suitable hyperparameters (e.g., the number of layers and number of nodes of each layer for NN; the number of trees and depth for RF) optimal for a specific data set? A critical point is that the higher complexity due to an increase of hyperparameters probably leads to the reduction of transparency and interpretability[8]. Noticeably, a higher number of hyperparameters also causes much longer training time. This issue is particularly true for the traditional NN algorithms. An important future research area is to develop general, automated tools to not only optimize the hyperparameters but also balance the depth/complexity and accuracy with tolerance.

(4) Model generalizability. How to ensure the generalizability of the trained ML model once the prediction is out of the scope of the data for training? Or how to train a model with extrapolative capability? One might keep in mind whether the solution to a given domain issue is still within the applicability range of the trained ML. For instance, if one constructs a predictive ML model, it should have the extrapolative ability to be generalizable to estimate spaces it has not "seen" during its prior training process. Only in the case that a trained model could at least partially generalize to what practitioners have not known, ML can then guide its applications in exploring unknown spaces in multiphase flow systems. To date, this is still a challenging problem, highlighting the necessity to give the priority of extrapolation as a measure of the trained model performance.

(5) Model interpretability. Up to now, many ML techniques have been applied for predicting key parameters or modeling closures for multiphase flow and transport systems, which have been demonstrated to outperform the traditional empirical correlations. However,

most ML models relatively lack physical interpretability because of their high dimensionality and nonlinearity although they are predictive and the feature inputs of ML can be physically motivated[10]. The recently proposed knowledge-informed ML further motivates the users to embed the additional physical or reactive knowledge into the ML architecture according to specific multiphase application scenarios, which will make the ML more robust, interpretable and generalizable. When re-designing the ML structure, one also has to balance the model complexity and interpretability. This is because the increases of interpretability will be accompanied by the increase in the structural complexity of ML. One potential direction is to develop optimization algorithms that can optimize the multiphase model performance (e.g., robustness, interpretability and generalization and computation cost) to achieve the "Pareto optimality". Finally, to achieve the goal of applying ML in decision making, the multiphase flow developers should try to make the prediction results more explainable and help users understand the fundamentals behind the decision.

(6) Model uncertainty. The origin of model uncertainty may include but not limited to model form, model parameter, model input, numerical approximation, and ML itself. How to establish a systematic method for quantification of the uncertainty induced by ML itself and multiphase data itself? Furthermore, how to determine the relative errors of ML models? It again comes back to the first question: which ML technique is the best for a given problem? It is advisable to explore ML's best range of applicability through more elaborate and rigorous comparisons of representative ML approaches as well as well-established traditional methods (e.g., computationally-demanding but high-precision numerical methods as baseline) so that disadvantages and advantages (e.g., in cost and accuracy) are clear. Some recent

studies[345-348] have increasingly promoted the development of relevant research areas and more efforts are suggested to contribute to better understanding and quantifying model uncertainty.

3.3 Future directions

After summarizing the shared challenges or the specific challenges in the domains of multiphase flows and reactors, several focused points for promising future directions are further presented below:

Future direction 1. Future efforts should establish *a large-scale, high-quality database* from highly-resolved simulations or high-resolution measurements, which can be used for developing more robust and generalizable closures for coarse simulations. In particular, the uncertainty in data should also be provided. Furthermore, *a large multiphase flow and transport (image) base* should also be established for regime identification and key parameter predictions. These large, homogeneous datasets covering a wide range of flow and transport conditions can be beneficial to better understanding of multiphase characteristics and rational design of multiphase devices.

Future direction 2. Physics-informed ML/DL, especially PINN, is a very promising, important future research field. Integrating the physical, chemical and mathematical knowledge into the ML structure can make the trained ML more explainable and generalizable with confidence for various multiphase flow and reactor systems even spanning a wide range of the flow, transport and reaction conditions.

Future direction 3. Development of open-source, reproducible, and automated toolkit, e.g., Augmented Reality (AR) and Mixed Reality (MR) based technologies, for

targeting multiphase flow and transport problems is required for realizing the practical value of ML in chemical engineering and multiphase flows. We note that there have been many automated robotic optimization platforms in the context of chemical reaction space. However, such a promising robotic platform for multiphase flow design of high-throughput experiments has received much less attention. This research direction is to develop automated optimization tools able to simultaneously optimize the hyperparameters of ML, model parameters of traditional physical models and the key flow and transport parameters.

Future direction 4. ML-based acceleration of computation is of critical importance for the practical use of numerical simulations for engineering design of multiphase devices. In particular, the CFD simulation of large-scale multiphase flow devices is very time-consuming and has been a long-standing, bottle-neck problem in chemical engineering and multiphase flows. A potential research direction is to correct or partially replace the traditional solver component mostly influencing the resolution loss in high-fidelity simulations, so that the learned interpolation and correction can be used in coarse simulations without sacrificing accuracy or generalization.

Future direction 5. Digital twin refers to the establishment of a dynamic virtual model of the physical entity through digital means, and the realization of simulation and mapping of real, multi-dimensional, multi-scale, multi-physical quantity attributes and behavior information of the physical entity in virtual space[349]. In recent years, with the rapid development of digital-based AI, engineering simulations, data fusion and analytics, and other emerging technologies (e.g., VR: Virtual reality; AR: Augmented reality), digital twin as a digital transformation technology has attracted more and more attentions[350,351]. In

particular, digital twin has achieved practical industrial application in aerospace[352], and process engineering industry represented by petrochemical industry[353]. From the perspective of multiphase flow and reactor engineering, the digital twin platform that is a combination of the digital processes and physical processes, involving modeling toolkit and experimental toolkit, is rarely reported in the literature. Such a mechanistic-AI augmented digital-twin platform for multiphase system engineering is illustrated in **Figure 23**. Notably, internet of things and metaverse can realize interconnection and creation that maps and interacts with the real world and a digital operating space with multiphase flow systems, and enables all ordinary objects in digital process and physical process to perform independent functions.
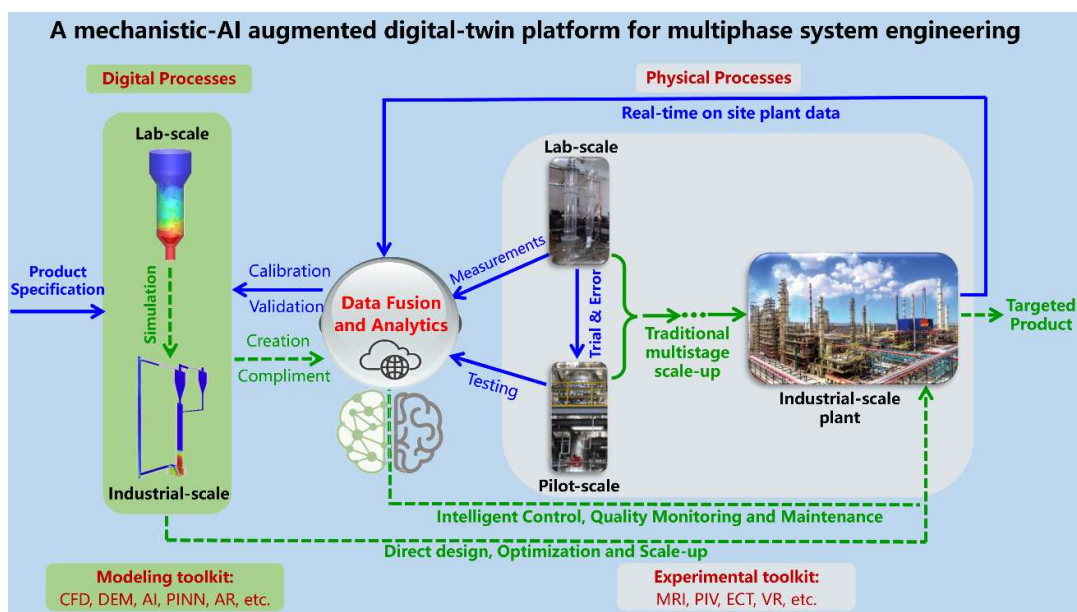
Figure 23 A mechanistic-AI augmented digital-twin platform for multiphase system engineering. The lab-scale simulation contour in the upper left was adapted with permission from ref 25. Copyright 2016 American Chemical Society. The industrial-scale simulation contour in the lower left was adapted with permission from ref 47. Copyright 2021 Elsevier. The pilot-scale reactor figure in the lower middle was adapted with permission from ref 354. Copyright 2015 Elsevier. The rightmost industrial-scale plant figure was adapted from ref 355. Copyright 2021 Elsevier. An open access article distributed under the terms of the Creative Commons CC BY license.

Finally, we would like to emphasize again that future development and research of multiphase flow reactors are envisaged to be accelerated by AI, especially ML. Overall, the

ultimate goal of ML applications is for more efficient and effective design, scale-up, optimization, and control of multiphase devices and systems. It is optimistic that ML will play a much larger impactful role in the fields of multiphase flow, transport and reaction processes in the coming years.

Acknowledgments

Supporting Information

Figure S1: The searched annual number of publications using the keywords such as 'Machine learning fluid dynamics' and 'Machine learning heat transfer'. **Figure S2**: Three types of fitting performance in a common regression and classification learning operation. Figure S3 Illustration of the survey processes and review summary. **Table S1**: Summary of typical ML algorithms for multiphase flows and devices. **Table S2**: Common activation functions, loss functions and optimizers of ML. **Table S3**: ML for processing flow images from the data measured by various experimental techniques. **Table S4**: ML for prediction of key flow and transport parameters. **Table S5**: ML for optimization of multiphase cyclone separators.

Abbreviations of machine learning algorithms

ANN: Artificial neural network

BO: Bayesian optimization

BP: Bayesian process

BPNN: Backpropagation neural network

CNN: Convolutional neural networks

CART: Classification and regression tree

DNN: deep neural networks

DT: Decision trees

FNN: Feedforward neural network

FCNN: Fully connected neural networks

GA: Genetic algorithm

GAN: Generative adversarial network

GBDT: Gradient boosting decision tree

GBoost: Gradient boosting

GPR: Gaussian process regression

GRU: Gated recurrent units

KNN: K-nearest neighbors

LNN: Linear nearest neighbor

LSTM: Long short-term memory network

NSGA-II: Non-dominated sorting genetic algorithm-II

RVR: relevance vector regression

PCA: principal component analysis

PINN: Physics-informed neural networks

POD: Proper orthogonal decomposition

RBFNN: Radial basis function neural network

RF: Random Forest

RNN: Recurrent neural networks

SOM: self-organizing map

SVM: Support vector machine

SVR: Support vector regression

XGBoost: eXtreme gradient boosting

References

1. Samuel, A. L. Some studies in machine learning using the game of checkers. *IBM J. Res. Dev.* **1959**, *3* (3), 210-229.

2. Mitchell, T. M. Machine Learning; McGraw-Hill, **1997**.

3. Venkatasubramanian, V. The promise of artificial intelligence in chemical engineering: Is it here, finally? *AIChE J.* **2019**, *65* (2), 466-478.

4. Haghighatlari, M.; Hachmann, J. Advances of machine learning in molecular modeling and simulation. *Curr. Opin. Chem. Eng.* **2019**, *23*, 51-57.

5. Brunton, S. L.; Noack, B. R.; Koumoutsakos, P. Machine learning for fluid mechanics. *Annu. Rev. Fluid Mech*. **2020**, 52, 477-508.

6. Beck, D. A.; Carothers, J. M.; Subramanian, V. R.; Pfaendtner, J. Data science: Accelerating innovation and discovery in chemical engineering. *AIChE J.* **2016**, *62* (5), 1402-1416.

7. Ding, J.; Xu, N.; Nguyen, M. T.; Qiao, Q.; Shi, Y.; He, Y.; Shao, Q. Machine learning for molecular thermodynamics. *Chin. J. Chem. Eng.* **2021**, *31*, 227-239.

8. Artrith, N.; Butler, K. T.; Coudert, F. X.; Han, S.; Isayev, O.; Jain, A.; Walsh, A. Best practices in machine learning for chemistry. *Nat. Chem.* **2021**, *13* (6), 505-508.

9. Weber, J. M.; Guo, Z.; Zhang, C.; Schweidtmann, A. M.; Lapkin, A. A. Chemical data intelligence for sustainable chemistry. *Chem. Soc. Rev.* **2021**, *50*, 12013-12036.

10. Goldsmith, B. R.; Esterhuizen, J.; Liu, J. X.; Bartel, C. J.; Sutton, C. Machine learning for heterogeneous catalyst design and discovery. *AIChE J.* **2018**, *64* (7), 2311-2323.

11. Ma, S.; Liu, Z. P. Machine learning for atomic simulation and activity prediction in heterogeneous catalysis: Current status and future. *ACS Catalysis*, **2020**, *10* (22), 13213-13226.

12. Guan, Y.; Chaffart, D.; Liu, G.; et al. Machine learning in solid heterogeneous catalysis: Recent developments, challenges and perspectives. *Chem. Eng. Sci*. **2022**, *248*, 117224.

13. Raccuglia, P.; Elbert, K. C.; Adler, P. D.; et al. Machine-learning-assisted materials discovery using failed experiments. *Nature*, **2016**, *533* (7601), 73-76.

14. Jackson, N. E.; Webb, M.A.; de Pablo, J.J. Recent advances in machine learning towards multiscale soft materials design. *Curr. Opin. Chem. Eng*. **2019**, *23*, 106-114.

15. Duraisamy, K.; Iaccarino, G.; Xiao, H. Turbulence modeling in the age of data. *Annu. Rev. Fluid Mech.* **2019**, *51*, 357-377.

16. Wang, B.; Wang, J. Application of Artificial Intelligence in Computational Fluid Dynamics. *Ind. Eng. Chem. Res.* **2021**, *60* (7), 2772-2790.

17. Chiang, L.; Lu, B.; Castillo, I. Big data analytics in chemical engineering. *Annu. Rev. Chem. Biomol. Eng.* **2017**, *8*, 63-85.

18. Karniadakis, G. E.; Kevrekidis, I. G.; Lu, L.; Perdikaris, P.; Wang, S.; Yang, L. Physics-informed machine learning. *Nat. Rev. Phys.* 2021, *3* (6), 422-440.

19. Sundaresan, S.; Ozel, A.; Kolehmainen, J. Toward constitutive models for momentum, species, and energy transport in gas–particle flows. *Annu. Rev. Chem. Biomol. Eng*. **2018**, *9*, 61-81.

20. Dixon, A. G.; Partopour, B. Computational fluid dynamics for fixed bed reactor design. *Annu. Rev. Chem. Biomol*. Eng., **2020**, *11*, 109-130.

21. Woo, M.; Stettler, M. E. Feasibility study on the use of artificial neural networks to model catalytic oxidation in a metallic foam reactor. *Ind. Eng. Chem. Res.* **2021**, 60(43), 15416-15427.

22. Lu, L.; Meng, X.; Mao, Z.; Karniadakis, G. E. DeepXDE: A deep learning library for solving differential equations. *SIAM Rev.* **2021**, *63* (1), 208-228.

23. Lagaris, I. E.; Likas, A.; Fotiadis, D. I. Artificial neural networks for solving ordinary and partial differential equations. *IEEE Trans. Neural Netw.* **1998**, *9* (5), 987-1000.

24. Coley, C. W.; Eyke, N. S.; Jensen, K. F. Autonomous discovery in the chemical sciences part I: Progress. *Angew. Chem. Int. Ed*. **2020**, *59* (51), 22858-22893.

25. Zhu, L. T.; Ye, M.; Luo, Z. H. Application of filtered model for reacting gas–solid flows and optimization in a large-scale methanol-to-olefin fluidized-bed reactor. *Ind. Eng. Chem. Res.* **2016**, *55* (46), 11887-11899.

26. Seyed-Ahmadi, A.; Wachs, A. Microstructure-informed probability-driven point-particle model for hydrodynamic forces and torques in particle-laden flows. *J. Fluid Mech.* **2020**, *900*, A12.

27. Deen, N. G.; Peters, E. A. J. F.; Padding, J. T.; Kuipers, J. A. M. Review of direct numerical simulation of fluid–particle mass, momentum and heat transfer in dense gas–solid flows. *Chem. Eng. Sci.* **2014**, *116*, 710-724.

28. Fox, R. O. Large-eddy-simulation tools for multiphase flows. *Annu. Rev. Fluid Mech.* **2012**, *44*, 47-76.

29. Wang, J. X.; Wu, J. L.; Xiao, H. Physics-informed machine learning approach for

reconstructing Reynolds stress modeling discrepancies based on DNS data. *Phys. Rev. Fluids*, **2017**, *2* (3), 034603.

30. Gidaspow, D. Multiphase flow and fluidization: continuum and kinetic theory descriptions. Academic press, **1994**.

31. Lei, H.; Zhu, L. T.; Luo, Z. H. Study of filtered interphase heat transfer using highly resolved CFD–DEM simulations. *AIChE J.* **2021**, *67* (4), e17121.

32. Esteghamatian, A.; Bernard, M.; Lance, M.; Hammouti, A.; Wachs, A. Micro/meso simulation of a fluidized bed in a homogeneous bubbling regime. *Int. J. Multiphase Flow* **2017**, *92*, 93-111.

33. Willard, J.; Jia, X.; Xu, S.; Steinbach, M.; Kumar, V. Integrating physics-based modeling with machine learning: A survey. *arXiv preprint arXiv: 2003.04919*, **2020**, *1* (1) 04919.

34. Zhu, L. T.; Chen, X. Z.; Luo, Z. H. Analysis and development of homogeneous drag closure for filtered mesoscale modeling of fluidized gas-particle flows. *Chem. Eng. Sci.* **2021**, *229*, 116147.

35. He, L.; Tafti, D.K. A supervisd machine learning approach for predicting variable drag forces on spherical particles in suspension. *Powder Technol*. **2019**, *345*, 379-389.

36. Jiang, Y.; Kolehmainen, J.; Gu, Y.; Kevrekidis, Y. G.; Ozel, A.; Sundaresan, S. Neural-network-based filtered drag model for gas-particle flows. *Powder Technol*. **2019**, *346*, 403-413.

37. Muralidhar, N.; Bu, J.; Cao, Z.; He, L.; Ramakrishnan, N.; Tafti, D.; Karpatne, A. Physics-guided deep learning for drag force prediction in dense fluid-particulate systems. *Big Data*, **2020**, *8* (5), 431-449.

38. Zhu, L. T.; Tang, J. X.; Luo, Z. H. Machine learning to assist filtered two-fluid model development for dense gas-particle flows. *AIChE J*. **2020**, *66* (6), e16973.

39. Nikolopoulos, A.; Samlis, C.; Zeneli, M.; Nikolopoulos, N.; Karellas, S.; Grammelis, P. Introducing an artificial neural network energy minimization multi-scale drag scheme for fluidized particles. *Chem. Eng. Sci*. **2021**, *229*, 116013.

40. Singh, A. P.; Medida, S.; Duraisamy, K. Machine-learning-augmented predictive modeling of turbulent separated flows over airfoils. *AIAA J*. **2017**, *55* (7), 2215-2227.

41. Yuan, Z.; Xie, C.; Wang, J. Deconvolutional artificial neural network models for large

eddy simulation of turbulence. *Phys. Fluids* **2020**, *32* (11), 115106.

42. Ling, J.; Kurzawski, A.; Templeton, J. Reynolds averaged turbulence modelling using deep neural networks with embedded invariance. *J. Fluid Mech.* **2016**, *807*, 155-166.

43. Ouyang B.; Zhu L. T.; Luo Z. H. Data-driven modeling of mesoscale solids stress closures for filtered two-fluid model in gas-particle flows. *AIChE J.* **2021**, *67* (7), e17290.

44. Kojić, P.; Omorjan, R. Predicting hydrodynamic parameters and volumetric gas–liquid mass transfer coefficient in an external-loop airlift reactor by support vector regression. *Chem. Eng. Res. Des.* **2017**, *125*, 398-407.

45. Zhu, L. T.; Ouyang, B.; Lei, H.; Luo, Z. H. Conventional and data-driven modeling of filtered drag, heat transfer and reaction rate in gas-particle flows. *AIChE J.* **2021**, *67* (8), e17299.

46. Wachs, A.; Hammouti, A.; Vinay, G.; Rahmani, M. Accuracy of finite volume/staggered grid distributed Lagrange multiplier/fictitious domain simulations of particulate flows. *Comput. Fluids*, **2015**, *115*, 154-172.

47. Li, J. S.; Zhu, L. T.; Yan, W. C.; Rashid, T. A. B.; Xu, Q. J.; Luo, Z. H. Coarse-grid simulations of full-loop gas-solid flows using a hybrid drag model: Investigations on turbulence models. *Powder Technol.* **2021**, *379*, 108-126.

48. Wang, W.; Lu, B.; Geng, J.; Li, F. Mesoscale drag modeling: a critical review. *Curr. Opin. Chem. Eng.* **2020**, *29*, 96-103.

49. Tafti, D. K. GenIDLEST-a scalable parallel computational tool for simulating complex turbulent flows, *Proc. ASME Int. Mech. Eng. Congr. Expo.* **2001**, *35722*, 347-356.

50. Yan, S.; He, Y.; Tang, T.; Wang, T. Drag coefficient prediction for non-spherical particles in dense gas–solid two-phase flow using artificial neural network. *Powder Technol.* **2019**, *354*, 115-124.

51. Hwang, S.; Pan, J.; Fan, L. S. A machine learning-based interaction force model for non-spherical and irregular particles in low Reynolds number incompressible flows. *Powder Technol.* **2021**, *392*, 632-638.

52. Ma, L.; Guo, Q.; Li, X.; Xu, S.; Zhou, J.; Ye, M.; Liu, Z. Drag correlations for flow past monodisperse arrays of spheres and porous spheres based on symbolic regression: effects of permeability, *Chem. Eng. J.* **2022**, 136653.

53. Luo, K.; Wang, D.; Jin, T.; Wang, S.; Wang, Z.; Tan, J.; Fan, J. Analysis and development of novel data-driven drag models based on direct numerical simulations of fluidized beds. *Chem. Eng. Sci.* **2021**, *231*, 116245.

54. Geldart, D. Types of gas fluidization. *Powder Technol.* **1973**, *7* (5), 285-292.

55. Zhang, Y.; Jiang, M.; Chen, X.; Yu, Y.; Zhou, Q. Modeling of the filtered drag force in gas–solid flows via a deep learning approach. *Chem. Eng. Sci.* **2020**, *225*, 115835.

56. Lu, L.; Gao, X.; Dietiker, J. F.; Shahnam, M.; Rogers, W. A. Development of a filtered CFD-DEM drag model with multiscale markers using an artificial neural network and nonlinear regression. *Ind. Eng. Chem. Res.* **2022**, *61* (1), 882–893.

57. Jiang, Y.; Chen, X.; Kolehmainen, J.; Kevrekidis, I. G.; Ozel, A.; Sundaresan, S. Development of data-driven filtered drag model for industrial-scale fluidized beds. *Chem. Eng. Sci.* **2021**, *230,* 116235.

58. Yang, Z.; Lu, B.; Wang, W. Coupling artificial neural network with EMMS drag for simulation of dense fluidized beds. *Chem. Eng. Sci.* **2021**, *246*, 117003.

59. Raissi, M.; Perdikaris, P.; Karniadakis, G. E. Physics-informed neural networks: A deep learning framework for solving forward and inverse problems involving nonlinear partial differential equations. *J. Comput. Phys.* **2019**, *378*, 686-707.

60. Moore, W. C.; Balachandar, S.; Akiki, G. A hybrid point-particle force model that combines physical and data-driven approaches. *J. Comput. Phys*. **2019**, *385*, 187-208.

61. Akiki, G.; Jackson, T. L.; Balachandar, S. Pairwise interaction extended point-particle model for a random array of monodisperse spheres. *J. Fluid Mech*. **2017**, *813*, 882-928.

62. Seyed-Ahmadi, A.; Wachs, A. Physics-inspired architecture for neural network modeling of forces and torques in particle-laden flows. *Comput. Fluids*, **2022**, *238*, 105379.

63. Iskhakov, A. S.; Dinh, N. T. Review of physics-based and data-driven multiscale simulation methods for computational fluid dynamics and nuclear thermal hydraulics. *arXiv preprint arXiv: 2102.01159*. **2021**.

64. Kennedy, D. 125. *Science*, **2005**, *309* (5731), 19-19.

65. Pandey, S.; Schumacher, J.; Sreenivasan, K. R. A perspective on machine learning in turbulent flows. *J. Turbul*. **2020**, *21* (9-10), 567-584.

66. Kutz, J. N. Deep learning in fluid dynamics. *J. Fluid Mech.* **2017**, *814*, 1-4.

67. Parish, E. J.; Duraisamy, K. A paradigm for data-driven predictive modeling using field inversion and machine learning. *J. Comput. Phys*. **2016**, *305*, 758-774.

68. Xiao, H.; Wu, J. L.; Wang, J. X.; Sun, R.; Roy, C. J. Quantifying and reducing model-form uncertainties in Reynolds-averaged Navier–Stokes simulations: A data-driven, physics-informed Bayesian approach. *J. Comput. Phys*. **2016**, *324*, 115-136.

69. Sarghini, F.; De Felice, G.; Santini, S. Neural networks based subgrid scale modeling in large eddy simulations. *Comput. Fluids*, **2003**, *32* (1), 97-108.

70. Wang, Z.; Luo, K.; Li, D.; Tan, J.; Fan, J. Investigations of data-driven closure for subgrid-scale stress in large-eddy simulation. *Phys. Fluids* **2018**, *30* (12), 125101.

71. Zhu, L.; Zhang, W.; Kou, J.; Liu, Y. Machine learning methods for turbulence modeling in subsonic flows around airfoils. *Phys. Fluids* **2019**, *31* (1), 015105.

72. Fang, R.; Sondak, D.; Protopapas, P.; Succi, S. Neural network models for the anisotropic Reynolds stress tensor in turbulent channel flow. *J. Turbul*. **2020**, *21* (9-10), 525-543.

73. Wu, J. L.; Xiao, H.; Paterson, E. Physics-informed machine learning approach for augmenting turbulence models: A comprehensive framework. *Phys. Rev. Fluids*, **2018**, *3* (7), 074602.

74. Park, J.; Choi, H. Toward neural-network-based large eddy simulation: application to turbulent channel flow. *J. Fluid Mech*. **2021**, *914*, A16.

75. Freund, A.; Ferrante, A. Large-eddy simulation of droplet-laden decaying isotropic turbulence using artificial neural networks. *Int. J. Multiphase Flow*, **2021**, *142*, 103704.

76. Yarlanki, S.; Rajendran, B.; Hamann, H. Estimation of turbulence closure coefficients for data centers using machine learning algorithms. *13th InterSociety Conference on Thermal and Thermomechanical Phenomena in Electronic Systems*. *IEEE*. **2012**, 38-42.

77. Matai, R.; Durbin, P. A. Zonal eddy viscosity models based on machine learning. *Flow, Turbul. Combust*. **2019**, *103* (1), 93-109.

78. Xie, C.; Yuan, Z.; Wang, J. Artificial neural network-based nonlinear algebraic models for large eddy simulation of turbulence. *Phys. Fluids* **2020**, *32* (11), 115101.

79. Stolz, S.; Adams, N. A. An approximate deconvolution procedure for large-eddy simulation. *Phys. Fluids* **1999**, *11* (7), 1699-1701.

80. Jiang, C.; Vinuesa, R.; Chen, R.; Mi, J.; Laima, S.; Li, H. An interpretable framework of

data-driven turbulence modeling using deep neural networks. *Phys. Fluids* **2021**, *33*, 055133.

81. Tracey, B. D.; Duraisamy, K.; Alonso, J. J. A machine learning strategy to assist turbulence model development. *53rd AIAA aerospace sciences meeting*, **2015**,1287.

82. Ma, M.; Lu, J.; Tryggvason, G. Using statistical learning to close two-fluid multiphase flow equations for a simple bubbly system. *Phys. Fluids* **2015**, *27* (9), 092101.

83. Ma, M.; Lu, J.; Tryggvason, G. Using statistical learning to close two-fluid multiphase flow equations for bubbly flows in vertical channels. *Int. J. Multiphase Flow*, **2016**, *85*, 336-347.

84. Babanezhad, M.; Pishnamazi, M.; Marjani, A.; Shirazian, S. Bubbly flow prediction with randomized neural cells artificial learning and fuzzy systems based on k–ε turbulence and Eulerian model data set. *Sci. Rep.* **2020**, *10* (1), 1-12.

85. Ouyang, B.; Zhu, L. T.; Su, Y. H.; Luo, Z. H. A hybrid mesoscale closure combining CFD and deep learning for coarse-grid prediction of gas-particle flow dynamics. *Chem. Eng. Sci.* **2022**, *248*, 117268.

86. Gao, X.; Li, T.; Rogers, W.A. Assessment of mesoscale solid stress in coarse-grid TFM simulation of Geldart A particles in all fluidization regimes. *AIChE J.* **2018**, *64* (10), 3565-3581.

87. Beetham, S.; Capecelatro, J. Formulating turbulence closures using sparse regression with embedded form invariance. *Phys. Rev. Fluids*, **2020**, *5* (8), 084611.

88. Weatheritt, J.; Sandberg, R. D. The development of algebraic stress models using a novel evolutionary algorithm. *Int. J. Heat Fluid Flow*, **2017**, *68*, 298-318.

89. Beetham, S.; Fox, R. O.; Capecelatro, J. Sparse identification of multiphase turbulence closures for coupled fluid–particle flows. *J. Fluid Mech.* **2021**, *914*, A11.

90. Hughes, M. T.; Kini, G.; Garimella, S. Status, Challenges, and potential for machine learning in understanding and applying heat transfer phenomena. *J. Heat Transfer*. **2021**, *143* (12), 120802.

91. Sobhanifar, N.; Ahmadloo, E.; Azizi, S. Prediction of two-phase heat transfer coefficients in a horizontal pipe for different inclined positions with artificial neural networks. *J. Heat Transfer*, **2015**, *137* (6), 061009.

92. Liu, Y.; Dinh, N.; Sato, Y.; Niceno, B. Data-driven modeling for boiling heat transfer:

using deep neural networks and high-fidelity simulation results. *Appl. Therm. Eng.* **2018**, *144*, 305-320.

93. Huang, J.; Zheng, G.; Li, M.; Xiao, Q.; Wang, H. Assessing the effects of fluids flow on heat transfer performance in direct contact heat transfer process through EMD-LSSVM model: An experimental study. *Appl. Therm. Eng*. **2021**, *189*, 116732.

94. Zhang, W.; Xie, P.; Li, Y.; Zhu, J. A machine learning model for predicting the mass transfer performance of rotating packed beds based on a least squares support vector machine approach. *Chem. Eng. Process*. **2021**, *165*, 108432.

95. Saeedan, M.; Nazar, A. R. S.; Abbasi, Y., Karimi, R. CFD Investigation and neutral network modeling of heat transfer and pressure drop of nanofluids in double pipe helically baffled heat exchanger with a 3-D fined tube. *Appl. Therm. Eng*. **2016**, *100*, 721-729.

96. Zhao, Z.; Wang, J.; Sun, B.; Arowo, M.; Shao, L. Mass transfer study of water deoxygenation in a rotor–stator reactor based on principal component regression method. *Chem. Eng. Res. Des*. **2018**, *132*, 677-685.

97. Xu, X.; Ooi, A. S.; Sandberg, R. D. Data-driven algebraic models of the turbulent Prandtl number for buoyancy-affected flow near a vertical surface. *Int. J. Heat Mass Transf.* **2021**, *179*, 121737.

98. Bansal, S.; Roy, S.; Larachi, F. Support vector regression models for trickle bed reactors. *Chem. Eng. J.* **2012**, *207*, 822-831.

99. Zhou, L.; Garg, D.; Qiu, Y.; Kim, S. M.; Mudawar, I.; Kharangate, C. R. Machine learning algorithms to predict flow condensation heat transfer coefficient in mini/micro-channel utilizing universal data. *Int. J. Heat Mass Transf.* **2020**, *162*, 120351.

100. Kwon, B.; Ejaz, F.; Hwang, L. K. Machine learning for heat transfer correlations. *Int. Commun. Heat Mass Transfer*, **2020**, *116*, 104694.

101. Qian, N.; Wang, X.; Fu, Y.; Zhao, Z.; Xu, J.; Chen, J. Predicting heat transfer of oscillating heat pipes for machining processes based on extreme gradient boosting algorithm. *Appl. Therm. Eng*. **2020**, *164*, 114521.

102. Alizadeh, R.; Mohebbi Najm Abad, J.; Fattahi, A.; Alhajri, E.; Karimi, N. Application of machine learning to investigation of heat and mass transfer over a cylinder surrounded by porous media—The radial basic function network. *J. Energy Resour. Technol.*

2020, *142* (11), 112109.

103.   Wei, H.; Bao, H.; Ruan, X. Machine learning prediction of thermal transport in porous media with physics-based descriptors. *Int. J. Heat Mass Transf*. **2020**, *160*, 120176.

104.   Su, Y.; Ng, T.; Li, Z.; Davidson, J. H. Sparse scattered high performance computing data driven artificial neural networks for multi-dimensional optimization of buoyancy driven heat and mass transfer in porous structures. *Chem. Eng. J.* **2020**, *397*, 125257.

105.   Marcato, A.; Boccardo, G.s Marchisio, D. A computational workflow to study particle transport and filtration in porous media: coupling CFD and deep learning. *Chem. Eng. J.* **2021**, *417*, 128936.

106.   Partopour, B.; Dixon, A. G. 110th anniversary: commentary: CFD as a modeling tool for fixed bed reactors. *Ind. Eng. Chem. Res*. **2019**, *58* (14), 5733-5736.

107.   Cai, S.; Wang, Z.; Wang, S.; Perdikaris, P.; Karniadakis, G. E. Physics-informed neural networks for heat transfer problems. *J. Heat Transfer*, **2021**, *143* (6), 060801.

108.   Zobeiry, N.; Humfeld, K. D. A physics-informed machine learning approach for solving heat transfer equation in advanced manufacturing and engineering applications. *Eng. Appl. Artif. Intell.* **2021**, *101*, 104232.

109.   Holland, J. R.; Baeder, J. D.; Duraisamy, K. Towards integrated field inversion and machine learning with embedded neural networks for rans modeling. In AIAA Scitech **2019** Forum (P. 1884).

110.   Sekar, V.; Jiang, Q.; Shu, C.; Khoo, B. C. Fast flow field prediction over airfoils using deep learning approach. *Phys. Fluids* **2019**, *31* (5), 057103.

111.   Zhao, X.; Luo, T.; Jin, H. Predicting diffusion coefficients of binary and ternary supercritical water mixtures via machine and transfer learning with deep neural network. *Ind. Eng. Chem. Res.* **2022**.

112.   Lemoine, R.; Morsi, B. I. An algorithm for predicting the hydrodynamic and mass transfer parameters in agitated reactors. *Chem. Eng. J.* **2005**, *114* (1-3), 9-31.

113.   Lemoine, R.; Behkish, A.; Sehabiague, L.; Heintz, Y. J.; Oukaci, R.; Morsi, B. I. An algorithm for predicting the hydrodynamic and mass transfer parameters in bubble column and slurry bubble column reactors. *Fuel Process. Technol.* **2008**, *89* (4), 322-343.

114.   Gandhi, A. B.; Gupta, P. P.; Joshi, J. B.; Jayaraman, V. K.; Kulkarni, B. D.

Development of unified correlations for volumetric mass-transfer coefficient and effective interfacial area in bubble column reactors for various gas− liquid systems using support vector regression. *Ind. Eng. Chem. Res.* **2009**, *48* (9), 4216-4236.

115. Bansal, S.; Roy, S.; Larachi, F. Support vector regression models for trickle bed reactors. *Chem. Eng. J.* **2012**, *207*, 822-831.

116. Patel, H. V.; Panda, A.; Kuipers, J. A. M.; Peters, E. A. J. F. Computing interface curvature from volume fractions: A machine learning approach. *Comput. Fluids*, **2019**, *193*, 104263.

117. Qi, Y.; Lu, J.; Scardovelli, R.; Zaleski, S.; Tryggvason, G. Computing curvature for volume of fluid methods using machine learning. *J. Comput. Phys.* **2019**, *377*, 155-161.

118. Theßeling, C.; Grünewald, M.; Biessey, P. Determination of bubble sizes in bubble column reactors with machine learning regression methods. *Chem. Eng. Res. Des*. **2020**, *163*, 47-57.

119. Ganti, H.; Khare, P. Data-driven surrogate modeling of multiphase flows using machine learning techniques. *Comput. Fluids*, **2020**, *211*, 104626.

120. Bao, H.; Feng, J.; Dinh, N.; Zhang, H. Computationally efficient CFD prediction of bubbly flow using physics-guided deep learning. *Int. J. Multiphase Flow*, **2020**, *131*, 103378.

121. Bao, H.; Feng, J.; Dinh, N.; Zhang, H. Deep learning interfacial momentum closures in coarse-mesh CFD two-phase flow simulation using validation data. *Int. J. Multiphase Flow*, **2021**, *135*, 103489.

122. Bao, H.; Dinh, N. T.; Lane, J. W.; Youngblood, R. W. A data-driven framework for error estimation and mesh-model optimization in system-level thermal-hydraulic simulation. *Nucl. Eng. Des.* **2019**, *349*, 27-45.

123. Silva, V. L. S.; Salinas, P.; Jackson, M. D.; Pain, C. C. Machine learning acceleration for nonlinear solvers applied to multiphase porous media flow. *Comput. Methods Appl. Mech. Eng.* **2021**, *384*, 113989.

124. Schmidt, D.; Maulik, R.; Lyras, K. Machine learning accelerated turbulence modeling of transient flashing jets. *Phys. Fluids*, **2021**, *33* (12), 127104.

125. Hasegawa, K.; Fukami, K.; Murata, T.; Fukagata, K. CNN-LSTM based reduced order modeling of two-dimensional unsteady flows around a circular cylinder at different

Reynolds numbers. *Fluid Dyn. Res.* **2020**, *52* (6), 065501.

126.   Regazzoni, F.; Dede, L.; Quarteroni, A. Machine learning for fast and reliable solution of time-dependent differential equations. *J. Comput. Phys.* **2019**, *397*, 108852.

127.   Lu, L.; Gao, X.; Dietiker, J. F.; Shahnama, M.; Rogers, W. A. Machine learning accelerated discrete element modeling of granular flows. *Chem. Eng. Sci*. **2021**, *245*, 116832.

128.   Liu, Y.; Hu, R.; Kraus, A.; Balaprakash, P.; Obabko, A. Data-driven modeling of coarse mesh turbulence for reactor transient analysis using convolutional recurrent neural networks. *Nucl. Eng. Des.* **2022**, *390*, 111716.

129.   Ladický, L. U.; Jeong, S.; Solenthaler, B.; Pollefeys, M.; Gross, M. Data-driven fluid simulations using regression forests. *ACM Trans. Graph.* **2015**, *34* (6), 1-9.

130.   Tompson, J.; Schlachter, K.; Sprechmann, P.; Perlin, K. Accelerating Eulerian fluid simulation with convolutional networks. *Proc. Machine Learning Res.* **2017**, 3424-3433.

131.   Kochkov, D.; Smith, J. A.; Alieva, A.; Wang, Q.; Brenner, M. P.; Hoyer, S. Machine learning accelerated computational fluid dynamics. *Proc. Natl. Acad. Sci.* **2021**, *118* (21), e2101784118.

132.   Reuther, A.; Michaleas, P.; Jones, M.; Gadepally, V.; Samsi, S.; Kepner, J. Survey of machine learning accelerators. *IEEE High Perform. Extreme Comput. Conf.* **2020**, 1-12.

133.   Warsito, W.; Fan, L. S. Neural network based multi-criterion optimization image reconstruction technique for imaging two-and three-phase flow systems using electrical capacitance tomography. *Meas. Sci. Technol.* **2001**, *12* (12), 2198.

134.   Xia, Z.; Cui, Z.; Chen, Y.; Hu, Y.; Wang, H. Generative adversarial networks for dual-modality electrical tomography in multi-phase flow measurement. *Measurement* **2021**, *173*, 108608.

135.   Tan, C.; Dong, F.; Wu, M. Identification of gas/liquid two-phase flow regime through ERT-based measurement and feature extraction. *Flow Meas. Instrum*. **2007**, *18* (5-6), 255-261.

136.   Alqahtani, N.; Alzubaidi, F.; Armstrong, R. T.; Swietojanski, P.; Mostaghimi, P. Machine learning for predicting properties of porous media from 2d X-ray images. *J. Petrol. Sci. Eng.* **2020**, *184*, 106514.

137.   Jin, X.; Laima, S.; Chen, W. L.; Li, H. Time-resolved reconstruction of flow field

around a circular cylinder by recurrent neural networks based on non-time-resolved particle image velocimetry measurements. *Exp. Fluids* **2020**, *61* (4), 1-23.

138. Ma, L.; Kashanj, S.; Xu, S.; Zhou, J.; Nobes, D. S.; Ye, M. Flow reconstruction and prediction based on small particle image velocimetry experimental datasets with convolutional neural networks. *Ind. Eng. Chem. Res.* **2022**.

139. Mallery, K.; Shao, S.; Hong, J. Dense particle tracking using a learned predictive model. *Exp. Fluids* **2020**, *61* (10), 1-14.

140. He, Y.; Hu, C.; Li, H.; Jiang, B.; Hu, X.; Wang, K.; Tang, D. A flexible image processing technique for measuring bubble parameters based on a neural network. *Chem. Eng. J.* **2022**, *429*, 132138.

141. Hasti, V. R.; Shin, D. Denoising and fuel spray droplet detection from light-scattered images using deep learning. *Energy AI*, **2022**, *7*, 100130.

142. Fathi, M. F.; Perez-Raya, I.; Baghaie, A.; Berg, P.; Janiga, G.; Arzani, A.; D'Souza, R. M. Super-resolution and denoising of 4D-Flow MRI using physics-informed deep neural nets. *Comput. Methods Prog. Biomed.* **2020**, *197*, 105729.

143. O'Mahony, N.; Campbell, S.; Carvalho, A.; et al. Deep learning vs. traditional computer vision. *Adv Intell Syst*. **2019**, *943*, 128-144.

144. Liu, L.; Bai, B. Flow regime identification of swirling gas-liquid flow with image processing technique and neural networks. *Chem. Eng. Sci.* **2019**, *199*, 588-601.

145. Haas, T.; Schubert, C.; Eickhoff, M.; Pfeifer, H. BubCNN: Bubble detection using faster RCNN and shape regression network. *Chem. Eng. Sci.* **2020**, *216*, 115467.

146. Cerqueira, R. F.; Paladino, E. E. Development of a deep learning-based image processing technique for bubble pattern recognition and shape reconstruction in dense bubbly flows. *Chem. Eng. Sci.* **2021**, *230*, 116163.

147. Wang, C.; Li, S.; Yang, Y.; et al. On flow regime transition in trickle bed: Development of a novel deep-learning-assisted image analysis method. *AIChE J*. **2020**, *66* (2), e16833.

148. Fukami, K.; Fukagata, K.; Taira, K. Machine-learning-based spatio-temporal super resolution reconstruction of turbulent flows. *J. Fluid Mech.* **2021**, *909*, A9.

149. Raissi, M.; Yazdani, A.; Karniadakis, G. E. Hidden fluid mechanics: Learning

velocity and pressure fields from flow visualizations. *Science*, **2020**, *367* (6481), 1026-1030.

150.   Wang, H.; Yang, Z.; Li, B.; Wang, S. Predicting the near-wall velocity of wall turbulence using a neural network for particle image velocimetry. *Phys. Fluids*, **2020**, *32* (11), 115105.

151.   Shen, C.; Zheng, Q.; Shang, M.; Zha, L.; Su, Y. Using deep learning to recognize liquid–liquid flow patterns in microchannels. *AIChE J.* **2020**, *66* (8), e16260.

152.   Patel, A. M.; Cocco, R. A.; Chew, J. W. Key influence of clusters of Geldart Group B particles in a circulating fluidized bed riser. *Chem. Eng. J.* **2020**, *413*, 127386.

153.   Wang, C.; Lan, X.; Sun, Z.; Han, M.; Gao, J.; Ye, M.; Zhu, J. Cluster identification by a K-means algorithm-assisted imaging method in a laboratory-scale circulating fluidized bed. *Ind. Eng. Chem. Res.* **2022**, *61* (1), 942–956

154.   Chew, J. W.; Cocco, R. A. Application of machine learning methods to understand and predict circulating fluidized bed riser flow characteristics. *Chem. Eng. Sci.* **2020**, *217*, 115503.

155.   Zhou, J.; Liu, D.; Ye, M.; Liu, Z. Data-driven prediction of minimum fluidization velocity in gas-fluidized beds using data extracted by text mining. *Ind. Eng. Chem. Res*. **2021**, *60* (37), 13727-13739.

156.   Elsayed, K.; Lacor, C. Modeling and Pareto optimization of gas cyclone separator performance using RBF type artificial neural networks and genetic algorithms. *Powder Technol*. **2012**, *217*, 84-99.

157.   Brar, L. S.; Elsayed, K. Analysis and optimization of cyclone separators with eccentric vortex finders using large eddy simulation and artificial neural network. *Sep. Purif. Technol*. **2018**, *207*, 269-283.

158.   Gbadago, D. Q.; Moon, J.; Kim, M.; Hwang, S. A unified framework for the mathematical modelling, predictive analysis, and optimization of reaction systems using computational fluid dynamics, deep neural network and genetic algorithm: A case of butadiene synthesis. *Chem. Eng. J.* **2021**, *409*, 128163.

159.   Yan, Y.; Wang, L.,;Wang, T.; Wang, X.; Hu, Y.; Duan, Q. Application of soft computing techniques to multiphase flow measurement: A review. *Flow Meas. Instrum*. **2018**, *60*, 30-43.

160.   Cai, S.; Liang, J.; Gao, Q.; Xu, C.; Wei, R. Particle image velocimetry based on a deep learning motion estimator. *IEEE Trans. Instrum. Meas.* **2019**, *69* (6), 3538-3554.

161.   Nooralahiyan, A. Y.; Hoyle, B. S. Three-component tomographic flow imaging using artificial neural network reconstruction. *Chem. Eng. Sci.* **1997**, *52* (13), 2139-2148.

162.   Warsito, W.; Fan, L. S. Neural network multi-criteria optimization image reconstruction technique (NN-MOIRT) for linear and non-linear process tomography. *Chem. Eng. Process.* **2003**, *42* (8-9), 663-674.

163.   Marashdeh, Q.; Warsito, W.; Fan, L. S.; Teixeira, F. L. A nonlinear image reconstruction technique for ECT using a combined neural network approach. *Meas. Sci. Technol.* **2006**, *17* (8), 2097.

164.   Yadav, A.; Gaurav, T. K.; Pant, H. J.; Roy, S. Machine learning based position-rendering algorithms for radioactive particle tracking experimentation. *AIChE J.* **2020**, *66* (6), e16954.

165.   Bazai, H.; Kargar, E.; Mehrabi, M. Using an encoder-decoder convolutional neural network to predict the solid holdup patterns in a pseudo-2d fluidized bed. *Chem. Eng. Sci.* **2021**, *246*, 116886.

166.   Deng, Z.; Chen, Y.; Liu, Y.; Kim, K. C. Time-resolved turbulent velocity field reconstruction using a long short-term memory (LSTM)-based artificial intelligence framework. *Phys. Fluids*, **2019**, *31* (7), 075108.

167.   Deabes, W.; Khayyat, K. M. J. Image reconstruction in electrical capacitance tomography based on deep neural networks. *IEEE Sens. J.* **2021**, *21* (22), 25818-25830.

168.   Lei, J.; Mu, H. P.; Liu, Q. B.; Wang, X. Y.; Liu, S. Data-driven reconstruction method for electrical capacitance tomography. *Neurocomputing*, **2018**, *273*, 333-345.

169.   Xu, Z.; Wu, F.; Yang, Y.; Li, Y. ECT Attention Reverse Mapping algorithm: visualization of flow pattern heatmap based on convolutional neural network and its impact on ECT image reconstruction. *Meas. Sci. Technol.* **2020**, *32* (3), 035403.

170.   Xu, Z.; Wu, F.; Yang, X.; Li, Y. Measurement of gas-oil two-phase flow patterns by using CNN algorithm based on dual ECT sensors with venturi tube. *Sensors*, **2020**, *20* (4), 1200.

171.   He, K.; Zhang, X.; Ren, S.; Sun, J. Deep residual learning for image recognition.

Proceedings of the IEEE conference on computer vision and pattern recognition. **2016**, 770-778.

172.   Wang, F.; Jiang, M.; Qian, C.; et al. Residual attention network for image classification. *CVPR*, **2017**, 3156-3164.

173.   Kani, J. N.; Elsheikh, A. H. Reduced-order modeling of subsurface multi-phase flow models using deep residual recurrent neural networks. *Transp. Porous Media*, **2019**, *126* (3), 713-741.

174.   Lei, J.; Liu, Q.; Wang, X. Deep learning-based inversion method for imaging problems in electrical capacitance tomography. *IEEE Trans. Instrum. Meas.* **2018**, *67* (9), 2107-2118.

175.   Vishnevskiy, V.; Walheim, J.; Kozerke, S. Deep variational network for rapid 4D flow MRI reconstruction. *Nat. Mach. Intell*. **2020**, *2* (4), 228-235.

176.   Kissas, G.; Yang, Y.; Hwuang, E.; Witschey, W. R.; Detre, J. A.; Perdikaris, P. Machine learning in cardiovascular flows modeling: Predicting arterial blood pressure from non-invasive 4D flow MRI data using physics-informed neural networks. *Comput. Methods Appl. Mech. Eng.* **2020**, *358*, 112623.

177.   Deng, Z.; He, C.; Liu, Y.; Kim, K. C. Super-resolution reconstruction of turbulent velocity fields using a generative adversarial network-based artificial intelligence framework. *Phys. Fluids*, **2019**, 31 (12), 125111.

178.   Kim, H.; Kim, J.; Won, S.; Lee, C. Unsupervised deep learning for super-resolution reconstruction of turbulence. *J. Fluid Mech.* **2021**, *910*, A29.

179.   Kong, C.; Chang, J. T.; Li, Y. F.; Chen, R. Y. Deep learning methods for super-resolution reconstruction of temperature fields in a supersonic combustor. *AIP Adv.* **2020**, *10* (11), 115021.

180.   Liu, T.; Li, Y.; Jing, Q.; Xie, Y.; Zhang, D. Supervised learning method for the physical field reconstruction in a nanofluid heat transfer problem. *Int. J. Heat Mass Transf.* **2021**, *165*, 120684.

181.   Mikhaylov, K.; Rigopoulos, S.; Papadakis, G. Reconstruction of large scale flow structures in a stirred tank from limited sensor data. *AIChE J.* **2021**, *67* (10), e17348.

182.   Mi, Y.; Ishii, M.; Tsoukalas, L. H. Vertical two-phase flow identification using

advanced instrumentation and neural networks. *Nucl. Eng. Des.* **1998**, *184* (2-3), 409-420.

183. Mi, Y.; Ishii, M.; Tsoukalas, L. H. Flow regime identification methodology with neural networks and two-phase flow models. *Nucl. Eng. Des.* **2001**, *204* (1-3), 87-100.

184. Trafalis, T. B.; Oladunni, O.; Papavassiliou, D. V. Two-phase flow regime identification with a multiclassification support vector machine (SVM) model. *Ind. Eng. Chem. Res.* **2005**, *44* (12), 4414-4426.

185. Wang, H. X.; Zhang, L. F. Identification of two-phase flow regimes based on support vector machine and electrical capacitance tomography. *Meas. Sci. Technol.* **2009**, *20* (11), 114007.

186. Quintino, A. M.; da Rocha, D. L. L. N.; Fonseca Júnior, R. Rodriguez, O. M. H. Flow pattern transition in pipes using data-driven and physics-informed machine learning. *J. Fluids Eng.* **2021**, *143* (3), 031401-1.

187. Ye, J.; Guo, L. Multiphase flow pattern recognition in pipeline–riser system by statistical feature clustering of pressure fluctuations. *Chem. Eng. Sci.* **2013**, *102*, 486-501.

188. Dong, F.; Zhang, S.; Shi, X.; Wu, H.; Tan, C. Flow regimes identification based multi-domain features for gas-liquid two-phase flow in horizontal pipe. *IEEE Trans. Instrum. Meas.* **2021**, *70*, 1-11.

189. Seal, M. K.; Abadi, S. N. R.; Mehrabi, M.; Meyer, J. P. Machine learning classification of in-tube condensation flow patterns using visualization. *Int. J. Multiphase Flow*, **2021**, *143*, 103755.

190. Ali, N.; Viggiano, B.; Tutkun, M.; Cal, R. B. Data-driven machine learning for accurate prediction and statistical quantification of two phase flow regimes. *J. Petrol. Sci. Eng.* **2021**, *202*, 108488.

191. Ahmad, H.; Kim, S. K.; Park, J. H.; Jung, S. Y. Development of two-phase flow regime map for thermally stimulated flows using deep learning and image segmentation technique. *Int. J. Multiphase Flow* **2022**, *146*, 103869.

192. Nie, F.; Wang, H.; Song, Q.; Zhao, Y.; Shen, J.; Gong, M. Image identification for two-phase flow patterns based on CNN algorithms. *Int. J. Multiphase Flow*, **2022**, *152*, 104067.

193. Hu, H. L.; Dong, J.; Zhang, J.; Cheng, Y. J.; Xu, T. M. Identification of gas/solid

two-phase flow regimes using electrostatic sensors and neural-network techniques. *Flow Meas. Instrum*. **2011**, *22* (5), 482-487.

194.   Li, J.; He, K.; Tan, M.; Cheng, X. An adaptive CEEMD-ANN algorithm and its application in pneumatic conveying flow pattern identification. *Flow Meas. Instrum*. **2021**, *77*, 101860.

195.   Hu, H. L.; Zhang, J.; Dong, J.; Luo, Z. Y.; Xu, T. M. Identification of gas–solid two-phase flow regimes using Hilbert–Huang transform and neural-network techniques. *Instrum. Sci. Technol.* **2011**, *39* (2), 198-210.

196.   Guo, Q.; Ye, M.; Yang, W.; Liu, Z. A machine learning approach for electrical capacitance tomography measurement of gas–solid fluidized beds. *AIChE J.* **2019**, *65* (6), e16583.

197.   Lin, Z.; Liu, X.; Lao, L.; Liu, H. Prediction of two-phase flow patterns in upward inclined pipes via deep learning. *Energy*, **2020**, *210*, 118541.

198.   Wang, C.; Zhong, Z.; Jiaqiang, E. Flow regime recognition in spouted bed based on recurrence plot method. *Powder Technol.* **2012**, *219*, 20-28.

199.   Tarca, L. A.; Grandjean, B. P.; Larachi, F. Feature selection methods for multiphase reactors data classification. *Ind. Eng. Chem. Res.* **2005**, *44* (4), 1073-1084.

200.   Poletaev, I.; Tokarev, M. P.; Pervunin, K. S. Bubble patterns recognition using neural networks: Application to the analysis of a two-phase bubbly jet. *Int. J. Multiphase Flow*, **2020**, *126*, 103194.

201.   Gong, C.; Song, Y.; Huang, G.; Chen, W.; Yin, J.; Wang, D. BubDepth: A neural network approach to three-dimensional reconstruction of bubble geometry from single-view images. *Int. J. Multiphase Flow* **2022**, *152*, 104100.

202.   Kim, Y.; Park, H. Deep learning-based automated and universal bubble detection and mask extraction in complex two-phase flows. *Sci. Rep.* **2021**, *11* (1), 1-11.

203.   Serra, P. L.; Masotti, P. H.; Rocha, M. S.; de Andrade, D. A.; Torres, W. M.; de Mesquita, R. N. Two-phase flow void fraction estimation based on bubble image segmentation using Randomized Hough Transform with Neural Network (RHTN). *Prog. Nucl. Energy*, **2020**, *118*, 103133.

204.   Wang, J.; Dong, T.; Cheng, Y.; Yan, W. C. Machine learning assisted spraying pattern

recognition for electrohydrodynamic atomization system. *Ind. Eng. Chem. Res.* **2022**, in press.

205. Li, C.; Gao, X.; Rowan, S.; Hughes, B.; Rogers, W. Measuring binary fluidization of non-spherical and spherical particles using machine learning aided image processing. *AIChE J.* **2022**, e17693.

206. Chew, J. W.; Cocco, R. A. Do particle-related parameters influence circulating fluidized bed (CFB) riser flux and elutriation? *Chem. Eng. Sci*. **2020**, *227*, 115935.

207. Arief, H. A. A.; Wiktorski, T.; Thomas, P. J. A survey on distributed fibre optic sensor data modelling techniques and machine learning algorithms for multiphase fluid flow estimation. *Sensors* **2021**, *21* (8), 2801.

208. Saraswathi K, S.; Bhosale, H.; Ovhal, P.; Parlikkad Rajan, N.; Valadi, J. K. Random forest and autoencoder data-driven models for prediction of dispersed-phase holdup and drop size in rotating disc contactors. *Ind. Eng. Chem. Res.* **2020**, *60* (1), 425-435.

209. Chew, J. W.; Cahyadi, A.; Hrenya, C. M.; Karri, R.; Cocco, R. A. Review of entrainment correlations in gas–solid fluidization. *Chem. Eng. J.* **2015**, *260*, 152-171.

210. Anantharaman, A.; Cocco, R. A.; Chew, J. W. Evaluation of correlations for minimum fluidization velocity (Umf) in gas-solid fluidization. *Powder Technol.* **2018**, *323*, 454-485.

211. Shaban, H.; Tavoularis, S. Measurement of gas and liquid flow rates in two-phase pipe flows by the application of machine learning techniques to differential pressure signals. *Int. J. Multiphase Flow*, **2014**, *67*, 106-117.

212. Zhang, P.; Yang, Y.; Huang, Z.; Sun, J.; Liao, Z.; Wang, J.; Yang, Y. Machine learning assisted measurement of solid mass flow rate in horizontal pneumatic conveying by acoustic emission detection. *Chem. Eng. Sci.* **2021**, *229*, 116083.

213. Tanudjaja, H. J.; Chew, J. W. Application of machine learning-based models to understand and predict critical flux of oil-in-water emulsion in crossflow microfiltration. *Ind. Eng. Chem. Res.* **2022**, in press.

214. Wang, H.; Hu, D.; Zhang, M.; Yang, Y. Multiphase flowrate measurement with time series sensing data and sequential model. *Int. J. Multiphase Flow*, **2022**, *146*, 103875.

215. Hosseini, S. H.; Moradkhani, M. A.; Rasteh, M.; Rahimi, M. New smart models for

minimum fluidization velocity forecasting in the tapered fluidized beds based on particle size distribution. *Ind. Eng. Chem. Res.* **2021**, *60* (42), 15289-15300.

216. Ratnayake, P.; Chandratilleke, R.; Bao, J.; Shen, Y. A soft-sensor approach to mixing rate determination in powder mixers. *Powder Technol.* **2018**, *336*, 493-505.

217. Xie, Z.; Gu, X.; Shen, Y. A machine learning study of predicting mixing and segregation behaviors in a bidisperse solid-liquid fluidized bed. *Ind. Eng. Chem. Res.* **2022**, in press.

218. Shaikh, A.; Al-Dahhan, M. Development of an artificial neural network correlation for prediction of overall gas holdup in bubble column reactors. *Chem. Eng. Process.* **2003**, *42* (8-9), 599-610.

219. Lahiri, S. K.; Ghanta, K. C. Development of an artificial neural network correlation for prediction of hold-up of slurry transport in pipelines. *Chem. Eng. Sci.* **2008**, *63* (6), 1497-1509.

220. Razzak, S. A.; Rahman, S. M.; Hossain, M. M.; Zhu, J. Investigation of artificial neural network methodology for modeling of a liquid–solid circulating fluidized bed riser. *Powder Technol.* **2012**, *229*, 71-77.

221. Pourtousi, M.; Sahu, J. N.; Ganesan, P.; Shamshirband, S.; Redzwan, G. A combination of computational fluid dynamics (CFD) and adaptive neuro-fuzzy system (ANFIS) for prediction of the bubble column hydrodynamics. *Powder Technol.* **2015**, *274*, 466-481.

222. Azizi, S.; Awad, M. M.; Ahmadloo, E. Prediction of water holdup in vertical and inclined oil–water two-phase flow using artificial neural network. *Int. J. Multiphase Flow* **2016**, *80*, 181-187.

223. Hwang, S.; Pottimurthy, Y.; Chen, Y. Y.; Xu, D.; Falascino, E.; Tong, A.; Fan, L. S. Characteristics of gas-solid mixture flows through a packed moving bed of coarse particles. *Ind. Eng. Chem. Res.* **2022**, *61* (6), 2615-2622.

224. Abdul-Majeed, G. H.; Kadhim, F. S.; Almahdawi, F. H.; Al-Dunainawi, Y.; Arabi, A.; Al-Azzawi, W. K. Application of artificial neural network to predict slug liquid holdup. *Int. J. Multiphase Flow* **2022**, *150*, 104004.

225. Lemoine, R.; Fillion, B.; Behkish, A.; Smith, A. E.; Morsi, B. I. Prediction of the

gas–liquid volumetric mass transfer coefficients in surface-aeration and gas-inducing reactors using neural networks. *Chem. Eng. Process.* **2003**, *42* (8-9), 621-643.

226.   Lahiri, S. K.; Ghanta, K. C. Prediction of pressure drop of slurry flow in pipeline by hybrid support vector regression and genetic algorithm model. *Chin. J. Chem. Eng.* **2008**, *16* (6), 841-848.

227.   Osgouei, R. E.; Ozbayoglu, A. M.; Ozbayoglu, E. M.; Yuksel, E.; Eresen, A. Pressure drop estimation in horizontal annuli for liquid–gas 2 phase flow: Comparison of mechanistic models and computational intelligence techniques. *Comput. Fluids* **2015**, *112*, 108-115.

228.   Najafi, B.; Ardam, K.; Hanušovský, A.; Rinaldi, F.; Colombo, L. P. M. Machine learning based models for pressure drop estimation of two-phase adiabatic air-water flow in micro-finned tubes: Determination of the most promising dimensionless feature set. *Chem. Eng. Res. Des.* **2021**, *167*, 252-267.

229.   Qiu, Y.; Garg, D.; Kim, S. M.; Mudawar, I.; Kharangate, C. R. Machine learning algorithms to predict flow boiling pressure drop in mini/micro-channels based on universal consolidated data. *Int. J. Heat Mass Transf.* **2021**, *178*, 121607.

230.   Shijo, J. S.; Behera, N. Performance prediction of pneumatic conveying of powders using artificial neural network method. *Powder Technol.* **2021**, *388*, 149-157.

231.   Liu, Y.; Li, C.; Gao, Z. A novel unified correlation model using ensemble support vector regression for prediction of flooding velocity in randomly packed towers. *J. Ind. Eng. Chem.* **2014**, *20* (3), 1109-1118.

232.   Mosavi, A.; Shamshirband, S.; Salwana, E.; Chau, K.W.; Tah, J. H. Prediction of multi-inputs bubble column reactor using a novel hybrid model of computational fluid dynamics and machine learning. *Eng. Appl. Comput. Fluid Mech.* **2019**, *13* (1), 482-492.

233.   Babanezhad, M.; Zabihi, S.; Behroyan, I.; Nakhjiri, A.T.; Marjani, A.; Shirazian, S. Prediction of gas velocity in two-phase flow using developed fuzzy logic system with differential evolution algorithm. *Sci. Rep.* **2021**, *11* (1), 1-14.

234.   Laubscher, R.; Rousseau, P. Application of generative deep learning to predict temperature, flow and species distributions using simulation data of a methane combustor. *Int. J. Heat Mass Transf.* **2020**, *163*, 120417.

235.   Asgari, S.; MirhoseiniNejad, S.; Moazamigoodarzi, H.; Gupta, R.; Zheng, R.; Puri, I. K. A gray-box model for real-time transient temperature predictions in data centers. *Appl. Therm. Eng.* **2021**, *185*, 116319.

236.   Laubscher, R. Simulation of multi-species flow and heat transfer using physics-informed neural networks. *Phys. Fluids* **2021**, *33*, 087101.

237.   Chen, X.; Wang, L. G.; Meng, F.; Luo, Z. H. Physics-informed deep learning for modelling particle aggregation and breakage processes. *Chem. Eng. J.* **2021**, *426*, 131220.

238.   Li, W.; Zhuo, Y.; Bao, J.; Shen, Y. A data-based soft-sensor approach to estimating raceway depth in ironmaking blast furnaces. *Powder Technol.* **2021**, *390*, 529-538.

239.   Li, Y.; Bao, J.; Yu, A.; Yang, R. A combined data-driven and discrete modelling approach to predict particle flow in rotating drums. *Chem. Eng. Sci.* **2021**, *231*, 116251.

240.   Gandhi, A. B.; Joshi, J. B.; Jayaraman, V. K.; Kulkarni, B. D. Development of support vector regression (SVR)-based correlation for prediction of overall gas hold-up in bubble column reactors for various gas–liquid systems. *Chem. Eng. Sci.* **2007**, *62* (24), 7078-7089.

241.   Gandhi, A.B.; Joshi, J.B.; Kulkarni, A.A.; Jayaraman, V.K.; Kulkarni, B.D. SVR-based prediction of point gas hold-up for bubble column reactor through recurrence quantification analysis of LDA time-series. *Int. J. Multiphase Flow*, **2008**, *34* (12), 1099-1107.

242.   Gandhi, A. B.; Joshi, J. B. Estimation of heat transfer coefficient in bubble column reactors using support vector regression. *Chem. Eng. J.* **2010**, *160* (1), 302-310.

243.   Ganti, H.; Kamin, M.; Khare, P. Design space exploration of turbulent multiphase flows using machine learning-based surrogate model. *Energies*, **2020**, *13* (17), 4565.

244.   Chew, J. W.; Cocco, R. A. Application of machine learning methods to understand and predict circulating fluidized bed riser flow characteristics. *Chem. Eng. Sci.* **2020**, *217*, 115503.

245.   Chew, J. W.; Cocco, R. A. Fast versus turbulent fluidization of Geldart Group B particles. *AIChE J.* **2021**, *67* (6), e17216.

246.   Li, Y.; Bao, J.; Yu, A.; Yang, R. ANN prediction of particle flow characteristics in a drum based on synthetic acoustic signals from DEM simulations. *Chem. Eng. Sci.* **2021**, *246*,

117012.

247.   Zhong, H.; Sun, Z.; Zhu, J.; Zhang, C. Prediction of solid holdup in a gas-solid circulating fluidized bed riser by artificial neural networks. *Ind. Eng. Chem. Res*. **2021**, *60* (8), 3452-3462.

248.   Li, C.; Liu, M.; Zhao, N.; Wang, F.; Zhao, Z.; Guo, S.; Fang, L.; Li, X. Void fraction measurement using modal decomposition and ensemble learning in vertical annular flow, *Chem. Eng. Sci.* **2022**, *247*, 116929.

249.   Barbosa, L. F. F.; Nascimento, A.; Mathias, M. H.; de Carvalho Jr, J. A. Machine learning methods applied to drilling rate of penetration prediction and optimization-A review. *J. Petrol. Sci. Eng.* **2019**, *183*, 106332.

250.   Rovira, M.; Engvall, K.; Duwig, C. Identifying key features in reactive flows: A tutorial on combining dimensionality reduction, unsupervised clustering, and feature correlation. *Chem. Eng. J.* **2022**, *438*, 135250.

251.   Wang, L.; Yan, Y.; Wang, X.; Wang, T. Input variable selection for data-driven models of Coriolis flowmeters for two-phase flow measurement. *Meas. Sci. Technol.* **2017**, *28* (3), 035305.

252.   Hussain, M. A. Review of the applications of neural networks in chemical process control—simulation and online implementation. *Artif. Intell. Eng*. **1999**, *13* (1), 55-68.

253.   Nascimento, C. A. O.; Giudici, R.; Guardani, R. Neural network based approach for optimization of industrial chemical processes. *Comput. Chem. Eng.* **2000**, *24* (9-10), 2303-2314.

254.   Luo, J.; Canuso, V.; Jang, J. B.; Wu, Z.; Morales-Guio, C. G.; Christofides, P. D. Machine learning-based operational modeling of an electrochemical reactor: Handling data variability and improving empirical models. *Ind. Eng. Chem. Res.* **2022**, in press.

255.   Müller, S.; Milano, M.; Koumoutsakos, P. Application of machine learning algorithms to flow modeling and optimization. *Annual Research Briefs*, **1999**, 169-178.

256.   Zhang, X.; Li, H. Neural-network-based control of discrete-phase concentration in a gas-particle corner flow with optimal energy consumption. *Comput. Math. Appl.* **2020**, *80* (5), 1360-1374.

257.   Nikita, S.; Tiwari, A.; Sonawat, D.; Kodamana, H.; Rathore, A. S. Reinforcement

learning based optimization of process chromatography for continuous processing of biopharmaceuticals. *Chem. Eng. Sci*. **2021**, *230*, 116171.

258.   Chen, T. Y.; Baker-Fales, M.; Vlachos, D. G. Operation and Optimization of Microwave-Heated Continuous-Flow Microfluidics. *Ind. Eng. Chem. Res.* **2020**, *59* (22), 10418-10427.

259.   Hamad, H. S.; Kapur, N.; Khatir, Z.; Querin, O. M.; Thompson, H. M.; Wang, Y.; Wilson, M. C. T. Computational fluid dynamics analysis and optimisation of polymerase chain reaction thermal flow systems. *Appl. Therm. Eng.* **2021**, *183*, 116122.

260.   Zhang, Z.; Wu, Z.; Rincon, D.; Christofides, P. D. Real-time optimization and control of nonlinear processes using machine learning. *Mathematics*, **2019**, *7* (10), 890.

261.   Wu, Z.; Tran, A.; Ren, Y. M.; Barnes, C. S.; Chen, S.; Christofides, P.D. Model predictive control of phthalic anhydride synthesis in a fixed-bed catalytic reactor via machine learning modeling. *Chem. Eng. Res. Des.* **2019**, *145*, 173-183.

262.   Brar, L. S.; Elsayed, K. Analysis and optimization of multi-inlet gas cyclones using large eddy simulation and artificial neural network. *Powder Technol.* **2017**, *311*, 465-483.

263.   Elsayed, K.; Lacor, C. Modeling, analysis and optimization of aircyclones using artificial neural network, response surface methodology and CFD simulation approaches. *Powder Technol.* **2011**, *212* (1), 115-133.

264.   Elsayed, K.; Lacor, C. CFD modeling and multi-objective optimization of cyclone geometry using desirability function, artificial neural networks and genetic algorithms. *Appl. Math. Model.* **2013**, *37* (8), 5680-5704.

265.   Ye, J.; Xu, Y.; Song, X.; Yu, J. Numerical modelling and multi-objective optimization of the novel hydrocyclone for ultra-fine particles classification. *Chem. Eng. Sci.* **2019**, *207*, 1072-1084.

266.   Deng, Y.; Yu, B.; Sun, D. Multi-objective optimization of guide vanes for axial flow cyclone using CFD, SVM, and NSGA II algorithm. *Powder Technol.* **2020**, *373*, 637-646.

267.   Komp, E.; Valleau, S. Machine learning quantum reaction rate constants. *J. Phys. Chem. A*, **2020**, *124* (41), 8607-8613.

268.   Grambow, C. A.; Pattanaik, L.; Green, W. H. Deep learning of activation energies. *J. Phys. Chem. Lett*. **2020**, *11* (8), 2992-2997.

269.   Ulissi, Z. W.; Medford, A. J.; Bligaard, T.; Nørskov, J. K. To address surface reaction network complexity using scaling relations machine learning and DFT calculations. *Nat. Commun.* **2017**, *8* (1), 1-7.

270.   Gusmão, G. S.; Retnanto, A. P.; da Cunha, S. C.; Medford, A. J. Kinetics-informed neural networks. *Catal. Today*, **2022**, in press.

271.   Ngo, S. I.; Lim, Y. I. Solution and parameter identification of a fixed-bed reactor model for catalytic CO_2 methanation using physics-informed neural networks. *Catalysts*, **2021**, *11* (11), 1304.

272.   Partopour, B.; Paffenroth, R. C.; Dixon, A. G. Random forests for mapping and analysis of microkinetics models. *Comput. Chem. Eng.* **2018**, *115*, 286-294.

273.   Ouyang, Y.; Vandewalle, L. A.; Chen, L.; Plehiers, P. P.; Dobbelaere, M. R.; Heynderickx, G. J.; Marin, G. B.; Van Geem, K. M. Speeding up turbulent reactive flow simulation via a deep artificial neural network: a methodology study, *Chem. Eng. J.* **2022**, *429*, 132442.

274.   Zhong, H.; Xiong, Q.; Yin, L.; Zhang, J.; Zhu, Y.; Liang, S.; Niu, B.; Zhang, X. CFD-based reduced-order modeling of fluidized-bed biomass fast pyrolysis using artificial neural network. *Renew. Energy*, **2020**, *152*, 613-626.

275.   Gao, H.; Struble, T. J.; Coley, C. W.; Wang, Y.; Green, W. H.; Jensen, K. F. Using machine learning to predict suitable conditions for organic reactions. *ACS Cent. Sci.* **2018**, *4* (11), 1465-1476.

276.   Amar, Y.; Schweidtmann, A. M.; Deutsch, P.; Cao, L.; Lapkin, A. Machine learning and molecular descriptors enable rational solvent selection in asymmetric catalysis. *Chem. Sci.* **2019**, *10* (27), 6697-6706.

277.   Li, J.; Pan, L.; Suvarna, M.; Wang, X. Machine learning aided supercritical water gasification for H_2-rich syngas production with process optimization and catalyst screening. *Chem. Eng. J.* **2021**, *426*, 131285.

278.   Mann, V.; Venkatasubramanian, V. Predicting chemical reaction outcomes: A grammar ontology-based transformer framework. *AIChE J.* **2021**, *67* (3), e17190.

279.   Unsleber, J. P.; Reiher, M. The exploration of chemical reaction networks. *Annu. Rev. Phys. Chem.* **2020**, *71*, 121-142.

280.   Vernuccio, S.; Broadbelt, L. J. Discerning complex reaction networks using automated generators. *AIChE J.* **2019**, *65* (8), e16663.

281.   Plehiers, P. P.; Lengyel, I.; West, D. H.; Marin, G. B.; Stevens, C. V.; Van Geem, K. M. Fast estimation of standard enthalpy of formation with chemical accuracy by artificial neural network correction of low-level-of-theory ab initio calculations. *Chem. Eng. J.* **2021**, *426*, 131304.

282.   Shi, Y.; Wang, J.; Wang, Q.; Jia, Q.; Yan, F.; Luo, Z. H.; Zhou, Y. N. Supervised machine learning algorithms for predicting rate constants of ozone reaction with micropollutants. *Ind. Eng. Chem. Res*. **2022**, in press.

283.   Komp, E.; Janulaitis, N.; Valleau, S. Progress towards machine learning reaction rate constants. *Phys. Chem. Chem. Phys.* **2022**, *24*, 2692-2705

284.   Taylor, C. J.; Booth, M.; Manson, J. A.; et al. Rapid, automated determination of reaction models and kinetic parameters. *Chem. Eng. J.* **2021**, *413*, 127017.

285.   Kunz, M. R.; Yonge, A.; Fang, Z.; Batchu, R.; Medford, A. J.; Constales, D.; Yablonsky, G.; Fushimi, R. Data Driven Reaction Mechanism Estimation via Transient Kinetics and Machine Learning. *Chem. Eng. J*. **2021**, *420*, 129610.

286.   Jorner, K.; Brinck, T.; Norrby, P. O.; Buttar, D. Machine learning meets mechanistic modelling for accurate prediction of experimental activation energies. *Chem. Sci*. **2021**, *12* (3), 1163-1175.

287.   Sanches-Neto, F. O.; Dias-Silva, J. R.; Keng Queiroz Junior, L. H.; Carvalho-Silva, V. H. "pySiRC": Machine learning combined with molecular fingerprints to predict the reaction rate constant of the radical-based oxidation processes of aqueous organic contaminants. *Environ. Sci. Technol*. **2021**, *55* (18), 12437-12448.

288.   Rizkin, B. A.; Shkolnik, A. S.; Ferraro, N. J.; Hartman, R. L. Combining automated microfluidic experimentation with machine learning for efficient polymerization design. *Nat. Mach. Intell.* **2020**, *2* (4), 200-209.

289.   Quaglio, M.; Roberts, L.; Jaapar, M. S. B.; Fraga, E. S.; Dua, V.; Galvanin, F. An artificial neural network approach to recognise kinetic models from experimental data. *Comput. Chem. Eng*. **2020**, *135*, 106759.

290.   Gonçalves, G. F.; Batchvarov, A.; Liu, Y.; Liu, Y.; Mason, L.R.; Pan, I.; Matar, O.K.

Data-driven surrogate modeling and benchmarking for process equipment. *Data-Centric Engineering*, **2020**, *1*, E7.

291.   Houston, P. L.; Nandi, A.; Bowman, J. M. A machine learning approach for prediction of rate constants. *J. Phys. Chem. Lett.* **2019**, *10* (17), 5250-5258.

292.   Ji, W.; Deng, S. Autonomous discovery of unknown reaction pathways from data by chemical reaction neural network. *J. Phys. Chem. A*, **2021**, *125* (4), 1082-1092.

293.   Ji, W.; Qiu, W.; Shi, Z.; Pan, S.; Deng, S. Stiff-PINN: Physics-informed neural network for stiff chemical kinetics. *J. Phys. Chem. A*, **2021**, *125* (36), 8098-8106.

294.   Owoyele, O.; Pal, P. ChemNODE: A Neural Ordinary Differential Equations Framework for Efficient Chemical Kinetic Solvers. *Energy AI*, **2021**, *7*, 100118.

295.   Plehiers, P. P.; Symoens, S. H.; Amghizar, I.; Marin, G. B.; Stevens, C. V.; Van Geem, K. M. Artificial intelligence in steam cracking modeling: a deep learning algorithm for detailed effluent prediction. *Engineering*, **2019**, *5* (6), 1027-1040.

296.   Hough, B. R.; Beck, D. A.; Schwartz, D. T.; Pfaendtner, J. Application of machine learning to pyrolysis reaction networks: Reducing model solution time to enable process optimization. *Comput. Chem. Eng*. **2017**, *104*, 56-63.

297.   Hua, F.; Fang, Z.; Qiu, T. Application of convolutional neural networks to large-scale naphtha pyrolysis kinetic modeling. *Chin. J. Chem. Eng.* **2018**, *26* (12), 2562-2572.

298.   Bi, K.; Zhang, C.; Qiu, T. An ingenious characterization of reaction network using sub-network reconstruction. *Comput. Chem. Eng.* **2020**, *134*, 106695.

299.   Katsoulakis, M. A.; Vilanova, P. Data-driven, variational model reduction of high-dimensional reaction networks. *J. Comput. Phys.* **2020**, *401*, 108997.

300.   Harirchi, F.; Kim, D.; Khalil, O.; et al. A. On sparse identification of complex dynamical systems: A study on discovering influential reactions in chemical reaction networks. *Fuel*, **2020**, *279*, 118204.

301.   Barwey, S.; Raman, V. A neural network-inspired matrix formulation of chemical kinetics for acceleration on GPUs. *Energies*, **2021**, *14* (9), 2710.

302.   Ghasemigoudarzi, P.; Hojjati, M. R.; Omidkhah, M.; Tavallali, M. S. Estimation of kinetic parameters and simulation of methylacetylene and propadiene liquid-phase selective hydrogenation reactor considering the catalyst deactivation. *Ind. Eng. Chem. Res*. **2021**, *60*

(34), 12474–12491.

303.   Spencer, R.; Gkinis, P.; Koronaki, E. D.; Gerogiorgis, D. I.; Bordas, S. P.; Boudouvis, A.G. Investigation of the chemical vapor deposition of Cu from copper amidinate through data driven efficient CFD modelling. *Comput. Chem. Eng.* **2021**, *149*, 107289.

304.   Chen, X.; Zhang, H.; Song, Y.; Xiao, R. Prediction of product distribution and bio-oil heating value of biomass fast pyrolysis. *Chem. Eng. Process.* **2018**, *130*, 36-42.

305.   Mutlu, A. Y.; Yucel, O. An artificial intelligence based approach to predicting syngas composition for downdraft biomass gasification. *Energy*, **2018**, *165*, 895-901.

306.   Agarwal, P.; Klein, M. T. Generating data-driven models from molecular-level kinetic models: A kinetic model speedup strategy. *Energy Fuels*, **2019**, *33* (10), 10372-10379.

307.   Zhu, X.; Li, Y.; Wang, X. Machine learning prediction of biochar yield and carbon contents in biochar based on biomass characteristics and pyrolysis conditions. *Bioresour. Technol.* **2019**, *288*, 121527.

308.   Zhao, S.; Li, J.; Chen, C.; Yan, B.; Tao, J.; Chen, G. Interpretable machine learning for predicting and evaluating hydrogen production via supercritical water gasification of biomass. *J. Cleaner Prod.* **2021**, *316*, 128244.

309.   Tang, Q.; Chen, Y.; Yang, H.; et al. Machine learning prediction of pyrolytic gas yield and compositions with feature reduction methods: Effects of pyrolysis conditions and biomass characteristics. *Bioresour. Technol*. **2021**, *339*, 125581.

310.   Ullah, Z.; Naqvi, S. R.; Farooq, W.; Yang, H.; Wang, S.; Vo, D. V. N. A Comparative study of machine learning methods for bio-oil yield prediction–A genetic algorithm-based features selection. *Bioresour. Technol*. **2021**, *335*, 125292.

311.   Bracconi, M.; Maestri, M. Training set design for machine learning techniques applied to the approximation of computationally intensive first-principles kinetic models. *Chem. Eng. J.* **2020**, *400*, 125469.

312.   Yang, F.; Dai, C.; Tang, J.; Xuan, J.; Cao, J. A hybrid deep learning and mechanistic kinetics model for the prediction of fluid catalytic cracking performance. *Chem. Eng. Res. Des.* **2020**, *155*, 202-210.

313.   Wan, K.; Barnaud, C.; Vervisch, L.; Domingo, P. Chemistry reduction using machine learning trained from non-premixed micro-mixing modeling: Application to DNS of a syngas

turbulent oxy-flame with side-wall effects. *Combust. Flame* **2020**, *220*, 119-129.

314.   Nakazawa, R.; Minamoto, Y.; Inoue, N.; Tanahashi, M. Species reaction rate modelling based on physics-guided machine learning. *Combust. Flame* **2022**, *235*, 111696.

315.   Franzoi, R. E.; Kelly, J. D.; Menezes, B. C.; Swartz, C. L. An adaptive sampling surrogate model building framework for the optimization of reaction systems. *Comput. Chem. Eng.* **2021**, *152*, 107371.

316.   Wang, Z.; Peng, X.; Xia, A., et al. The role of machine learning to boost the bioenergy and biofuels conversion. *Bioresour. Technol.* **2022**, *343*, 126099.

317.   Venkatasubramanian, V.; Mann, V. Artificial intelligence in reaction prediction and chemical synthesis. *Curr. Opin. Chem. Eng.* **2022**, *36*, 100749.

318.   Meuwly, M. Machine Learning for Chemical Reactions. *Chem. Rev.* **2021**, *121* (16), 10218-10239.

319.   Chaffart, D.; Ricardez-Sandoval, L. A. Optimization and control of a thin film growth process: A hybrid first principles/artificial neural network based multiscale modelling approach. *Comput. Chem. Eng.* **2018**, *119*, 465-479.

320.   Ding, Y.; Zhang, Y.; Ren, Y. M.; Orkoulas, G.; Christofides, P. D. Machine learning-based modeling and operation for ALD of SiO2 thin-films using data from a multiscale CFD simulation. *Chem. Eng. Res. Des.* **2019**, *151*, 131-145.

321.   Liang, R.; Duan, X.; Zhang, J.; Yuan, Z. Bayesian based reaction optimization for complex continuous gas–liquid–solid reactions. *React. Chem. Eng.* **2022**, *7*, 590-598.

322.   Wang, C.; Yang, Q.; Wang, J.; Zhao, J.; Wan, X.; Guo, Z.; Yang, Y. Application of support vector machine on controlling the silanol groups of silica xerogel with the aid of segmented continuous flow reactor. *Chem. Eng. Sci.* **2019**, *199*, 486-495.

323.   Neumann, M.; Palkovits, D. S. Reinforcement learning approaches for the optimization of the partial oxidation reaction of methane. *Ind. Eng. Chem. Res.* **2022**.

324.   Li, J.; Zhu, X.; Li, Y.; Tong, Y. W.; Ok, Y. S.; Wang, X. Multi-task prediction and optimization of hydrochar properties from high-moisture municipal solid waste: Application of machine learning on waste-to-resource. *J. Cleaner Prod.* **2021**, *278*, 123928.

325.   Zhang, W.; Li, J.; Liu, T.; et al. Machine learning prediction and optimization of bio-oil production from hydrothermal liquefaction of algae. *Bioresour. Technol.* **2021**, *342*,

126011.

326. Garcia, A. C.; Shuo, C.; Cross, J. S. Machine learning based analysis of reaction phenomena in catalytic lignin depolymerization. *Bioresour. Technol*. **2022**, *345*, 126503.

327. Zhou, Z.; Li, X.; Zare, R. N. Optimizing chemical reactions with deep reinforcement learning. *ACS Cent. Sci*. **2017**, *3* (12), 1337-1344.

328. Schweidtmann, A. M.; Clayton, A. D.; Holmes, N.; Bradford, E.; Bourne, R. A.; Lapkin, A. A. Machine learning meets continuous flow chemistry: Automated optimization towards the Pareto front of multiple objectives. *Chem. Eng. J.* **2018**, *352*, 277-282.

329. Clayton, A. D.; Schweidtmann, A. M.; Clemens, G.; Manson, J. A.; Taylor, C. J.; Niño, C. G.; Chamberlain, T. W.; Kapur, N.; Blacker, A. J.; Lapkin, A. A.; Bourne, R. A. Automated self-optimisation of multi-step reaction and separation processes using machine learning. *Chem. Eng. J.* **2020**, *384*, 123340.

330. Kim, H. W.; Lee, S. W.; Na, G. S.; et al. Reaction condition optimization for non-oxidative conversion of methane using artificial intelligence. *React. Chem. Eng*. **2021**, *6* (2), 235-243.

331. Houben, C.; Lapkin, A. A. Automatic discovery and optimization of chemical processes. *Curr. Opin. Chem. Eng.* **2015**, *9*, 1-7.

332. Zhang, C.; Amar, Y.; Cao, L.; Lapkin, A. A. Solvent selection for Mitsunobu reaction driven by an active learning surrogate model. *Org. Process Res. Dev.* **2020**, *24* (12), 2864-2873.

333. Felton, K.; Rittig, J.; Lapkin, A. Summit: Benchmarking machine learning methods for reaction optimisation, *Chemistry-Methods*, **2021**, *1*, 116-122.

334. Coley, C. W.; Thomas, D. A.; Lummiss, J. A.; et al. A robotic platform for flow synthesis of organic compounds informed by AI planning. *Science*, **2019**, *365*, 6453.

335. Burger, B.; Maffettone, P. M.; Gusev, V. V.; et al. A mobile robotic chemist. *Nature*, **2020**, *583*, 237-241.

336. Shields, B. J.; Stevens, J.; Li, J.; et al. Bayesian reaction optimization as a tool for chemical synthesis. *Nature*, **2021**, *590* (7844), 89-96.

337. Cao, L.; Russo, D.; Felton, K.; Salley, D.; Sharma, A.; Keenan, G.; Mauer, W.; Gao, H. H.; Cronin, L.; Lapkin, A. A. Optimization of Formulations Using Robotic Experiments

Driven by Machine Learning DoE. *Cell Rep. Phys. Sci.* **2021**, *2* (1), 100295.

338.   Cao, L.; Russo, D.; Lapkin, A. A. Automated robotic platforms in design and development of formulations. *AIChE J.* **2021**, *67* (5), e17248.

339.   Yuan, W. K. Targeting the dominating-scale structure of a multiscale complex system: A methodological problem. *Chem. Eng. Sci.* **2007**, *62* (13), 3335-3345.

340.   Sivaram, A.; Venkatasubramanian, V. XAI-MEG: Combining symbolic AI and machine learning to generate first-principles models and causal explanations. *AIChE J.* **2022**, e17687, in press.

341.   Toyao, T.; Maeno, Z.; Takakusagi, S.; Kamachi, T.; Takigawa, I.; Shimizu, K. I. Machine learning for catalysis informatics: recent applications and prospects. *ACS Catalysis*, **2019**, *10* (3), 2260-2297.

342.   Selvaratnam, B.; Koodali, R.T. Machine learning in experimental materials chemistry. *Catal. Today*, **2021**, *371*, 77-84.

343.   Wen, M.; Blau, S. M.; Xie, X.; Dwaraknath, S.; Persson, K. Improving machine learning performance on small chemical reaction data with unsupervised contrastive pretraining. *Chem. Sci.* **2022**, *13*, 1446-1458.

344.   Rajulapati, L.; Chinta, S.; Shyamala, B.; Rengaswamy, R. Integration of machine learning and first principles models. *AIChEJ.* **2022**, e17715, in press.

345.   Kotteda, V. K.; Stephens, J. A.; Spotz, W.; Kumar, V.; Kommu, A. Uncertainty quantification of fluidized beds using a data-driven framework. *Powder Technol.* **2019**, *354*, 709-718.

346.   Xiao, H.; Cinnella, P. Quantification of model uncertainty in RANS simulations: A review. *Prog. Aerosp. Sci.* **2019**, *108*, 1-31.

347.   Liu, Y.; Dinh, N. T.; Smith, R. C.; Sun, X. Uncertainty quantification of two-phase flow and boiling heat transfer simulations through a data-driven modular Bayesian approach. *Int. J. Heat Mass Transf.* **2019**, *138*, 1096-1116.

348.   Scillitoe, A.; Seshadri, P.; Girolami, M. Uncertainty quantification for data-driven turbulence modelling with Mondrian forests. *J. Comput. Phys.* **2021**, *430*, 110116.

349.   Grieves, M.; Vickers, J. Digital twin: Mitigating unpredictable, undesirable emergent behavior in complex systems. *Transdiscipl. Perspect. Complex Syst*. **2017**. 85-113.

350. Wang, L. G.; Ge, R.; Chen, X.; Zhou, R.; Chen, H. M. Multiscale digital twin for particle breakage in milling: From nanoindentation to population balance model. *Powder Technol.* **2021**, *386*, 247-261.

351. Pan, I.; Mason, L. R.; Matar, O. K. Data-centric Engineering: integrating simulation, machine learning and statistics. Challenges and opportunities. *Chem. Eng. Sci.* **2022**, *249*, 117271.

352. Tuegel, E. J.; Ingraffea, A. R.; Eason, T. G.; Spottswood, S. M. Reengineering aircraft structural life prediction using a digital twin. *Int. J. Aerosp*, **2011**, *2011*, 4.

353. Min, Q.; Lu, Y.; Liu, Z.; Su, C.; Wang, B. Machine learning based digital twin framework for production optimization in petrochemical industry. *Int. J. Inf. Manage.* **2019**, *49*, 502-519.

354. Che, Y.; Tian, Z.; Liu, Z.; et al. CFD prediction of scale-up effect on the hydrodynamic behaviors of a pilot-plant fluidized bed reactor and preliminary exploration of its application for non-pelletizing polyethylene process. *Powder Technol.* **2015**, *278*, 94-110.

355. Ye, M.; Tian, P.; Liu, Z. DMTO: a sustainable methanol-to-olefins technology. *Engineering* **2021**, *7* (1), 17-21.
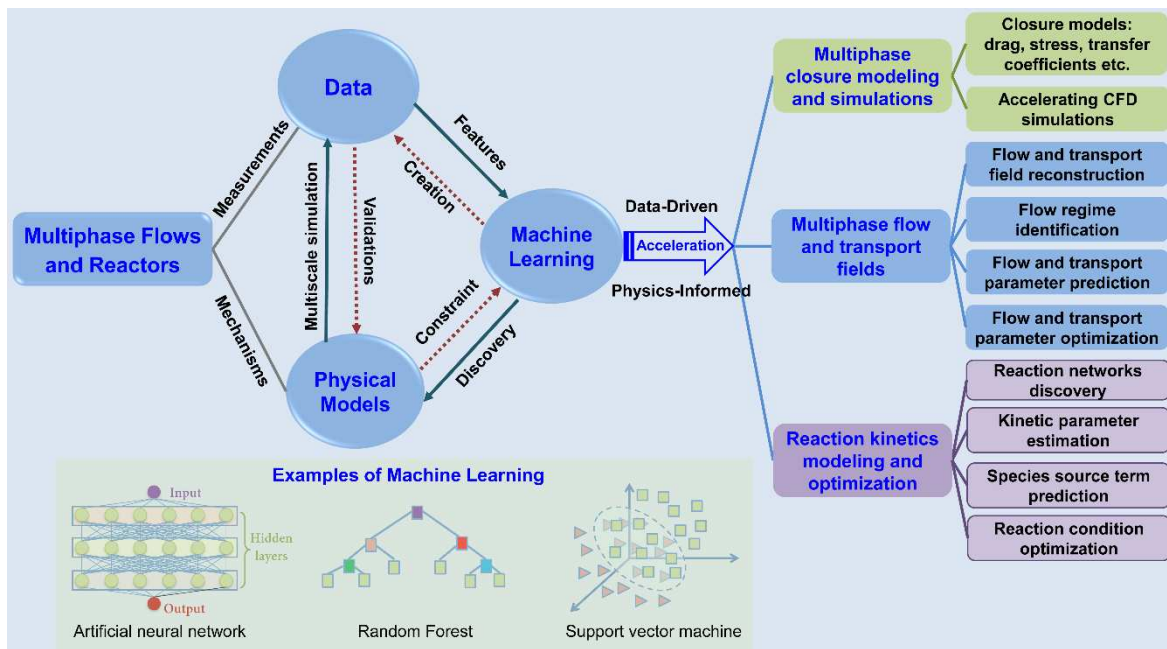
Table of Contents Graphic